NAVAL POSTGRADUATE SCHOOL
MONTEREY, CALIFORNIA

THESIS

A CHARACTERIZATION OF THE MAXIMUM BENDING STRESS OF THE SLICE HULL IN RANDOM SEAS

by

Dennis W. McFadden

March, 1996

Thesis Advisor: Fotis A. Papoulias

Approved for public release; distribution is unlimited.

REPORT DOCUMENTATION PAGE

Form Approved OMB No. 0704-0188

1. AGENCY USE ONLY *(Leave blank)*	2. REPORT DATE March 1996	3. REPORT TYPE AND DATES COVERED Master's Thesis

4. TITLE AND SUBTITLE A CHARACTERIZATION OF THE MAXIMUM BENDING STRESS OF THE SLICE HULL IN RANDOM SEAS.

5. FUNDING NUMBERS

6. AUTHOR(S) : Dennis W. McFadden

7. PERFORMING ORGANIZATION NAME(S) AND ADDRESS(ES)
Naval Postgraduate School
Monterey CA 93943-5000

8. PERFORMING ORGANIZATION REPORT NUMBER

9. SPONSORING/MONITORING AGENCY NAME(S) AND ADDRESS(ES)

10. SPONSORING/MONITORING AGENCY REPORT NUMBER

11. SUPPLEMENTARY NOTES The views expressed in this thesis are those of the author and do not reflect the official policy or position of the Department of Defense or the U.S. Government.

12a. DISTRIBUTION/AVAILABILITY STATEMENT
Approved for public release; distribution is unlimited.

12b. DISTRIBUTION CODE

13. ABSTRACT *(maximum 200 words)*

A study of the effects of speed, heading and sea state on the maximum longitudinal bending stress of the SLICE Advanced Technology Demonstrator is presented. Strip Theory is applied to a model of the SLICE hull. The hull is modeled using data from a current design and with ship loading weight information for ferry operations. Stress results are based on conventional beam theory applied to the hull girder. Bending moment distributions are presented for random, fully-developed, uni-directional seas. The maximum expected bending stress is calculated for varying sea states, ship speeds, and wave directions. Operability of the SLICE based on limiting material stress is evaluated for sea states through sea state 6. The results of this study indicate that increased stiffening of the hull could be considered in the vicinity just aft of the forward pods.

14. SUBJECT TERMS SLICE, HULL STRESS, WAVE INDUCED STRESS, OPERABILITY, STRIP THEORY

15. NUMBER OF PAGES 142

16. PRICE CODE

17. SECURITY CLASSIFICATION OF REPORT	18. SECURITY CLASSIFICATION OF THIS PAGE	19. SECURITY CLASSIFICATION OF ABSTRACT	20. LIMITATION OF ABSTRACT
Unclassified	Unclassified	Unclassified	UL

NSN 7540-01-280-5500

Standard Form 298 (Rev. 2-89)
Prescribed by ANSI Std. 239-18 298-102

Approved for public release; distribution is unlimited.

A CHARACTERIZATION OF THE MAXIMUM BENDING STRESS OF THE SLICE HULL IN RANDOM SEAS

Dennis W. McFadden
Lieutenant, United States Navy
B.S., University of Oklahoma, 1988

Submitted in partial fulfillment
of the requirements for the degree of

MASTER OF SCIENCE IN MECHANICAL ENGINEERING

from the

NAVAL POSTGRADUATE SCHOOL
March 1996

Author: 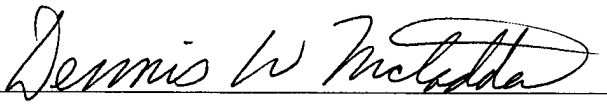

Dennis W. McFadden

Approved by: 

Fotis A. Papoulias, Thesis Advisor

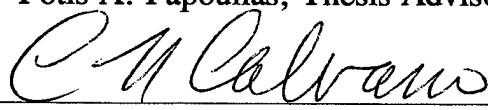

Charles N. Calvano, Second Reader

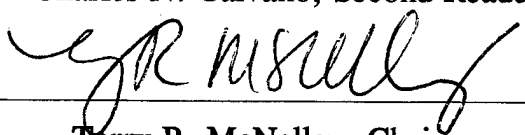

Terry R. McNelley, Chairman
Department of Mechanical Engineering

ABSTRACT

A study of the effects of speed, heading and sea state on the maximum longitudinal bending stress of the SLICE Advanced Technology Demonstrator is presented. Strip Theory is applied to a model of the SLICE hull. The hull is modeled using data from a current design and with ship loading weight information for ferry operations. Stress results are based on conventional beam theory applied to the hull girder. Bending moment distributions are presented for random, fully-developed, uni-directional seas. The maximum expected bending stress is calculated for varying sea states, ship speeds, and wave directions. Operability of the SLICE based on limiting material stress is evaluated for sea states through sea state 6. The results of this study indicate that increased stiffening of the hull could be considered in the vicinity just aft of the forward pods.

TABLE OF CONTENTS

I. INTRODUCTION

A. SMALL WATERPLANE TWIN HULL CONCEPT

The Small Waterplane Twin Hull (SWATH) structure has several advantages over that of the conventional monohull. Some of the improved operating conditions are: improved seakeeping in high seas, reduced deck wetness, reduced slamming in waves and better crew effectiveness and safety due to a more stable work environment (Gupta, 1986). Most of these improvements result from reduced dynamic response of the hull to waves. Much of a ship's dynamic response to waves is directly related to the waterplane area of the hull. For the most part, a reduction in dynamic response will follow a reduction in the waterplane area of the hull (Muckle, 1989). A newer adaptation of this concept is the SLICE Advanced Technology Demonstrator (ATD). The 170 ton SLICE design, by Lockheed Missile and Space Company, enjoys the seakeeping benefits of the SWATH but has a slightly different hull geometry. Recent studies of the SLICE hull have been done by Rodriguez (1995), Roberts (1995) and Lesh (1995). Rodriguez (1995) investigated the structural reaction to three different wave angle heading loads at sea state 5 and 8. Roberts (1995) analyzed the effect of prying forces, squeezing forces and a combination of racking forces on the forward struts and prying forces on the after struts. Lesh (1995) conducted a motion study of the SLICE to

evaluate the ship's seakeeping characteristics. The SLICE hull consists of an upper hull supported by four independent pods or struts vice two running the length of the ship. Advantages of this modification are a reduction in area that is subjected to side forces and a further reduction in water plane area. Figure (1) illustrates the basic geometry of SWATH and SLICE hulls. The overall structure and dimensions of the SLICE are shown in Figure (2) and Table (1).

B. LONGITUDINAL BENDING OF THE SLICE HULL

With the use of a fore and aft strut (on each side of the hull) instead of a long strut, the response of the hull to bending moments is significantly different. With the SLICE, static and dynamic loads are transmitted via the four struts to a hull of considerably reduced cross section near midships compared to the traditional SWATH. The focus of this study is to better understand the factors that affect bending moment imparted on the hull due to the wave loads via the four strut configuration. Strip Theory is applied to a model of the ship for the resolution of wave loads on the hull. A portion of the hull is identified as the limiting area of the hull and is evaluated for its ability to withstand normal bending stress induced by wave loads. Based on a limiting stress for the hull material the operability of the SLICE is evaluated for speeds of 10 to 30 kts in sea states up to and including sea state 6.

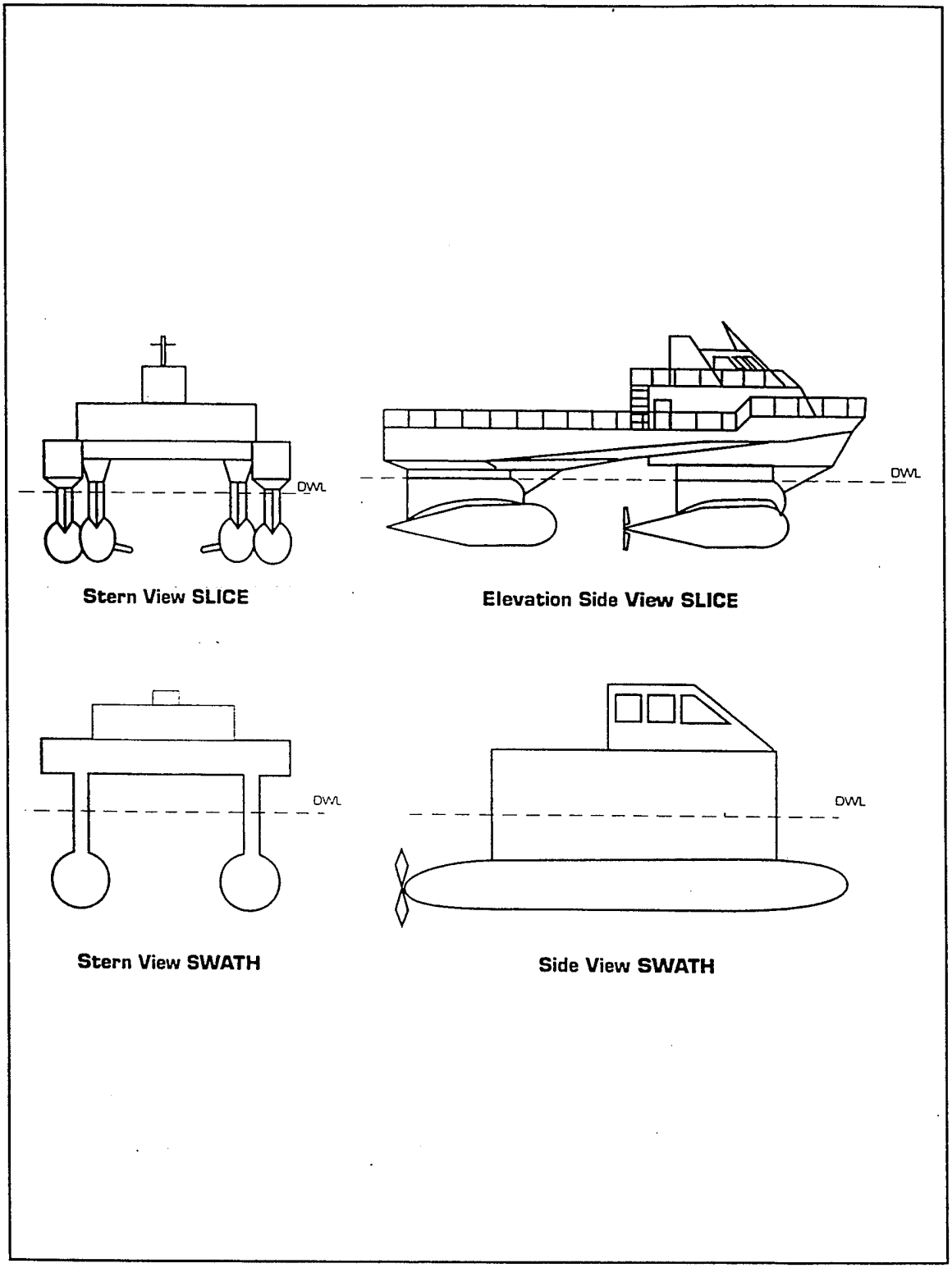

Figure 1. Comparison of SLICE and SWATH Hull Geometry, After LMSC, 1994.

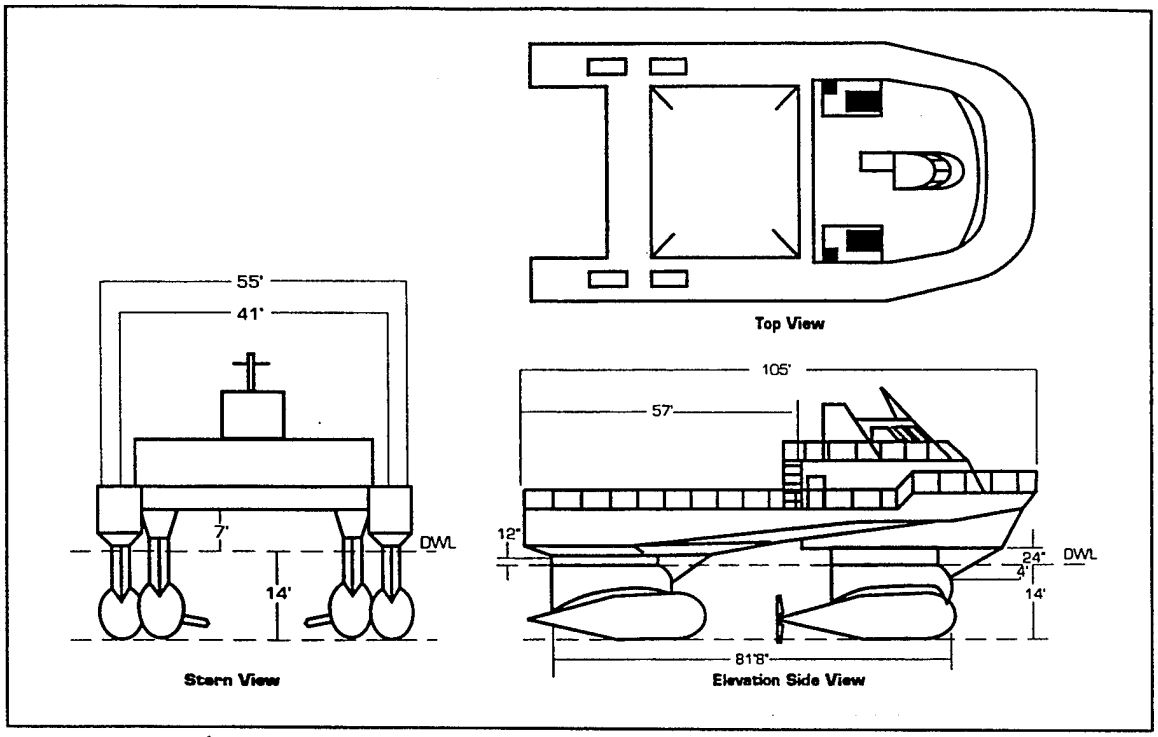

Figure 2 The SLICE (ATD), From LMSC, 1994.

Length Overall	105' - 0"
Length Between Perpendiculars	81' - 8"
Length of Forward Lower Hull	33' - 9"
Length of Aft Lower Hull	36' - 0"
Length of Struts	24' - 0"
Breadth overall	55' - 0"
Diameter (max.) Lower Hull	8' - 0"
Depth Molded to Main Deck	25' - 0"
Depth Molded to Design Water Line	14' - 0"
Length on Design Water Line	89' - 1 1/2"
Forward Hull Offset From Centerline	16' - 6"
Aft Hull Offset From Centerline	23' - 6"

Table (1). SLICE Principal Dimensions, From Lesh, 1995.

II. MODELING

A. OBJECTIVE OF THE STUDY

This study focuses on the relationship between hull bending moments and sea state, relative heading and ship speed. The operability of the SLICE is evaluated based on headings and sea states that do not result in exceeding an acceptable limit and is reported for speeds between 10 and 30 kts. The SLICE hull is modeled using Strip Theory with the use of the computer code SHIPMO.BM (Beck, 1989). Weight curve data that is representative of ferrying operations is used to model an anticipated application for the 170 ton hull. The model is subjected to sea states 2 through 6 at speed between 10 and 30 kts and relative wave headings from following to head seas. The longitudinal stress is evaluated at a portion of the hull that consistently experiences high bending moments and has the lowest section modulus.

B. THE SHIPMO PROGRAM

The FORTRAN 77 code SHIPMO is used in this study to model the SLICE hull. It is based on the Strip Theory of Salvenson, Tuck and Faltinsen (Salvenson, 1970) and is written by Beck and Troech (Beck, 1989). Strip theory is a method for solving three dimensional hydrodynamic problems. The first portion of the solution involves the solution of a

two dimensional problem at each station. These solutions are then integrated along the length of the hull, producing the three dimensional solution. The primary code SHIPMO.BM controls the numerical modeling procedure with the use of several self contained subroutines. All portions of the program are well documented, allowing the user to follow the operational procedure of the code. The program predicts motion in six directions, two shear distributions and three bending moment distributions. The compressive shear stress distribution along the length of the hull is not determined because of a lack of faith in the accuracy of the calculation.

The calculation of motions, shear stress and bending moment are based on sea state and on the following ship characteristics: hull geometry, weight curve data, fluid dynamic properties, heading and speed. These characteristics are read into the program with the use of an input file SHIPMO.IN. A sample input file is located in Appendix A. The information that is provided in the file contains the hull's dimensions, damping coefficients, weight curve distribution speed and heading and the type of wave spectra used to approximate the sea state. A thorough description of the input data is available in Appendix A of Beck (1989). The geometry of the hull is described using twenty stations along the hull (see Figure (3)). Uniform

spacing was not used due to the unique shape of the hull. The locations of the twenty stations were selected so as to better describe the unique details of the hull shape. The weight curve information is based on the SLICE employed in ferry applications and is from Roberts (1995). The SLICE weight curve used in this study is shown in Figure (4) from Lesh (1995).

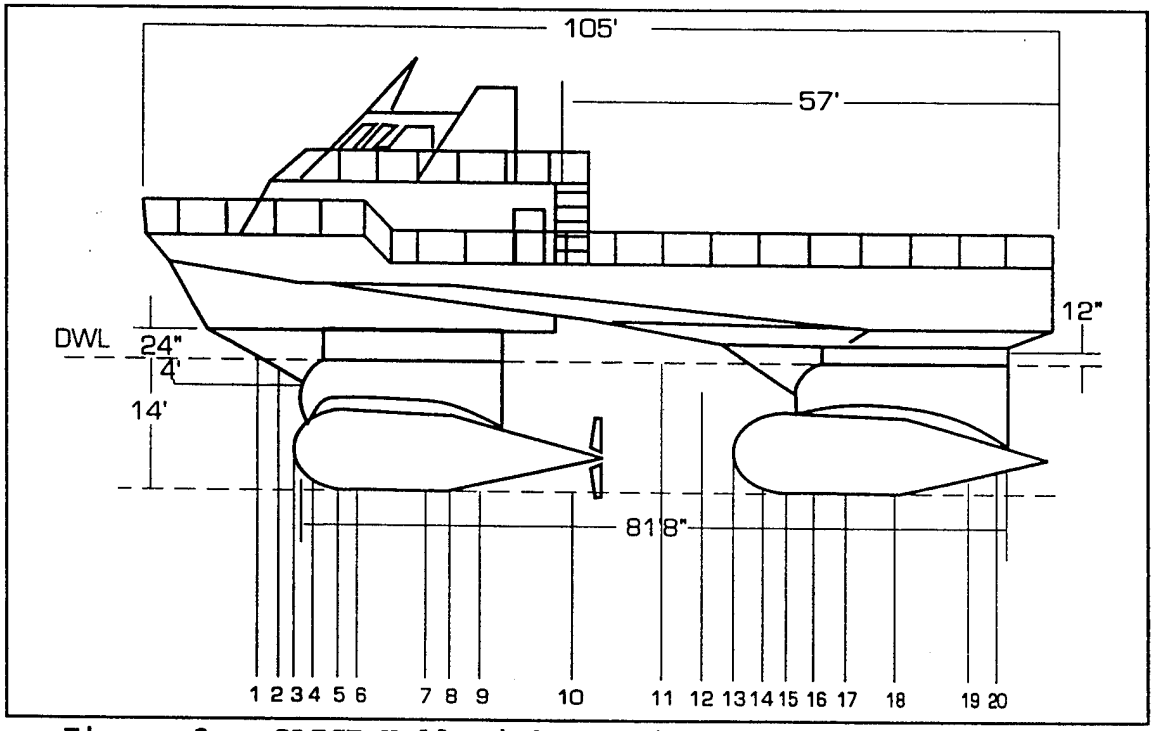

Figure 3. SLICE Hull with Stations, After LMSC, 1994.

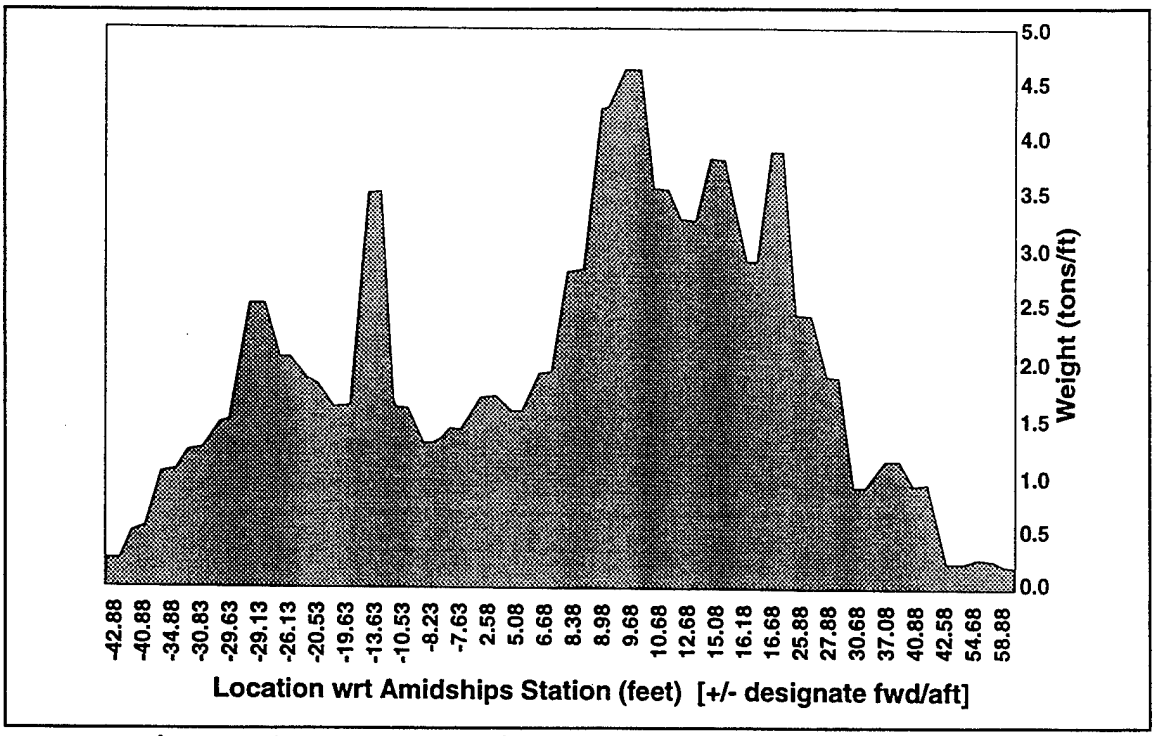

Figure 4. SLICE Weight Curve, From Lesh, 1995.

C. CALM WATER BENDING MOMENTS

The primary hydrostatic forces on a ship hull at rest are due to the combination of the upward vertical buoyancy forces and the downward vertical gravitational forces. When the hull of a ship is modeled as a beam, referred to as a hull girder, it can be treated as a beam with distributed loads. The weight per unit length load is simply the ship's mass as a function of position along the hull multiplied by the gravitational acceleration. The buoyancy per unit length load is the submerged cross-sectional area multiplied by the specific weight of the displaced fluid (Muckle, 1987). The static bending moment about the transverse axis

or in the vertical plane are referred to as the calm water bending moment (CWBM) in the SHIPMO program. The CWBM is determined by a double numerical integration of the difference between weight per unit length and the buoyancy per unit length along the length of the hull (Beck, 1989). A plot of the calm water bending moment is located in Figure (1) of Appendix B.

$$CWBM=\int\int (mg-\varrho ga)\,dx \qquad (1)$$

where mg = weight per unit length of the ship

ϱ = density of displaced water

g = acceleration of gravity

a = cross sectional area of hull

D. DYNAMIC FORCES ON SHIP HULL

A ship at sea has six degrees of freedom in rigid body motion: heaving, pitching, rolling, surging, swaying and yawing, see Figure (5). When a ship interacts with sea waves, the primary types of forces that cause these motions are: inertial, hydrostatic, exciting and radiation forces.

$$Force_{Total}=(Inertial-Hydrostatic-Exciting-Radiaton)\,forces \qquad (2)$$

When a ship moves in one or more degrees of freedom the change in inertia or acceleration results in forces on the ship hull. Static or hydrostatic forces, although by name

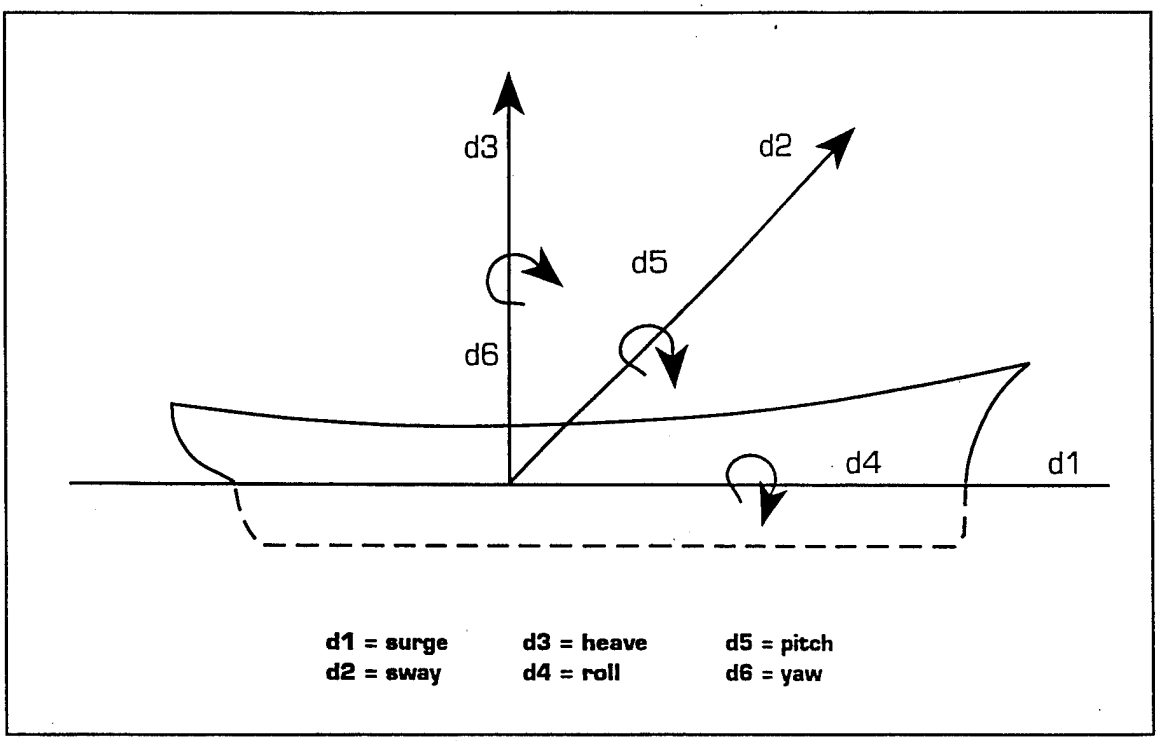

Figure 5. Six Degrees of Freedom in Rigid Body Motion, Lewis, 1989.

are expected to be unchanging, change as the ship and waves move. As more or less of the hull is submerged the distribution of buoyancy forces changes producing hydrostatic loading patterns on the hull. Exciting forces result from pressure that exists in the wave system and wave formation by the hull. The first portion of the exciting force is known as the Froude-Krylov exciting force. The Froude-Krylov exciting force is determined by integrating, over the submerged surface of the hull, the pressure that would exist if the ship was not affecting the wave system. The second component of the exciting force is due to diffraction of the waves by the hull and is known as the

diffraction exciting force. Radiation forces result from the water's resistance to the ship's oscillatory motion. As the ship oscillates vertically, waves are radiated into the fluid, the resulting force on the hull is referred to as the radiation force (Lewis, 1989).

E. PIERSON - MOSKOWITZ SPECTRUM

The spectral energy density is a convenient way of representing random, fully-developed, unidirectional sea waves. A useful approximation of this spectral energy density is the Pierson - Moskowitz (P-M) spectrum as defined by

$$S(\omega) = \alpha \frac{g^2}{\omega^5} \exp[-\beta[\frac{g}{h\omega^2}]^2] \qquad (3)$$

where $\alpha = 8.1 \times 10^{3}$

$\beta = 0.032$

h = significant wave height, defined as the average of one-third of the highest values.

g = acceleration of gravity

Using input data the SHIPMO program generates a P-M spectrum based on wave height that is consistent with the sea state of interest and a frequency range that sufficiently bounds the spectrum. Table (2) list sea states and wave heights used in this study (Lewis, 1989). Hull bending moments predicted with these wave spectra and various heading and

speed combinations are displayed in Figures (2) through (76) in Appendix B.

Sea State	Wave Height (ft)
2	0.95
3	2.85
4	6.15
5	10.65
6	16.40

Table 2. Sea States and Wave Height, From Lewis, 1989.

When the sea waves are modeled statistically, a variety of parameters can be evaluated: mean, variance, mean amplitude, significant amplitude and average of the upper tenth highest amplitude. Since the stresses due to larger waves are of more importance, the significant wave height is a useful parameter as representative wave height for a particular sea state. Bending moments associated with the significant values are used as representative bending moments for a particular sea state. The significant wave height is defined as

$$H_{1/3} = \frac{2\int Ap(\zeta)\,d\zeta}{\int p(\zeta)\,d\zeta} \qquad \textbf{(4)}$$

where A = amplitude or 1/2 the wave height

$p(\zeta)$ = normalized probability distribution function

ζ = normalized wave amplitude.

The significant wave height be can numerically determined as

$$\overline{\eta_{1/3}} = 2.0\sigma \tag{5}$$

twice the root mean square of the spectrum.

The Significant wave height is a good estimate (which would err on the high side) for the most likely wave to be encountered, but a better estimate can be determined by considering the most probable extreme amplitude. Out of N waves the most probable extreme value is

$$A = [2m_o \ln(N)]^{1/2} \tag{6}$$

where m_o = total energy of the spectrum

N = number of statistically independent waves.

The Design Extreme value is defined as the wave amplitude that will be exceeded in N encounters by only one percent.

$$1 - P^N = 1 - [1 - \exp(-\frac{\zeta^2}{2})]^N \tag{7}$$

$$P = e^{(1/N)\ln(0.99)} \cong - e^{-0.01/N} = 1 - \frac{0.01}{N} \tag{8}$$

$$A = (2m_0 \ln(\frac{N}{0.01}))^2 \quad \textbf{(9)}$$

This estimate of amplitude is the Design Extreme amplitude and can be made more useful by comparing it with the Significant wave height, giving the ratio

$$\frac{Design\ Extreme}{Significant} = (\frac{1}{2}\ln\frac{N}{0.01}) \quad \textbf{(10)}$$

For N = 100, the ratio has a value of 2.15.

Completely analogous expressions can be used for the bending moments. The only difference is that we need to use the bending moment spectrum, S_{BM}, instead of the wave spectrum, S. For linear systems, the two spectra are related by

$$S_{BM} = |RAO_{BM}(\omega)|^2 S(\omega) \quad \textbf{(11)}$$

where RAO_{BM} is the Response Amplitude Operator for the bending moment, defined as the bending moment for a unit amplitude regular sinusoidal wave. For the spectrum of the seaway $S(\omega)$, we use long-crested, fully-developed seas modeled by the Pierson - Moskowitz spectrum defined previously (Papoulias, 1993).

F. BEAM THEORY FOR THE SHIP HULL

The longitudinally continuous structural members of the hull of a ship can be treated as a large girder or beam. This is commonly referred to as the "hull girder" (Muckle, 1989). The most significant stress imposed on this girder is due to the vertical plane bending moment resulting from the weight distribution and sea loads. The hull girder can be analyzed with simple beam theory governed by

$$\sigma = \frac{Mc}{I} \tag{12}$$

where M = bending moment

c = distance between the neutral axis and the point of interest on the beam's cross-section

I = moment of inertia for the cross-section

The longitudinal bending stress is a result of the combination of the calm water bending moment and the dynamic bending moment represented by the design extreme value. The structural members of the hull are made with 5083 - H32 Aluminum. The yield strength of the 5083 - H32 alloy is 36 kpsi (ASM, 1979). A factor of safety of 2.0 was applied to the yield strength to account for various stress concentration factors that might occur in the structure resulting in a limiting stress of 18 kpsi. The longitudinal

stress was calculated using the limiting cross section near frame 18 (the section modulus information for the hull at frame 18 is in Appendix C) and is graphically displayed in the form of operability limits in Figures 77 to 83 of Appendix B. These figures represent the acceptable sea state and heading combinations for a given speed with respect to the endurance limit of the hull material. Data for these plots are located in Appendix D.

III. RESULTS

A. OVERVIEW

In order to investigate the stress that the mid section of the SLICE hull was likely to experience, the model was subjected to a variety of sea states at different headings and speeds. After a review of preliminary data, the critical or limiting area of the hull was identified based on the magnitude of the bending moment and the section modulus. The complete bending moment data was used to evaluate the relationships between the bending moment and speed, heading and sea state. The hull cross section near frame 18 was determined to be the limiting cross section. This area is located just aft of the forward pod. This area consistently experiences some of the largest bending moments and also had the smallest section modulus. The cross sectional properties of this area derived in Appendix C. Once the limiting cross section was identified, a stress limit with a combination of speed, heading and sea state was used to evaluate the SLICE hull's operability in the sea way environment. The results reported in this study are for speeds 10 to 30 kts, sea states 2 through 6 and relative headings of the wave from following seas to head seas (0 to 180 degrees). Figure (6) shows wave angle headings.

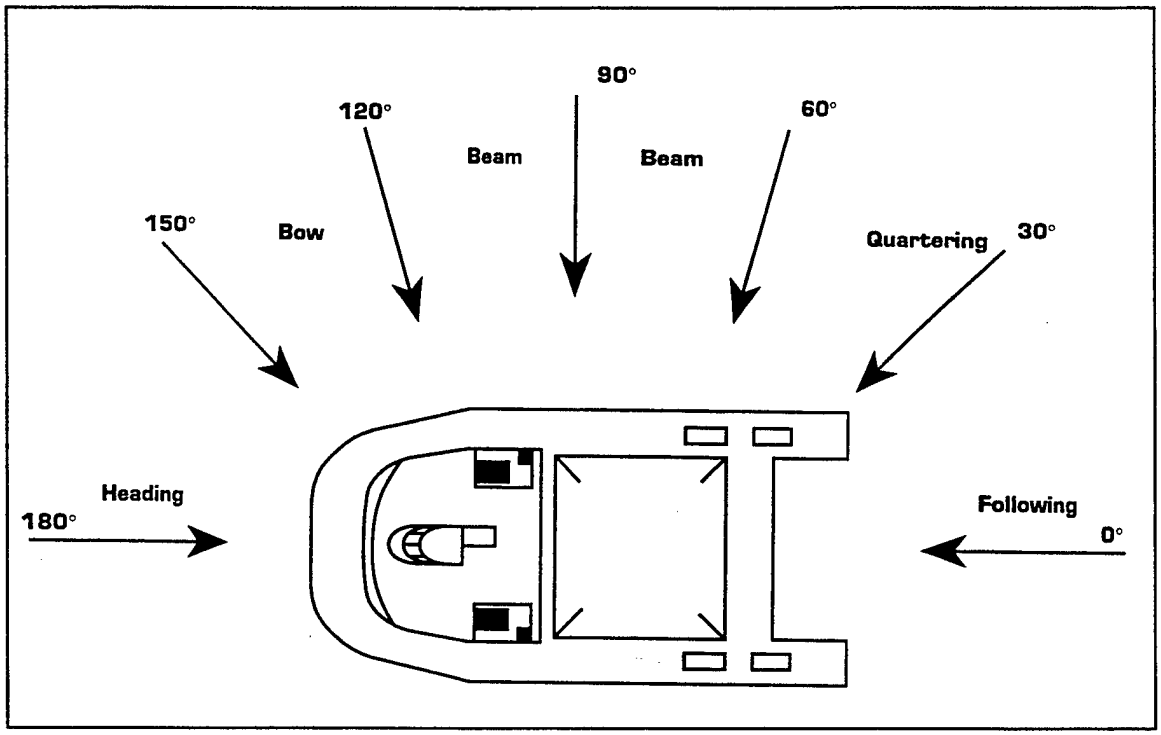

Figure 6. Wave Heading Angles, After Lewis, 1989 and LMSC, 1994.

B. BENDING MOMENT AND SEA STATE RELATIONSHIP

The bending moment experienced by the hull directly relates to the sea state of the seaway environment. For a given heading and speed the largest bending moment corresponded to the greatest sea state. This trend can be seen in Figures 2 to 26; each plot depicts a family of sea state curves for sea states 2 through 6 for each heading and speed combination. As sea state increases, the dominant wave environment characteristic that increases is wave height. The increase in bending moment is probably related to these larger waves which will result in increased force from inertial loads, wave diffraction and wave radiation.

Increased vertical plane motion that is predicted to increase with sea state is also suspected to contribute to this increased bending moment (Lesh, 1995).

C. BENDING MOMENT AND SPEED RELATIONSHIP

The bending moment experienced by the hull was not significantly affected by the speed of the ship in sea states 2 and 3. For all combinations of speed and heading there is no significant change (see Figures 27 though 36 in Appendix B). Above sea state 3, speeds of 10 and 30 knots tend to result in bending moments larger then the other speeds. At sea states 5 and 6 the combination of seas (in the range from 135 to 180 degrees), and the changes in speed result in proportionally larger changes in bending moment (see Figures 45, 46, 50 and 51 in Appendix B).

D. BENDING MOMENT AND HEADING RELATIONSHIP

The bending moment experienced by the hull is directly related to the heading of the ship. For sea states 2 and 3 relative changes in heading between the waves and the hull do not affect the bending moment on the hull. Above sea state 3, heading has a direct impact on the hull bending moment. Most notable is the tendency for head seas to produce larger bending moments than oblique seas. An unexpected prediction for following seas is noted for sea states 3 through 6. Following seas are predicted to produce bending moments that are larger than those for head sea at

the same speed and sea state. This occurs at 20 and 30 kts in sea state 3 and 4, and at 10 kts in sea state 5 and 6 (see Figures 59, 61, 64, 66, 67 and 72 in Appendix B). When the ship is in sea state 6 head and bow seas produce dominant bending moments (see Figures 72 through 76 in Appendix B). This behavior is probably due to a combination of wave height, period, ship speed and heave.

E. OPERABILITY BASED ON STRESS LIMITATIONS

A ship at sea often "rides best" with the seas at a particular relative heading. This human sensing of a comfortable ride with respect to a ship's heading and speed for a given sea state can easily be likened to the acceptable headings and speeds in sea states for stress limitations. Operability can be thought of as the ratio of acceptable heading and sea state combinations to the total possible heading and sea state combinations. Figures 77 to 82 in Appendix B are graphical displays of headings and sea states based on acceptable hull stresses at speeds 10 to 30 kts. On the operability diagrams, sea states are plotted along the radius and heading or wave angle plotted from 0 to 360 degrees. The results of this portion of the study indicate that the ship should be able to withstand seas up to sea state 6 on the beam and aft at all speeds between 10 and 30 kts. At 10 kts the limiting wave headings are 45 degrees off the port and starboard bows (135 and 225

degrees) which result in stress that limits sea state to sea state 4 and 5. Between 15 kts and 25 kts operability improves. At 15 kts the only limiting headings are 60 degrees off of the port and starboard bows with a sea state 5 limit. As speed increases to 20 kts, seas +/- 30 degrees on the bow also result in a sea state 4 and 5 limit. At 25 kts operability is limited to sea state 5 for seas on the head and at 60 degrees off of the head. As speed increases to 30 kts seas on the head and up to 15 degrees off of the limit operability to sea state 5. The operability index of the SLICE at a speed for seas up through sea state 6 is graphically represented on a sea state-heading plot as the ratio of the area inside the stress limit curve to the area of a circle with radius of sea state 6 (which would indicate complete operability at sea state 6). Figure (82) in Appendix B shows the normalized operability index of the SLICE based of stress limitations for speeds of 10 to 30 kts for sea state 6. For sea states up to sea state 6 the operability is between 87 and 97.5 percent. Operability is best over the speed of range of 13 to 26 kts and then drops off slightly above and below this range. Figure (83) shows a family of speed curves for operability. Over the entire speed range for all heading and sea state combinations the operability index is nearly 80 percent. Based on these operability trends a good rule of thumb for the mariner is

to keep the heavy seas on the beam or abaft the beam when traveling at 20 kts and below. At higher speeds, the seas can be taken closer to the head.

IV. CONCLUSIONS AND RECOMMENDATIONS

A. CONCLUSIONS

This study has shown a method by which the dynamic bending moment and operability of a ship design can be evaluated based on sea state, heading and speed. Based solely on blueprint data and expected operating conditions, Strip Theory can be used to predict some important characteristics of the ship's response in the seaway environment. Based on the criteria employed in this study, the operability of the SLICE hull is shown to be limited to less than sea state 6 when seas are on the bow or head. The limiting factor was excessive stress at the hull's weakest area. The SLICE hull is predicted to experience fairly consistent dynamic bending in sea states below sea state 4 regardless of heading or speed. The dynamic bending moment developed in the SLICE hull is most significantly affected by the sea state or wave height in the seaway. In all cases, the dynamic bending moment increases as the characteristic wave height increases. As the ship increases speed the dynamic bending moment increases. For the most part there is a direct correlation between speed and dynamic bending, but at a speed as low as 10 kts in a particular sea state the dynamic bending moment can be surprisingly large. The orientation between the hull and the incident wave has

the most significant effect when the heading results in head or following seas.

The operability study and dynamic bending analysis predicts that excessive stress will occur in the hull when it is subjected to the seaway environments modeled. Since the yield strength of the material is essentially fixed, the option of designing to allow for reduced factors of safety would allow operability to be increased to 100 percent for seas up to and including seas state 6. Without design changes, the operation of the SLICE in heavy seas should be limited so as to keep the seas on the beam or better yet abaft the beam. In addition to these options, reduction in vertical plane motion may reduce the magnitude of dynamic bending moment experienced. The use of both active and passive control surfaces could be employed to reduce some of the hull's undesirable dynamic motions and there by reducing undesirable dynamic bending stresses characteristics.

B. RECOMMENDATIONS

The following is a list of recommendations for further research on the SLICE hull configuration:

Strip Theory utilizes two dimensional potential theory for the solution of a hydrodynamic problem and provides motion, shear distributions and bending moment distributions information about the hull in a sea wave environment.

Addition calculations are required to evaluate structural stress due to bending and shear. A more useful solution could be obtained through finite element modeling. Actually modeling the forces experienced by the ship as it translates and rotates in six degrees of freedom in the seaway could produce a more accurate stress picture for design and analysis.

Investigate the potential for reduction in the dynamic bending stress through the active and passive control of the hull's motion in response to the seaway. A controls study could be used to determine the relationship between the ship's motion responses, controls surface orientation and operation and resultant dynamic bending stresses. Information gained from this type of study could be employed to improve the ship's seakeeping characteristics and reduce the dynamic bending experienced by the hull.

APPENDIX A. SHIPMO.BM INPUT FILE

This sample input file of SHIPMO.IN is for running irregular wave analysis on the SLICE hull form. Appendix A of the SHIPMO.BM User's Manual provides detailed line content description and format (Beck, 1989).

```
SLICE HULL  10 - 30 kts by 5, 0 - 180 seas by 15, sig wave height 16,4 ft, SS 6
  0  64     0    2    1    0    3    0    0    0    0    0    7   20    1
105.0000    1.9905   32.1740        1.26E-05      1.6557E+02     0.0000
 33.0000  -26.0000    1.0000
  1   48.6000    0.0000    0
 16.5000    0.0000
  5   44.8750    0.0000    0
 16.0000    0.0000
 16.2500   -0.9000
 16.5000   -1.8000
 16.7500   -0.9000
 17.0000    0.0000
  8   40.8750    0.0000    0
 15.5000    0.0000
 15.8000   -2.0000
 16.1000   -4.0000
 16.1000  -10.0000
 16.9000  -10.0000
 16.9000   -4.0000
 17.2000   -2.0000
 17.5000    0.0000
 15   39.8750    0.0000    0
 15.4000    0.0000
 15.6000   -1.5000
 15.5500   -7.3100
 14.6250   -8.9200
 14.5000  -10.0000
 14.6250  -11.1000
 15.0850  -11.4100
 16.5000  -12.0000
 17.9000  -11.4100
 18.3750  -11.1000
 18.5000  -10.0000
 18.3750   -8.9200
 17.4500   -7.3100
 17.4000   -1.5000
 17.6000    0.0000
 11   37.8750    0.0000    0
 15.0000    0.0000
 15.0000   -5.7500
 13.5800   -8.3125
 13.3000  -10.0000
 14.7000  -11.7900
 16.5000  -13.2000
 18.2900  -11.7900
 19.7000  -10.0000
 19.4200   -8.3125
 18.0000   -5.7500
 18.0000    0.0000
```

```
15   33.8750    0.0000    0
14.8750    0.0000
14.8750   -4.8000
14.8500   -4.9100
13.0400   -8.0000
12.5000  -10.0000
13.0400  -12.0000
14.5000  -13.4600
16.5000  -14.0000
18.5000  -13.4600
20.0000  -12.0000
20.5000  -10.0000
20.0000   -8.0000
18.1500   -4.9100
18.1250   -4.8000
18.1250    0.0000
13   23.8750    0.0000    0
15.2000    0.0000
15.2000   -6.9200
13.0400   -8.0000
12.5000  -10.0000
13.0400  -12.0000
14.5000  -13.4600
16.5000  -14.0000
18.5000  -13.4600
20.0000  -12.0000
20.5000  -10.0000
20.0000   -8.0000
17.8000   -6.9200
17.8000    0.0000
13   19.8750    0.0000    0
15.8750    0.0000
15.9100   -6.1200
15.6640   -6.5500
13.0380  -10.0000
13.5000  -11.7300
14.7700  -13.0000
16.5000  -13.4600
18.2300  -13.0000
19.5000  -11.7300
20.0000  -10.0000
17.3400   -6.5500
17.1000   -6.1200
17.1250    0.0000
15   16.8750    0.0000    0
16.4000    0.0000
16.4000   -7.2500
15.0600   -7.5100
14.0100   -8.5600
13.6200  -10.0000
14.0100  -11.4400
15.0600  -12.4900
16.5000  -12.8800
18.0000  -12.4900
19.1000  -11.4400
19.3800  -10.0000
19.1000   -8.5600
18.0000   -7.5100
16.6000   -7.2500
16.6000    0.0000
```

```
13    7.1250    0.0000    1
16.5000   -9.2800
16.1400   -9.3800
15.8800   -9.6400
15.7800  -10.0000
15.8800  -10.3600
16.1400  -10.6200
16.5000  -10.7200
16.8600  -10.6200
17.1200  -10.3600
17.2200  -10.0000
17.1200   -9.6400
16.8600   -9.3800
16.5000   -9.2800
 1    0.0000    0.0000    1
23.5000    0.0000
 1  -10.1250    0.0000    1
23.5000  -10.0000
13  -11.3000    0.0000    1
23.5000   -7.8000
22.4000   -8.0900
21.5900   -8.9000
21.3000  -10.0000
21.5900  -11.1000
22.4000  -11.9100
23.5000  -12.2000
24.6000  -11.9100
25.4000  -11.1000
25.7000  -10.0000
25.4000   -8.9000
24.6000   -8.0900
23.5000   -7.8000
13  -13.3500    0.0000    1
23.5000   -7.1000
22.1000   -7.4800
21.0800   -8.5500
20.6000  -10.0000
21.1800  -11.4500
22.1500  -12.5200
23.5000  -12.9000
25.0000  -12.5200
26.0000  -11.4500
26.4000  -10.0000
26.0000   -8.5500
25.0000   -7.4800
23.5000   -7.1000
15  -16.7900    0.0000    0
22.4000    0.0000
23.4000   -6.0000
21.5000   -6.5400
20.0000   -8.0000
19.5000  -10.0000
20.0000  -12.0000
21.5000  -13.4600
23.5000  -14.0000
25.5000  -13.4600
27.0000  -12.0000
27.5000  -10.0000
27.0000   -8.0000
25.5000   -6.5400
23.6000   -6.0000
24.6000    0.0000
```

58.8800	0.2210	7.2289	16.5000
54.6800	0.2210	7.2289	16.5000
54.6800	0.2710	8.2937	16.5000
42.5800	0.2710	8.2937	16.5060
42.5800	0.2210	7.2289	16.5060
40.8800	0.2210	7.2289	16.5101
40.8800	0.9063	5.7590	16.5101
37.0800	0.9063	5.7590	16.6123
37.0800	1.1196	2.8272	16.6123
30.6800	1.1196	2.8272	16.6479
30.6800	0.9063	5.7590	16.6479
27.8800	0.9063	5.7590	16.6479
27.8800	1.8746	-1.8491	16.6479
25.8800	1.8746	-1.8491	16.6504
25.8800	2.4336	0.2640	16.6504
16.6800	2.4336	0.2640	16.6166
16.6800	3.8786	1.3690	16.6166
16.1800	3.8786	1.3690	16.6061
16.1800	2.9103	4.8089	16.6061
15.0800	2.9103	4.8089	16.5913
15.0800	3.8303	1.2664	16.5913
12.6800	3.8303	1.2664	16.5591
12.6800	3.2713	0.2268	16.5591
10.6800	3.2713	0.2268	16.5371
10.6800	3.5580	0.7831	16.5371
9.6800	3.5580	0.7831	16.5285
9.6800	4.6180	4.7786	16.5285
8.9800	4.6180	4.7786	16.5220
8.9800	4.2741	5.7263	16.5220
8.3800	4.2741	5.7263	16.5170
8.3800	2.8291	7.0013	16.5170
6.6800	2.8291	7.0013	16.5079
6.6800	1.9091	15.1654	16.5079
5.0800	1.9091	15.1654	16.5000
5.0800	1.5677	14.6222	16.5000
2.5800	1.5677	14.6222	16.5000
2.5800	1.7066	14.1646	16.5000
-7.6300	1.7066	14.1646	23.5000
-7.6300	1.4199	15.5850	23.5000
-8.2300	1.4199	15.5850	23.5000
-8.2300	1.2810	16.2290	23.5000
-10.5300	1.2810	16.2290	23.5000
-10.5300	1.6034	11.6142	23.5000
-13.6300	1.6034	11.6142	23.6038
-13.6300	3.5304	-0.2817	23.6038
-19.6300	3.5304	-0.2817	23.6046
-19.6300	1.6034	11.6142	23.6046
-20.5300	1.6034	11.6142	23.6046
-20.5300	1.8334	9.2979	23.6046
-26.1300	1.8334	9.2979	23.5921
-26.1300	2.0534	7.1596	23.5921
-29.1300	2.0534	7.1596	23.5765
-29.1300	2.5276	7.0734	23.5765
-29.6300	2.5276	7.0734	23.5720
-29.6300	1.4676	-0.9558	23.5720
-30.8300	1.4676	-0.9558	23.5658
-30.8300	1.2376	0.1396	23.5658
-34.8800	1.2376	0.1396	23.5352
-34.8800	1.0176	2.4744	23.5352
-40.8800	1.0176	2.4744	23.5087
-40.8800	0.5434	-1.2131	23.5087
-42.8800	0.5434	-1.2131	23.5063
-42.8800	0.2210	7.2289	23.5063
-46.1250	0.2210	7.2289	23.5000

```
0.0000  246.9000 5924.8000 -296.2000  740.6000  987.5000  987.5000
0  7.1200   16.5000  -10.0000
1.0000     .20000     8.000     0.2000    16.89    50.6700     8.44500
0.1000
0.0000  180.0000   15.0000
16.400
```

APPENDIX B. DYNAMIC BENDING MOMENT PLOTS

The following plots are presented as group to make comparison between that plots as easy as possible and to minimize the disruption to chapters II through IV. The first figure is the calm water bending moment. Figures 2 through 26 are plots of the dynamic bending moments arranged as families of sea states for all headings and speeds. Figures 27 through 51 are plots of the dynamic bending moments arranged as families of speeds for all headings and sea states. Figures 52 through 76 are plots of the dynamic bending moments arranged as families of headings for all speeds and sea states. Figures 77 through 81 are plots of operability at speeds of 10 to 30 kts. Figure (82) is a plot of operability over the speed range of 10 to 30 kts and Figure (83) is a plot of operability for a family of speeds.

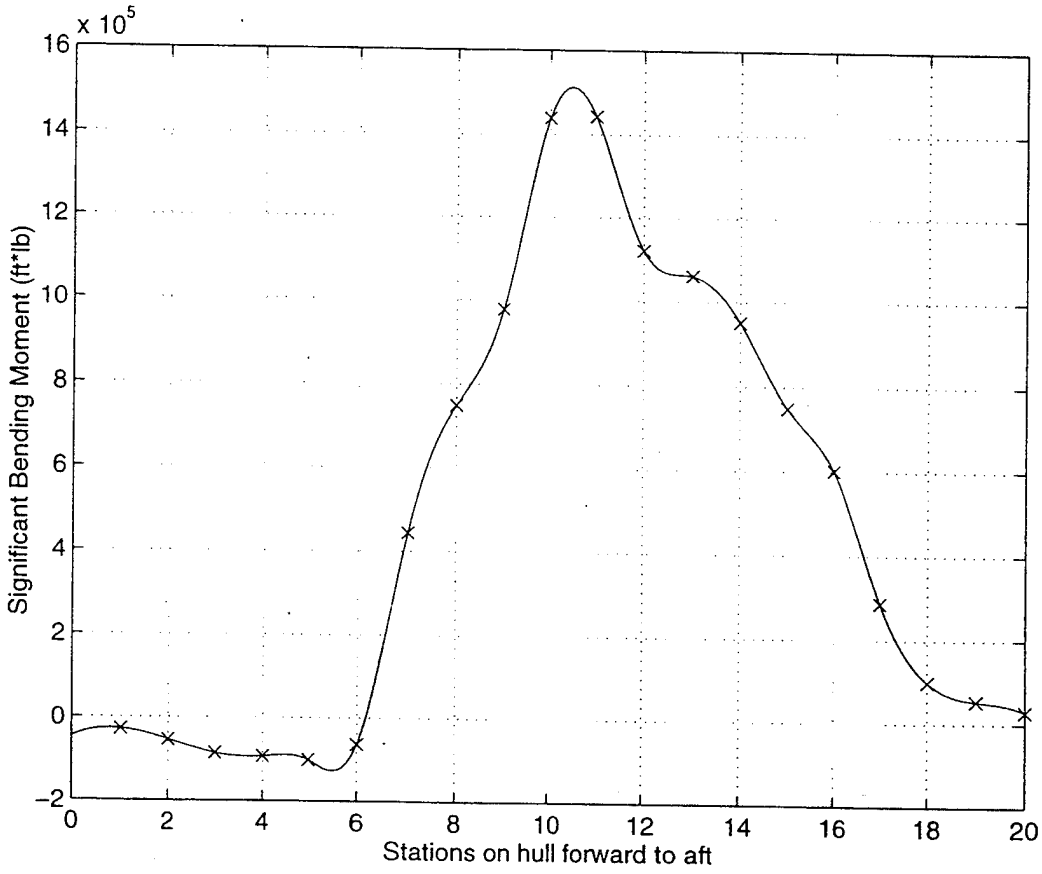

Figure (1). Calm Water Bending Moment.

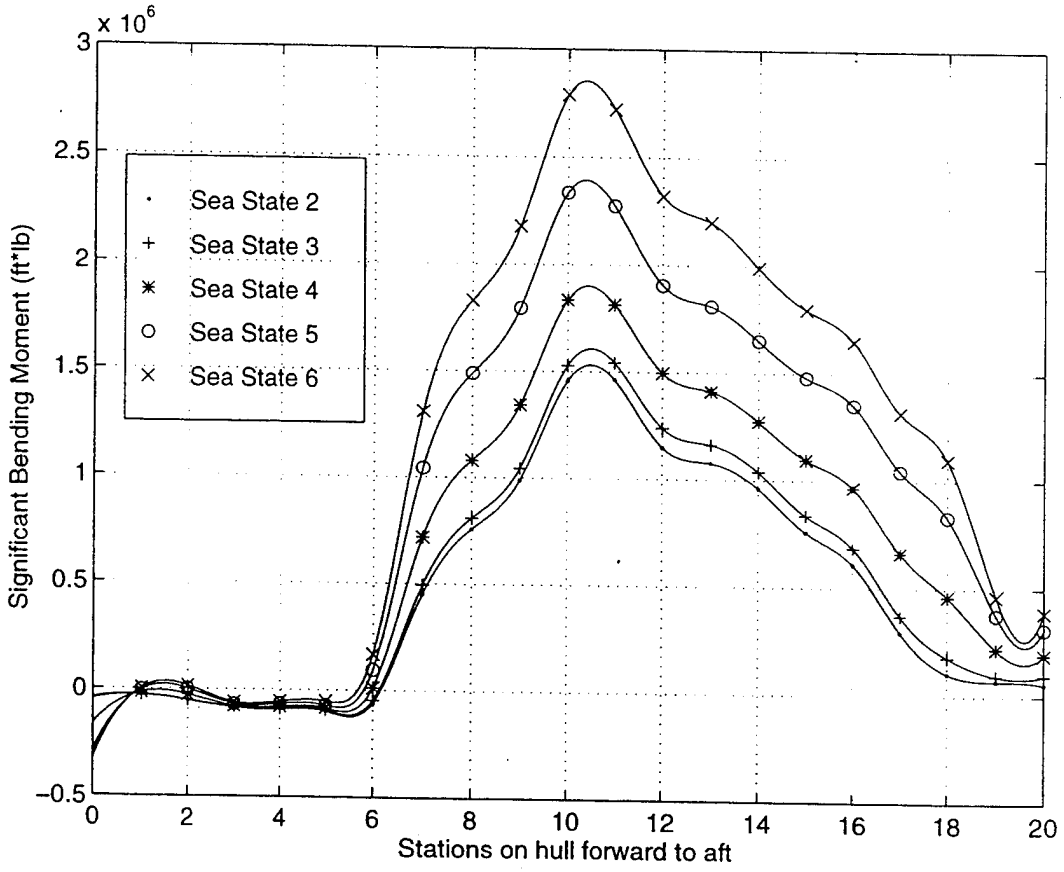

Figure (2). Dynamic Bending Moments for Following Seas and 10 Knots.

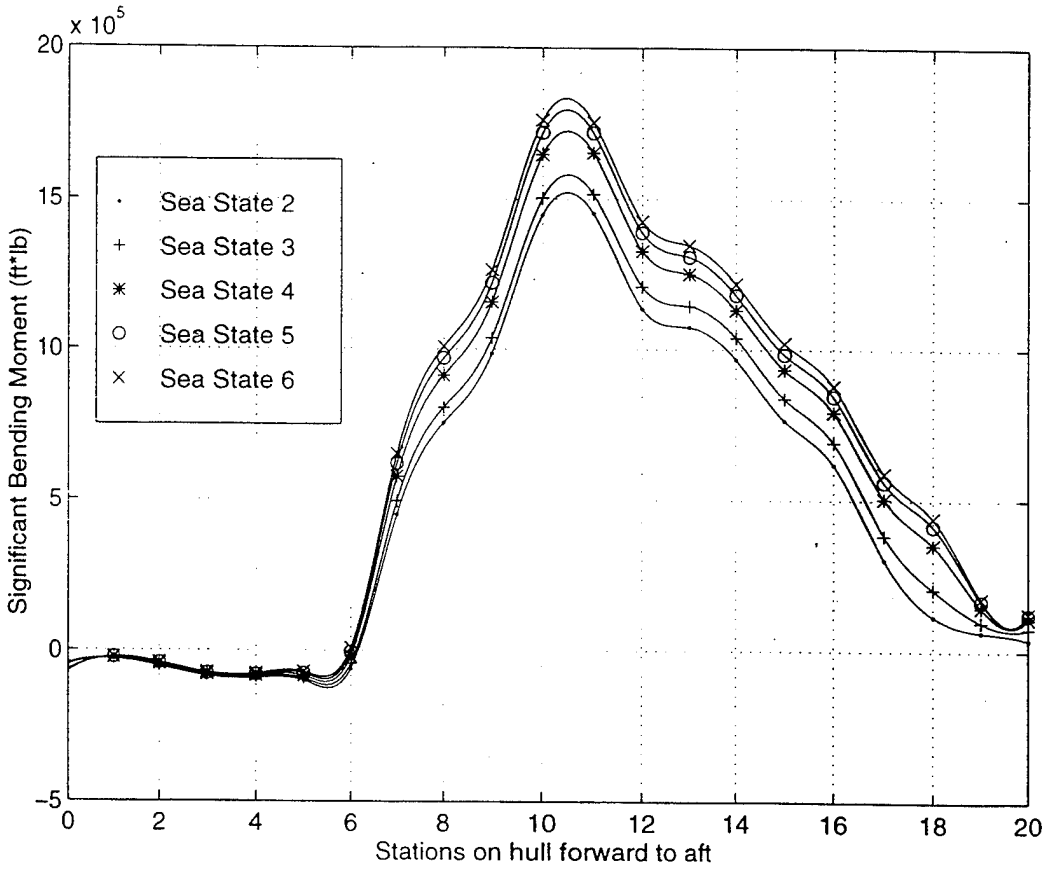

Figure (3). Dynamic Bending Moments for Following Seas and 15 Knots.

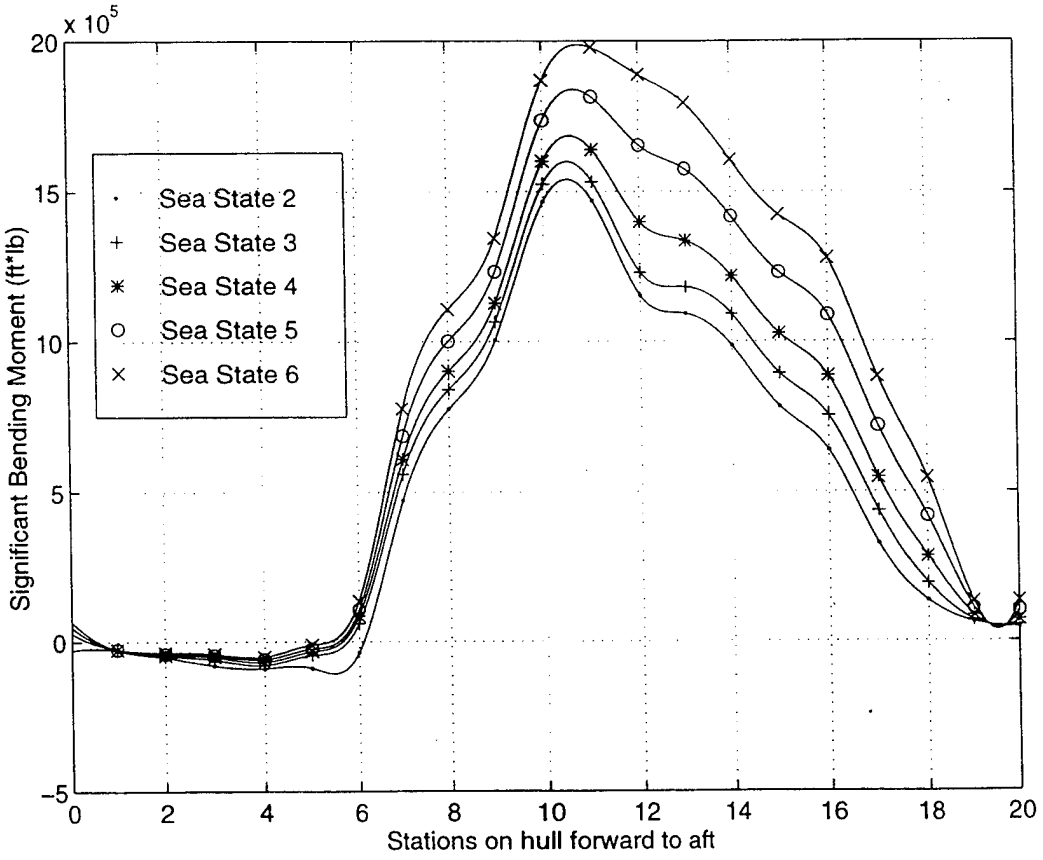

Figure (4). Dynamic Bending Moments for Following Seas and 20 Knots.

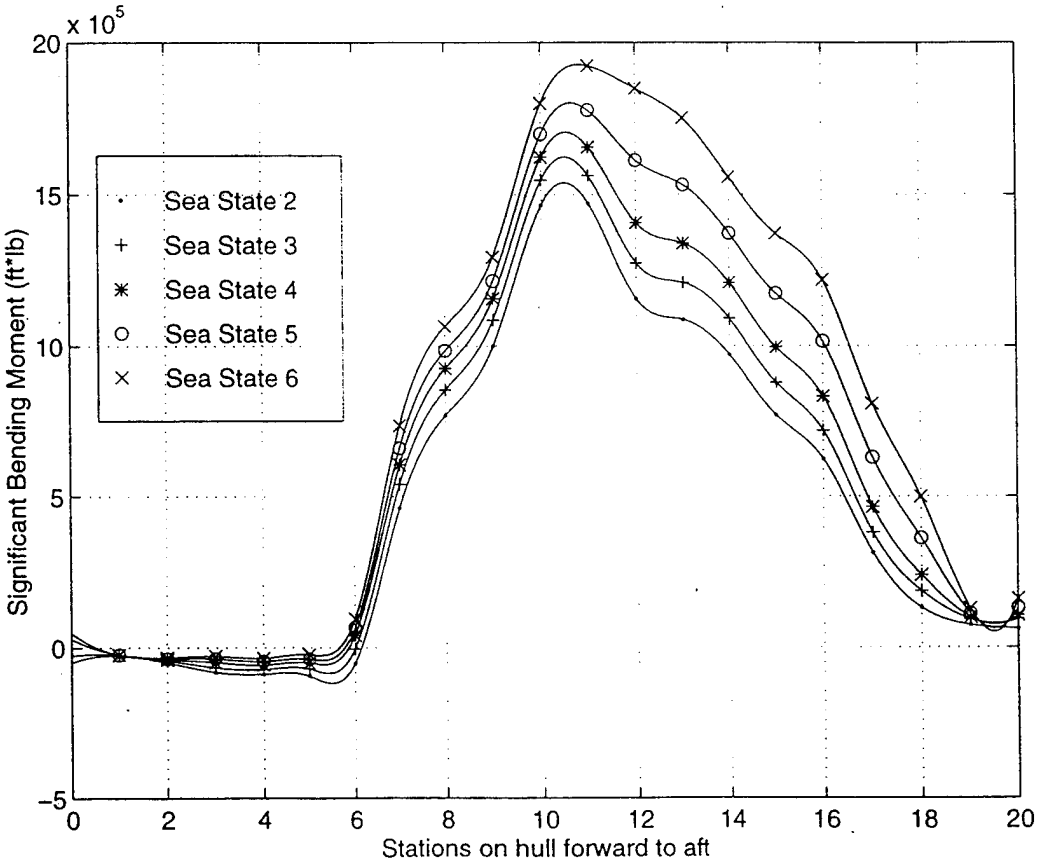

Figure (5). Dynamic Bending Moments for Following Seas and 25 Knots.

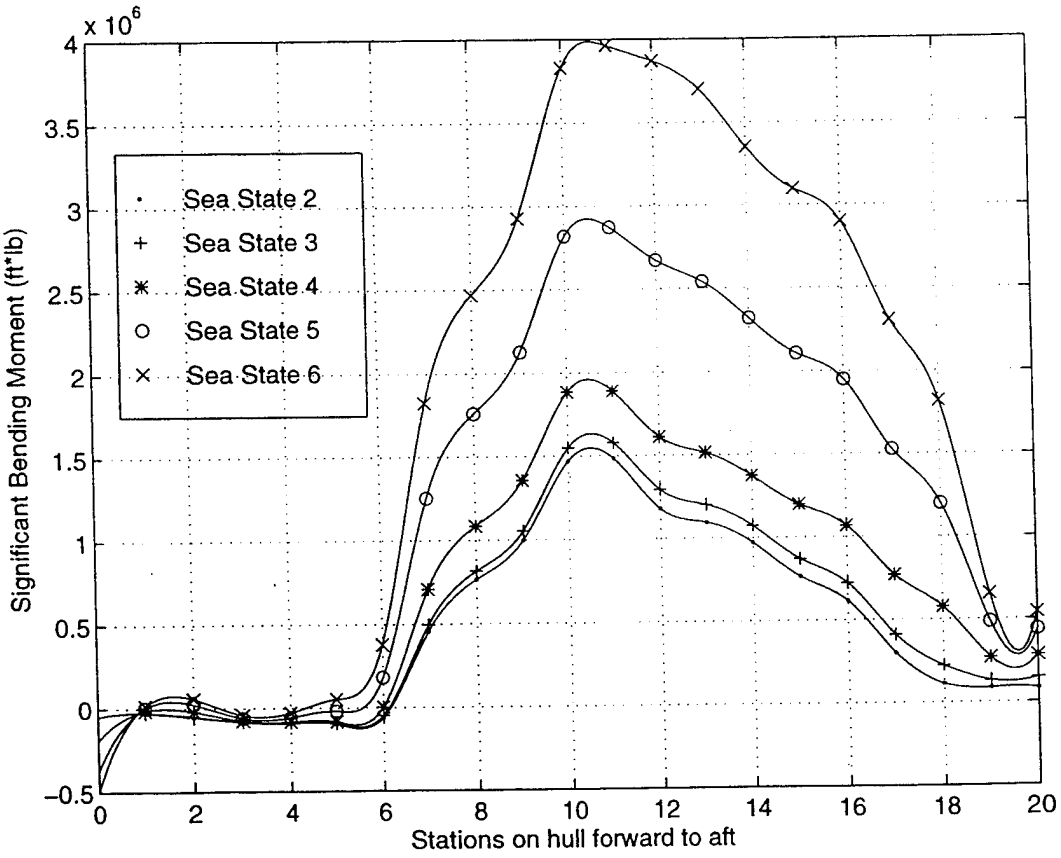

Figure (6). Dynamic Bending Moments for Following Seas and 30 Knots.

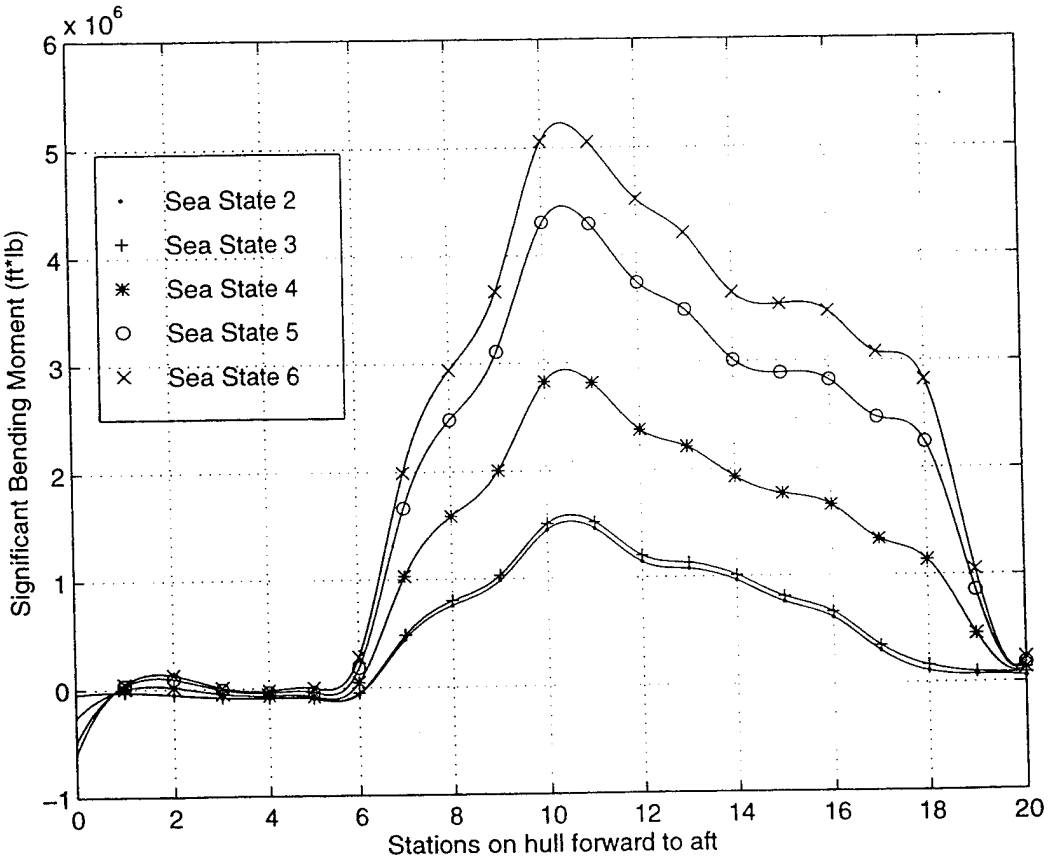

Figure (7). Dynamic Bending Moments for Quartering Seas and 10 Knots.

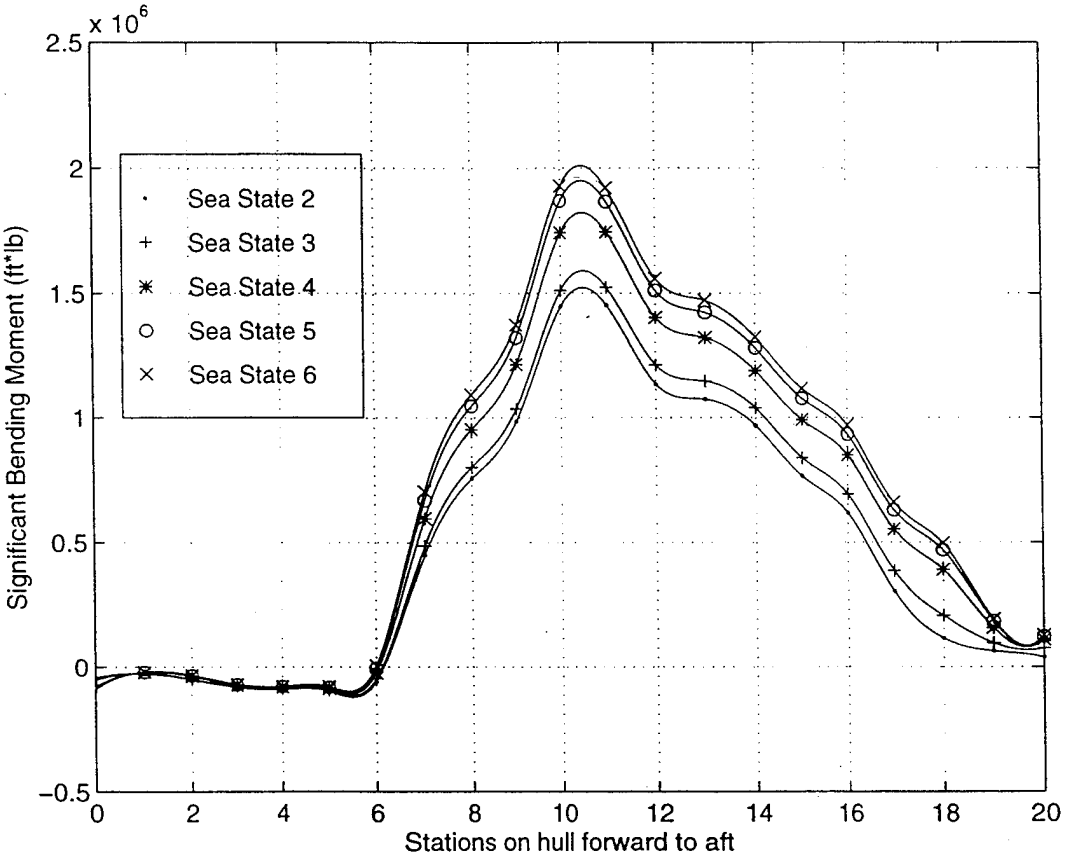

Figure (8). Dynamic Bending Moments for Quartering Seas and 15 Knots.

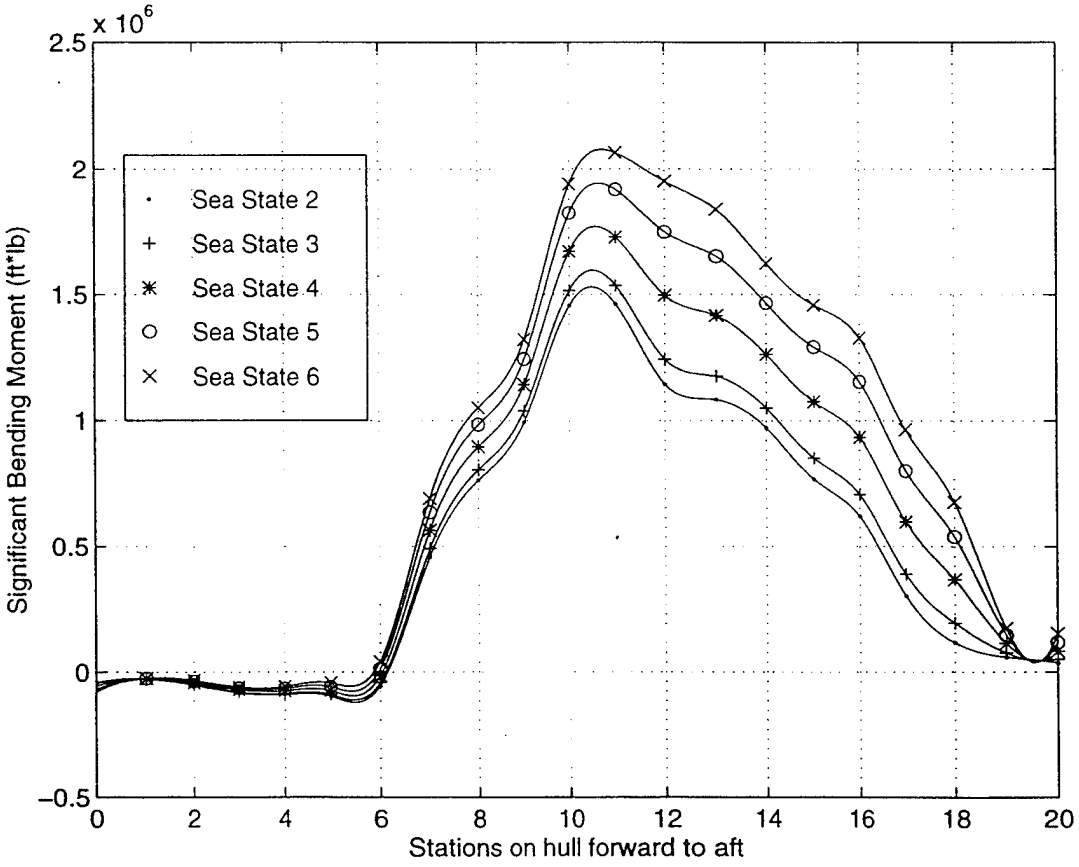

Figure (9). Dynamic Bending Moments for Quartering Seas and 20 Knots.

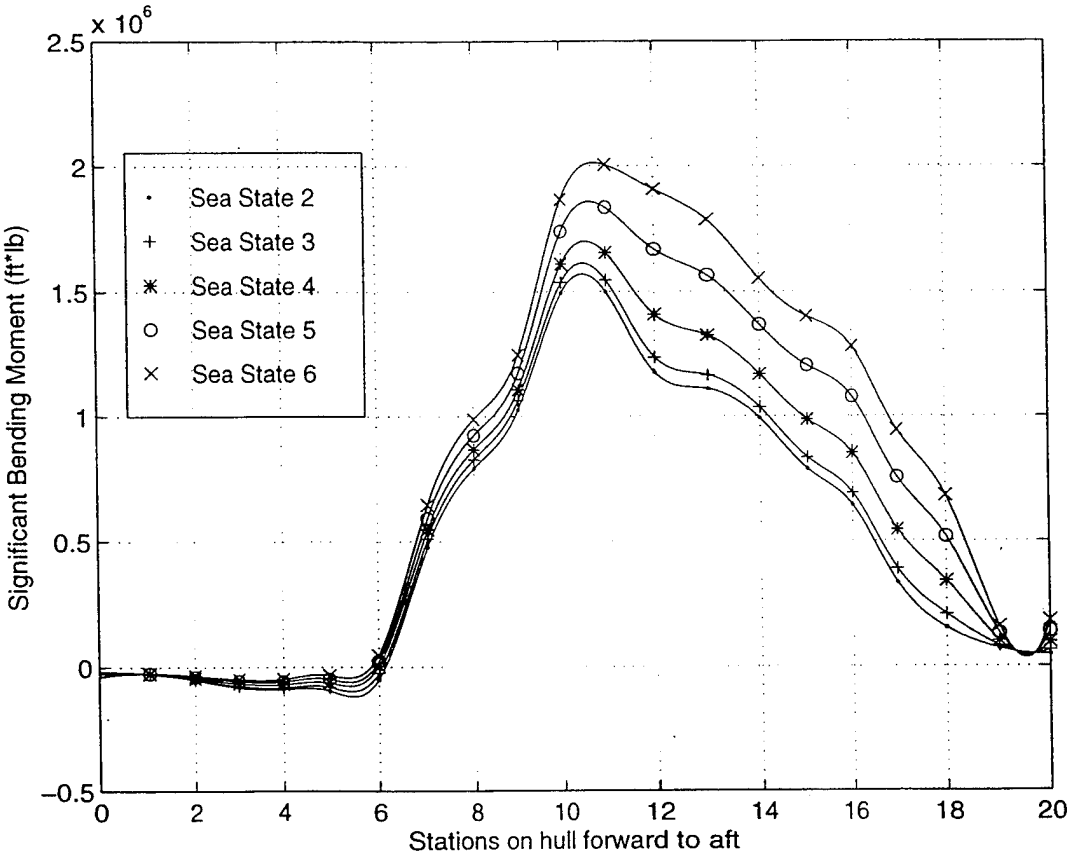

Figure (10). Dynamic Bending Moments for Quartering Seas and 25 Knots.

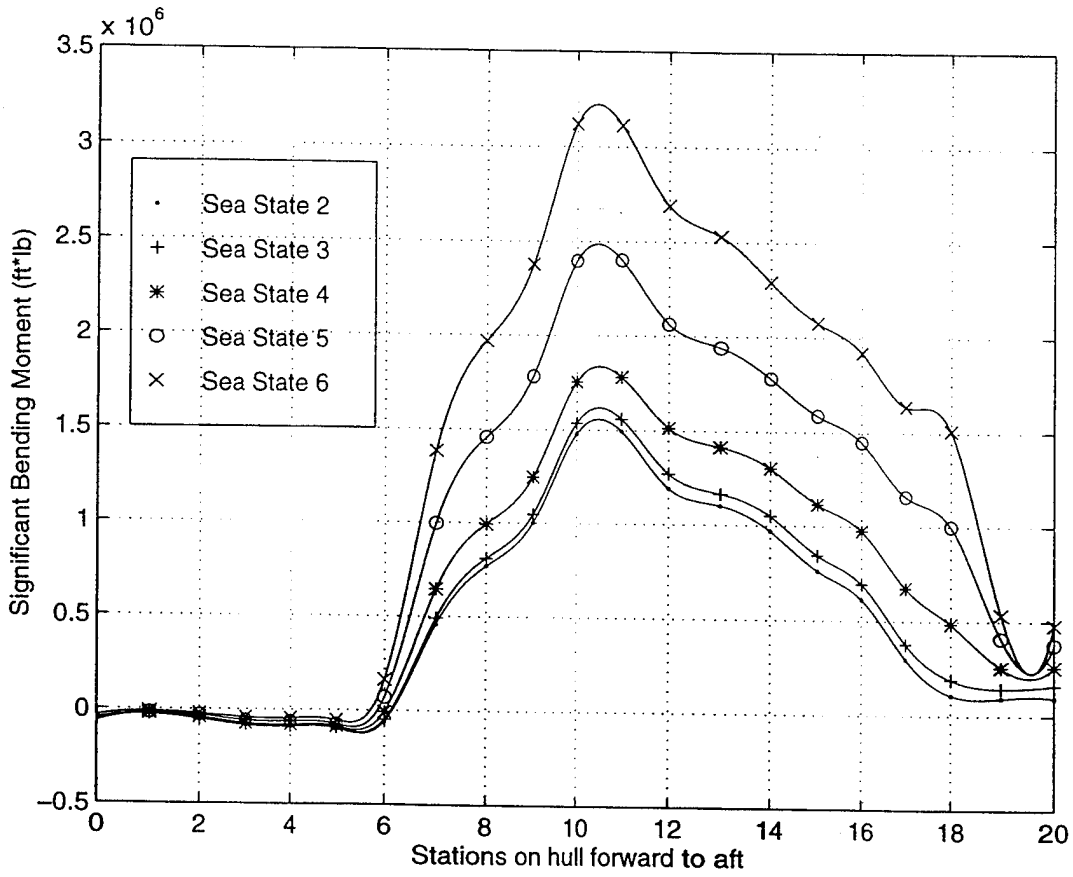

Figure (11). Dynamic Bending Moments for Quartering Seas and 30 Knots.

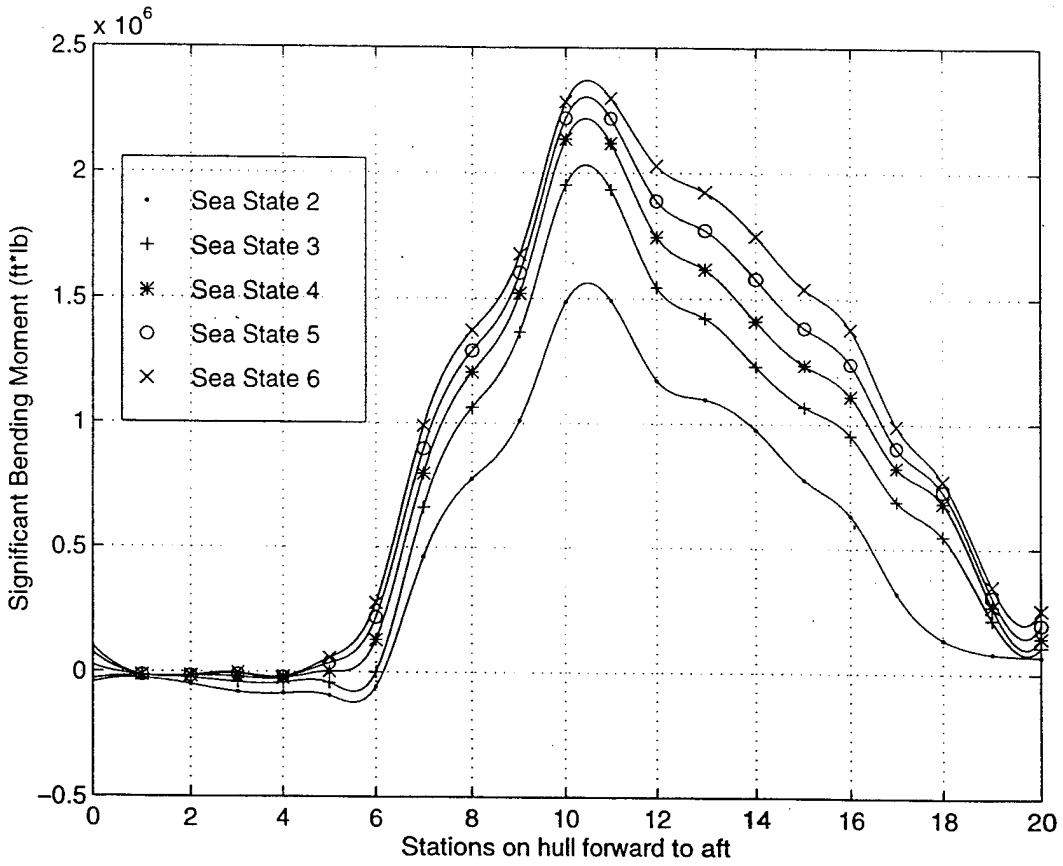

Figure (12). Dynamic Bending Moments for Beam Seas and 10 Knots.

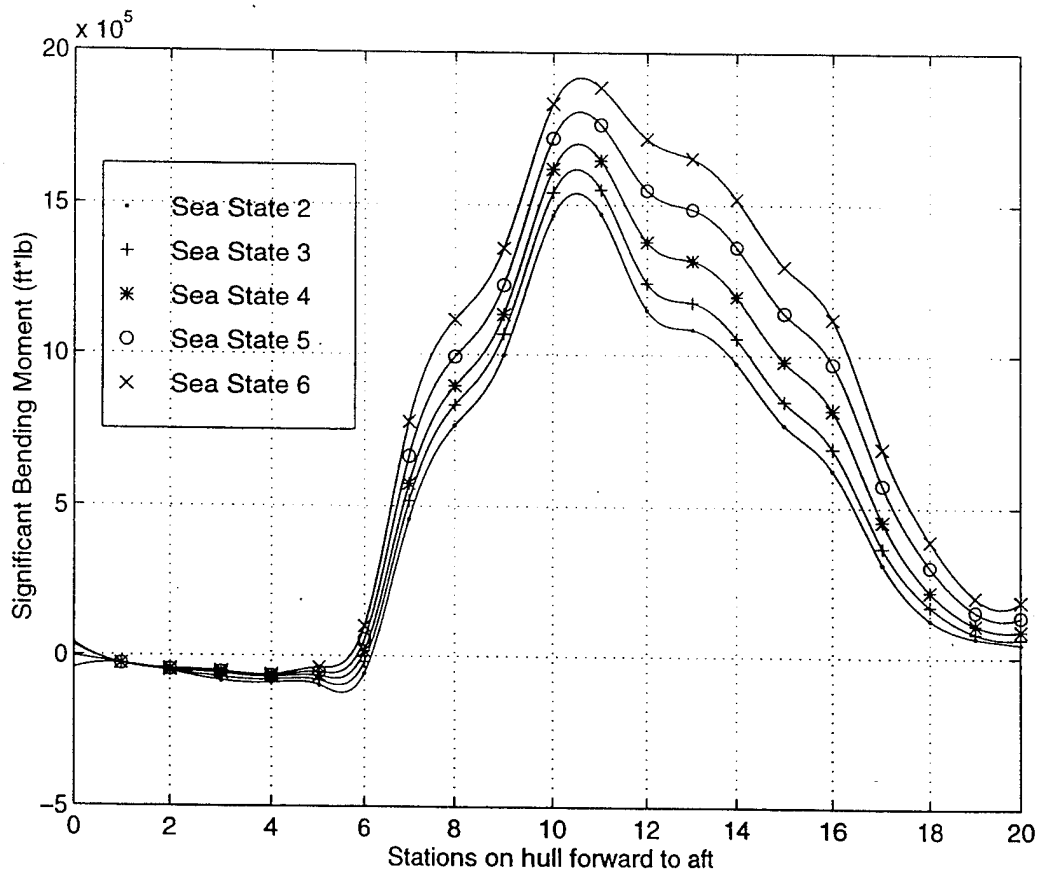

Figure (13). Dynamic Bending Moments for Beam Seas and 15 Knots.

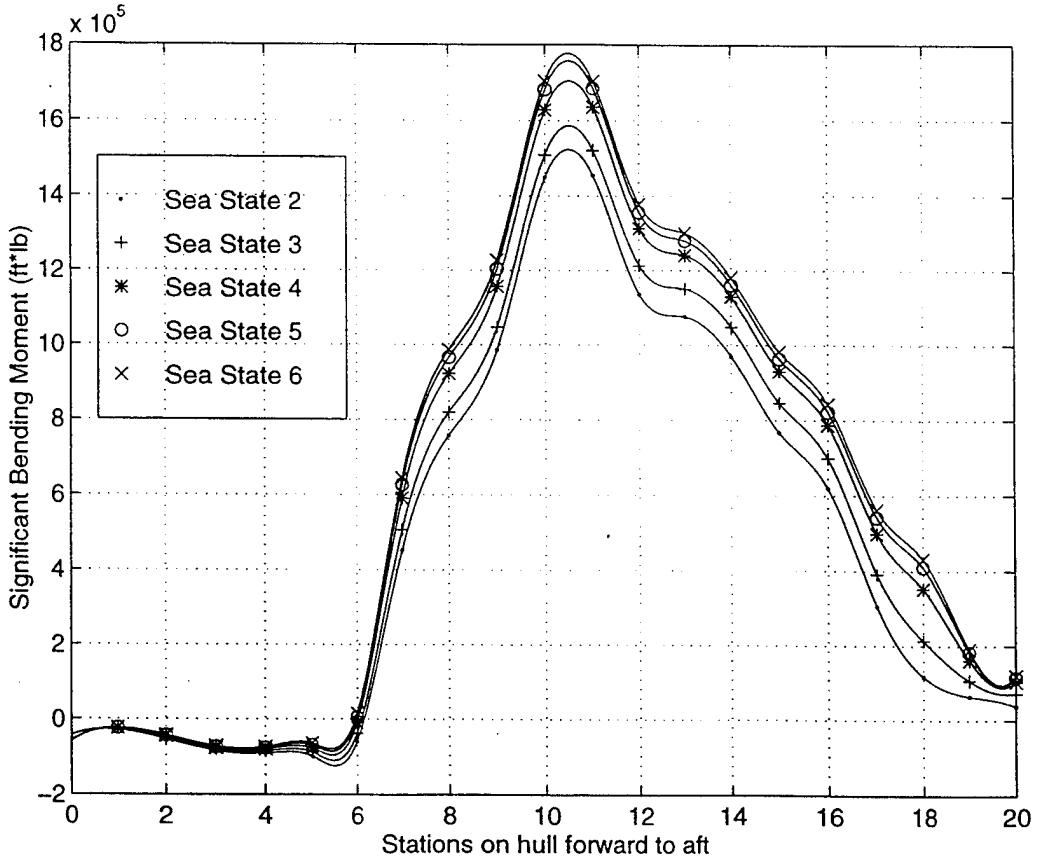

Figure (14). Dynamic Bending Moments for Beam Seas and 20 Knots.

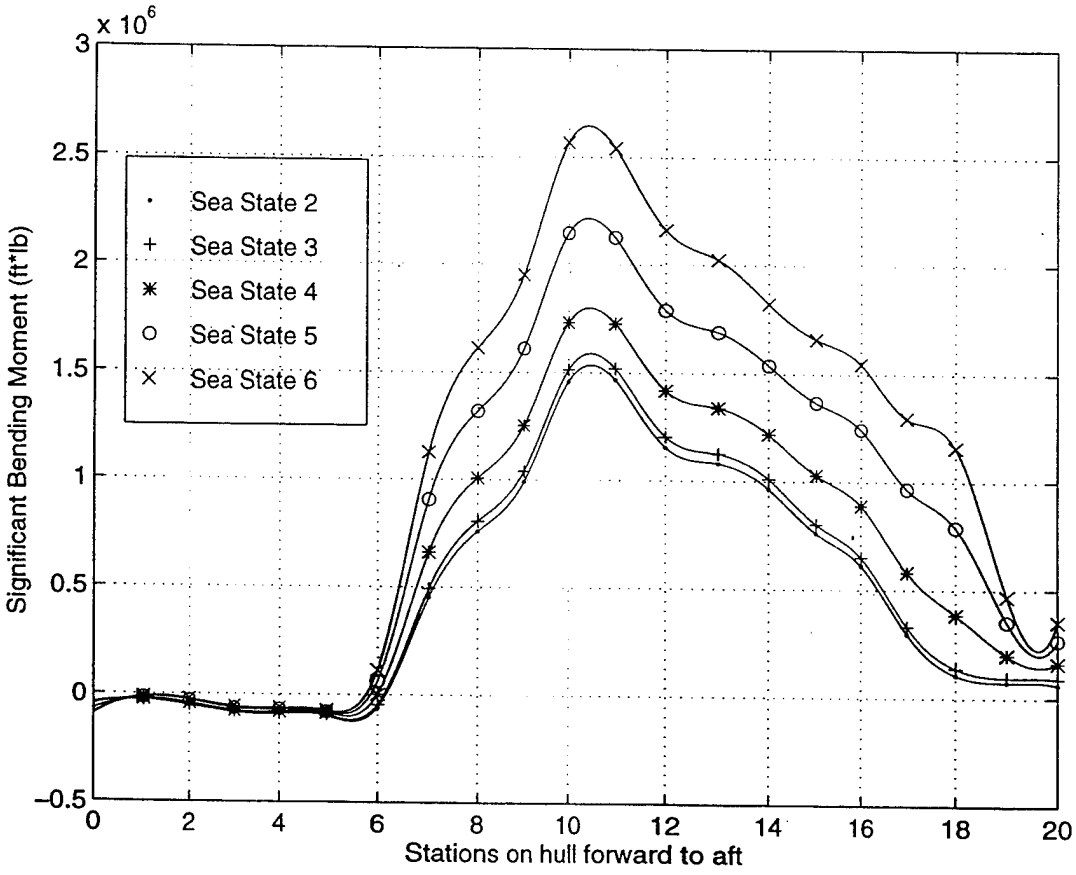

Figure (15). Dynamic Bending Moments for Beam Seas and 25 Knots.

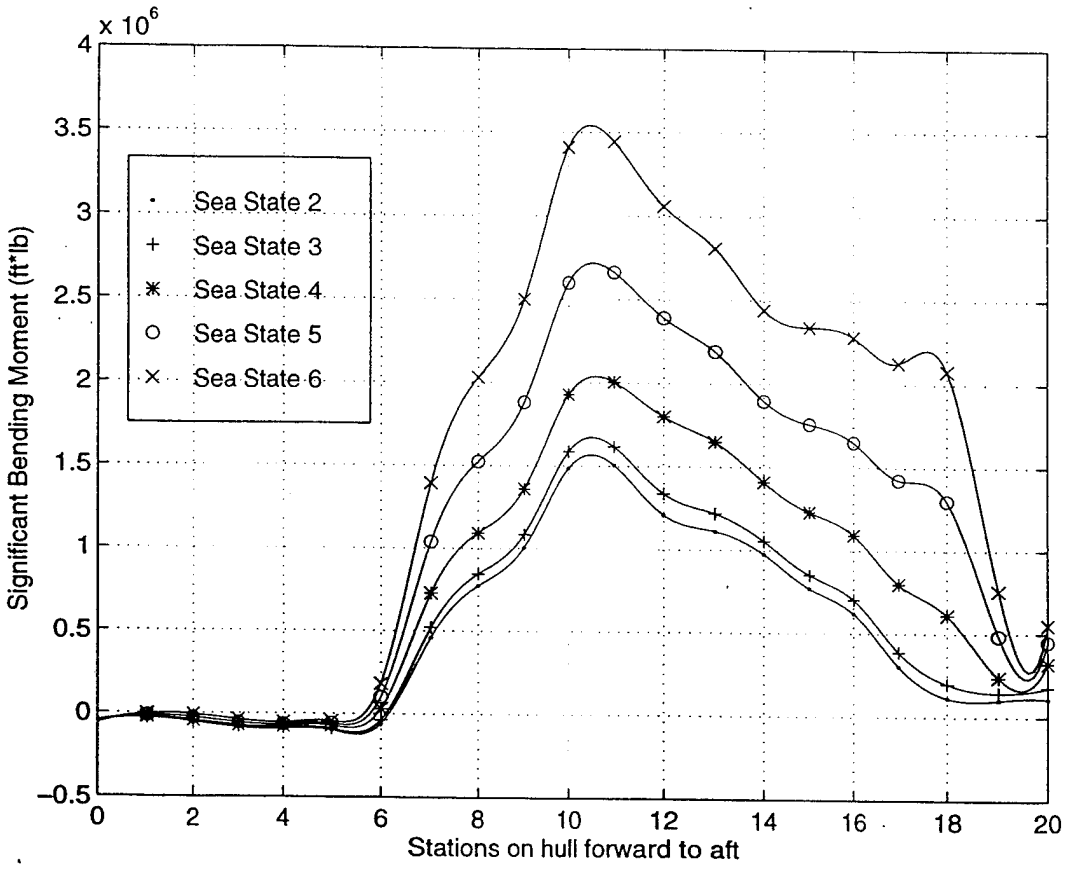

Figure (16). Dynamic Bending Moments for Beam Seas and 30 Knots.

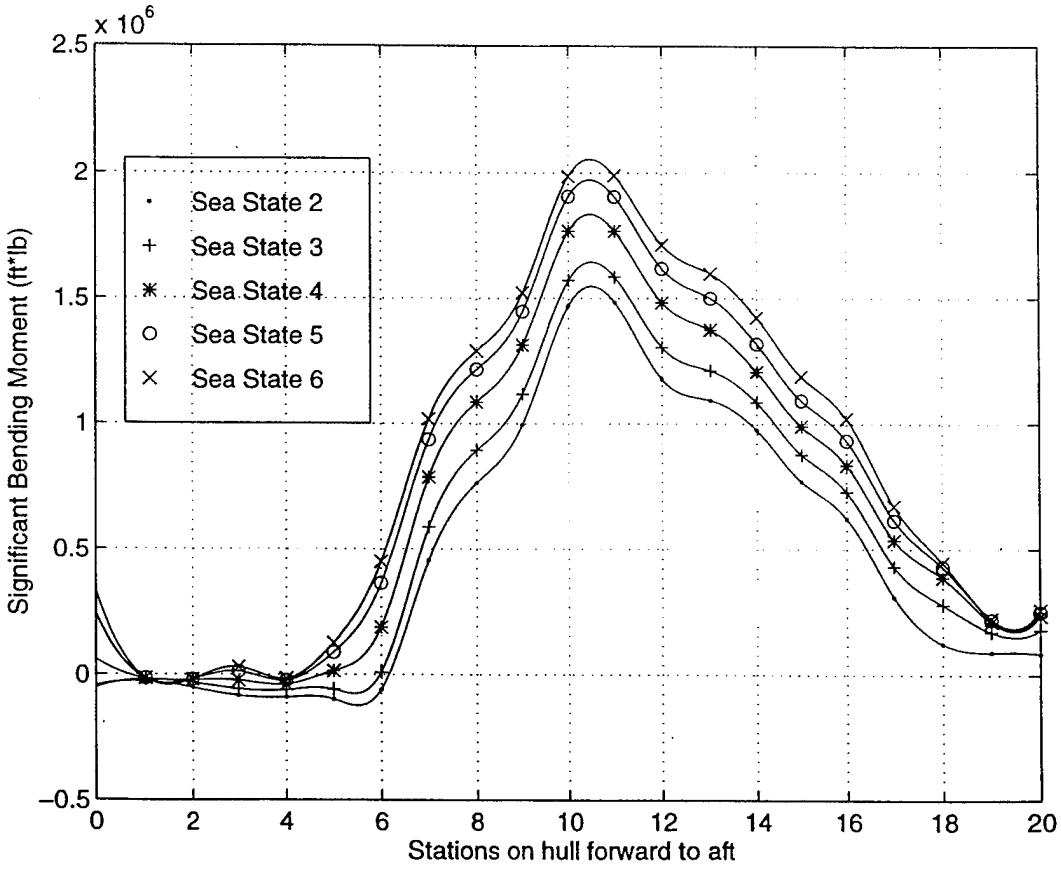

Figure (17). Dynamic Bending Moments for Bow Seas and 10 Knots.

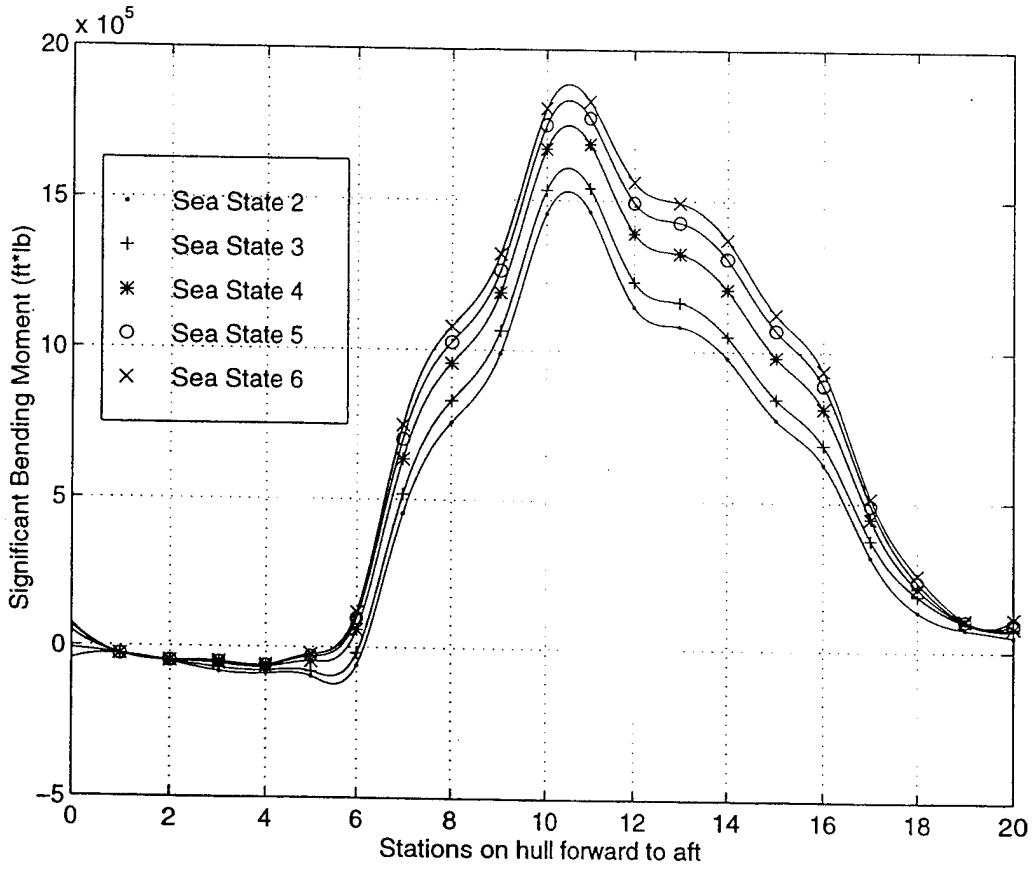

Figure (18). Dynamic Bending Moments for Bow Seas and 15 Knots.

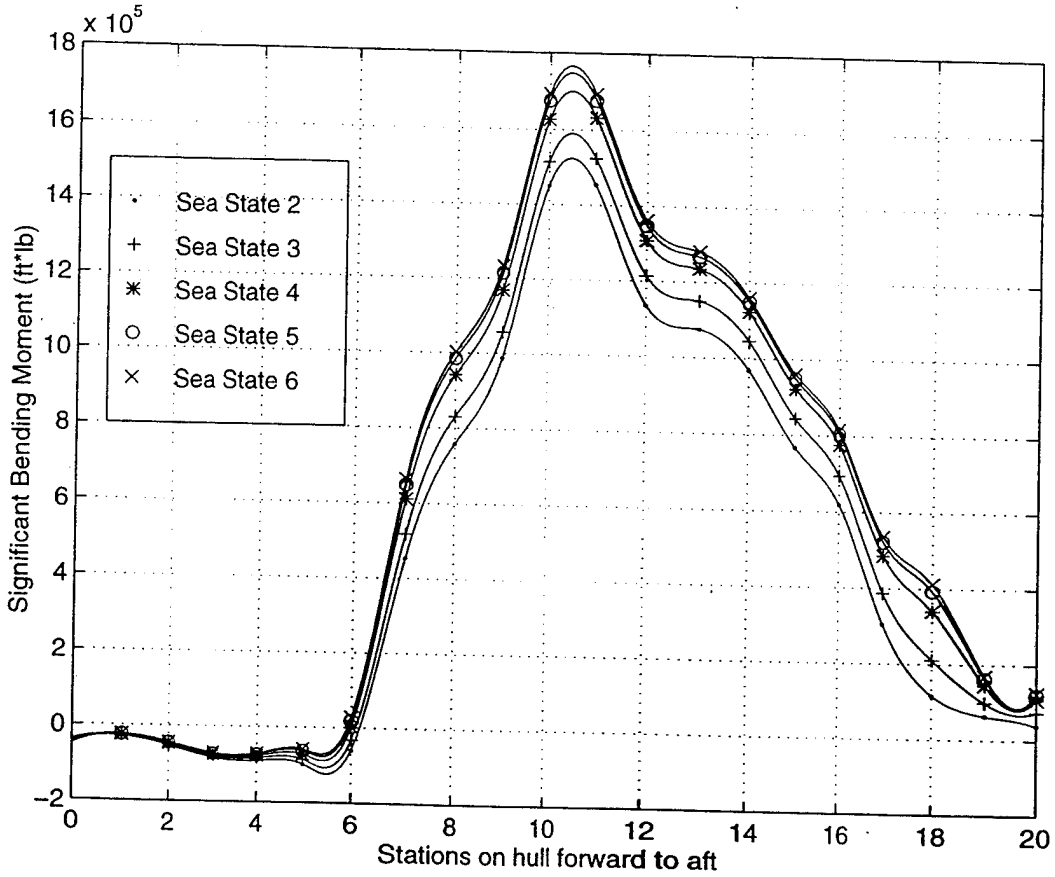

Figure (19). Dynamic Bending Moments for Bow Seas and 20 Knots.

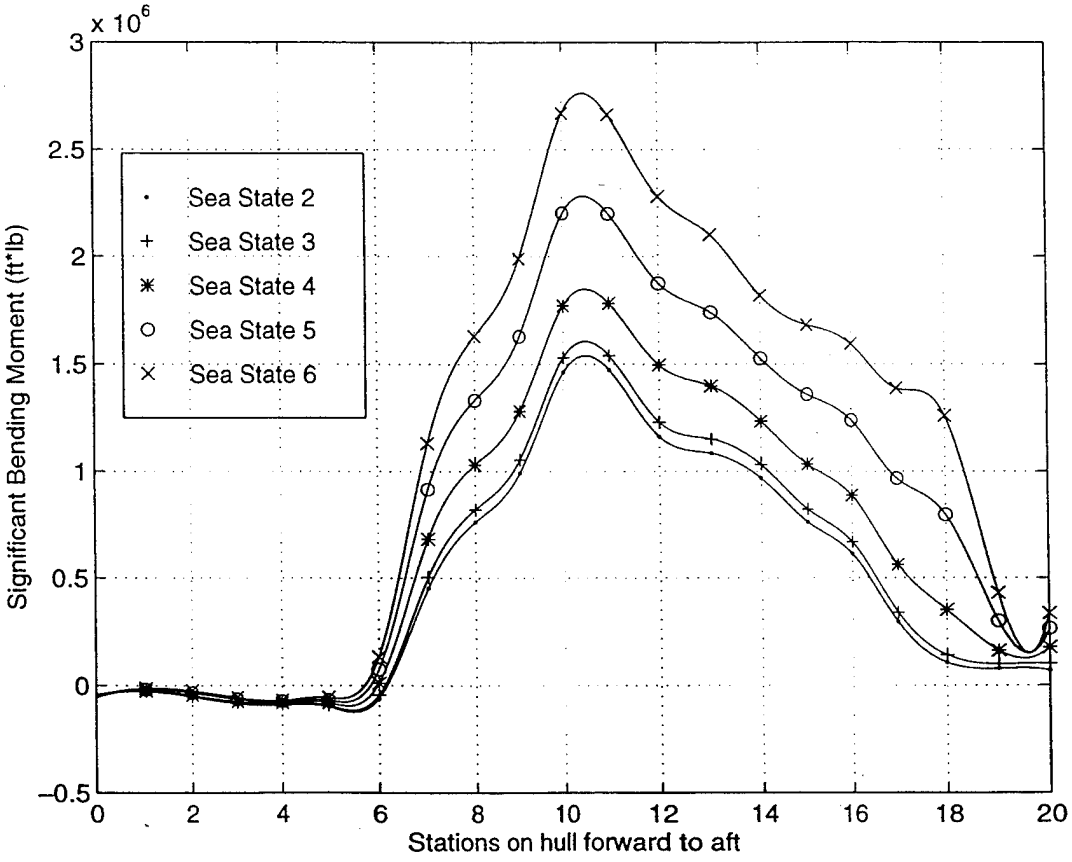

Figure (20). Dynamic Bending Moments for Bow Seas and 25 Knots.

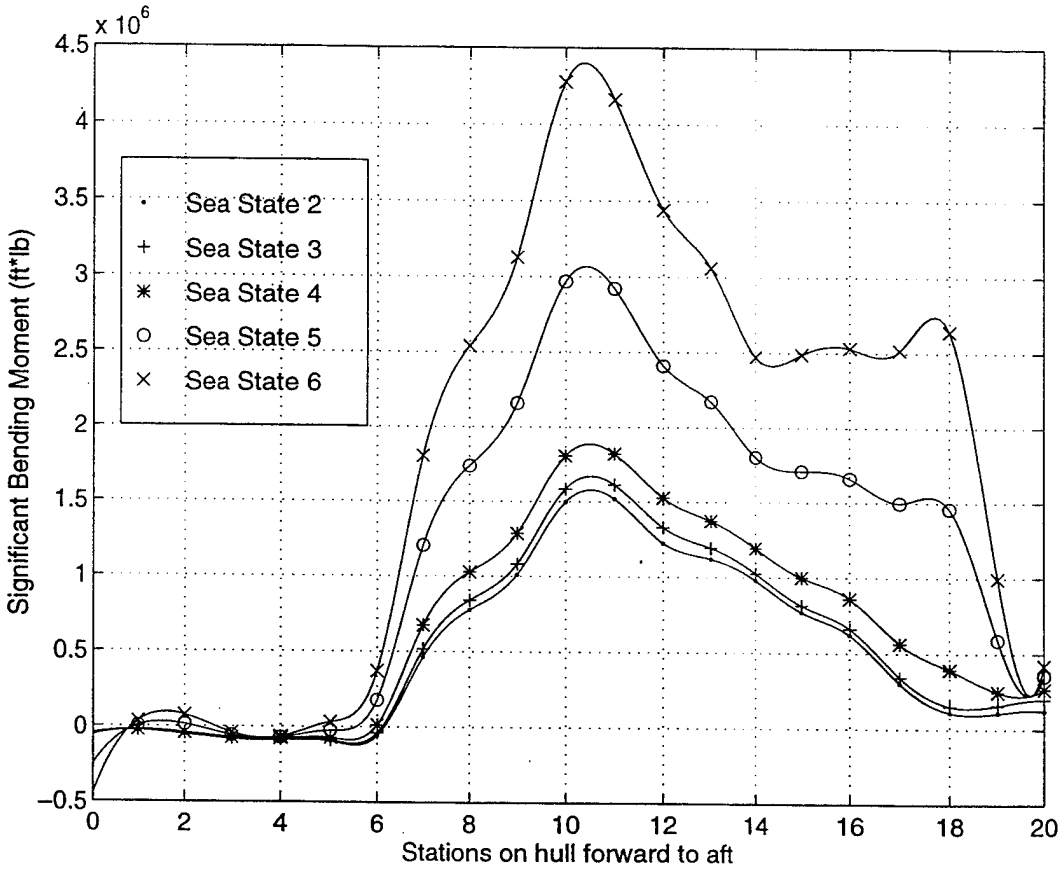

Figure (21). Dynamic Bending Moments for Bow Seas and 30 Knots.

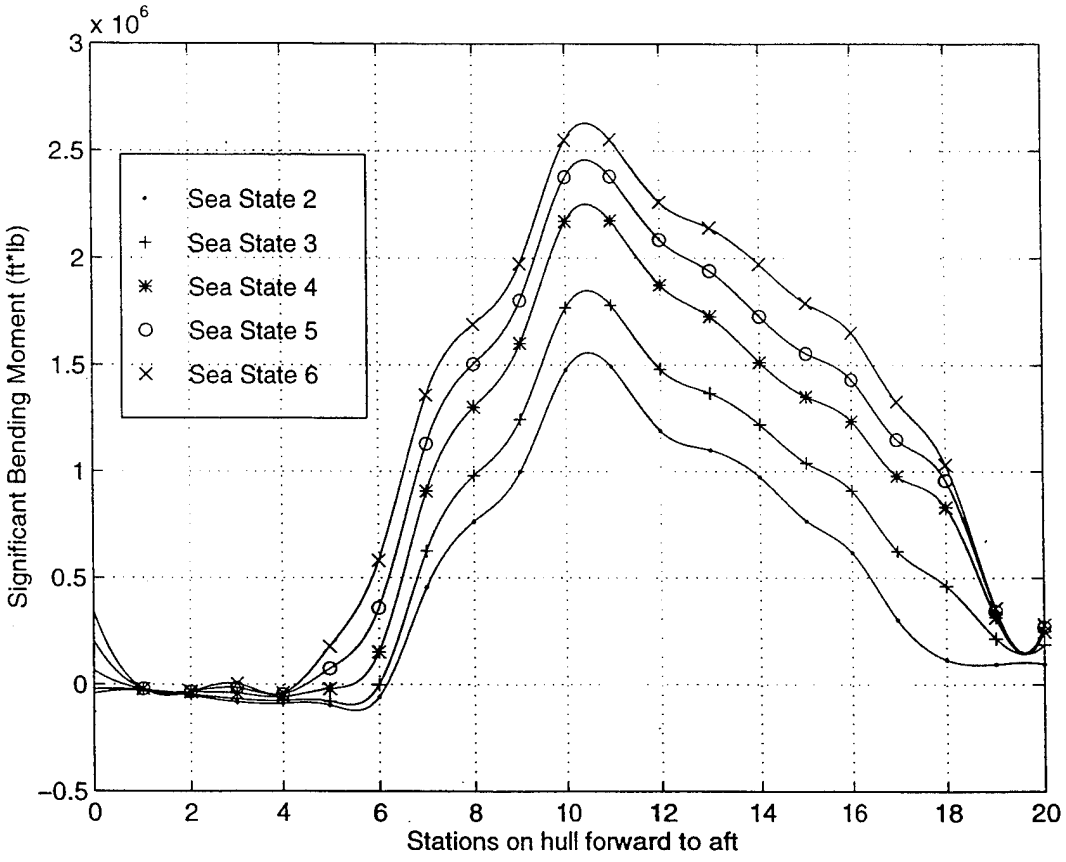

Figure (22). Dynamic Bending Moments for Head Seas and 10 Knots.

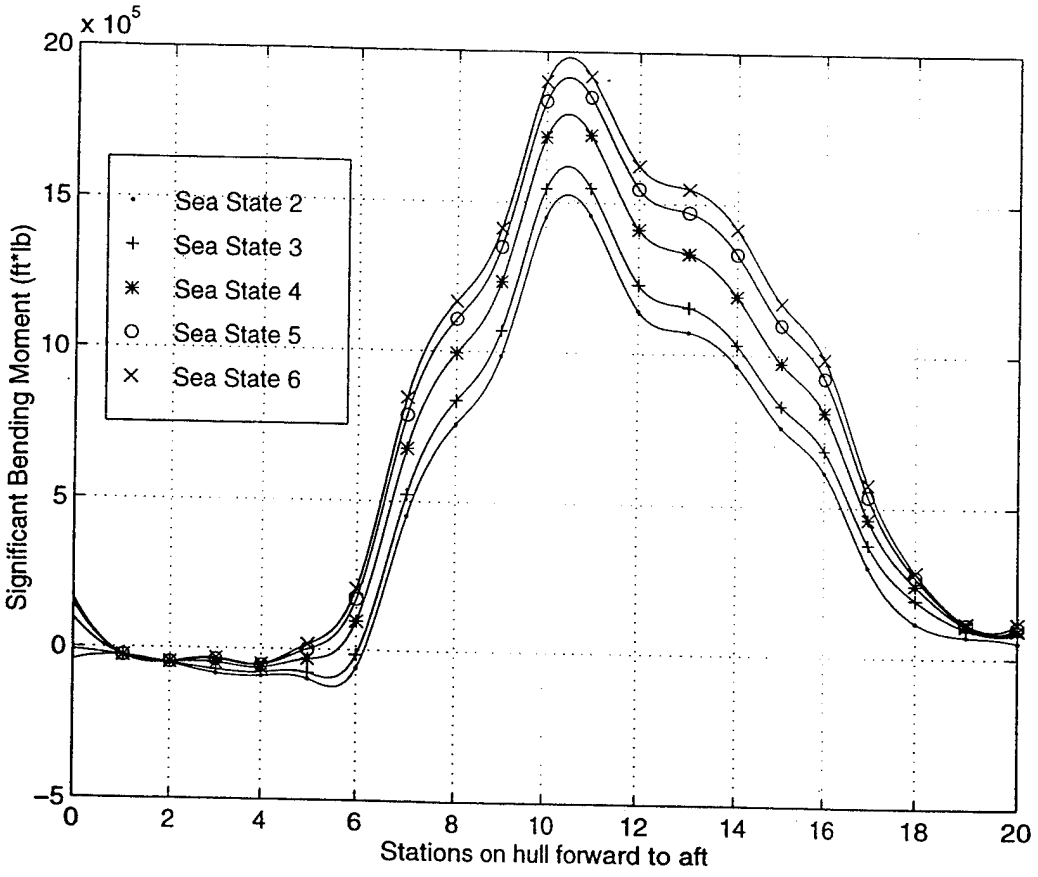

Figure (23). Dynamic Bending Moments for Head Seas and 15 Knots.

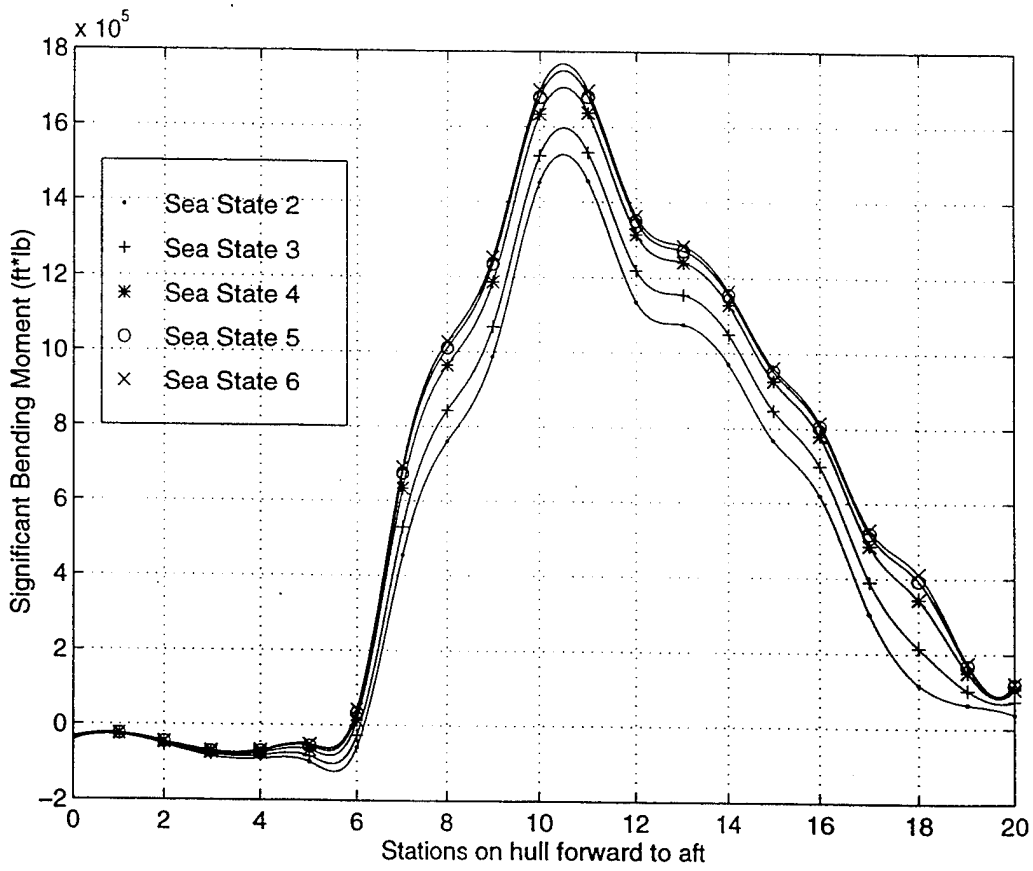

Figure (24). Dynamic Bending Moments for Head Seas and 20 Knots.

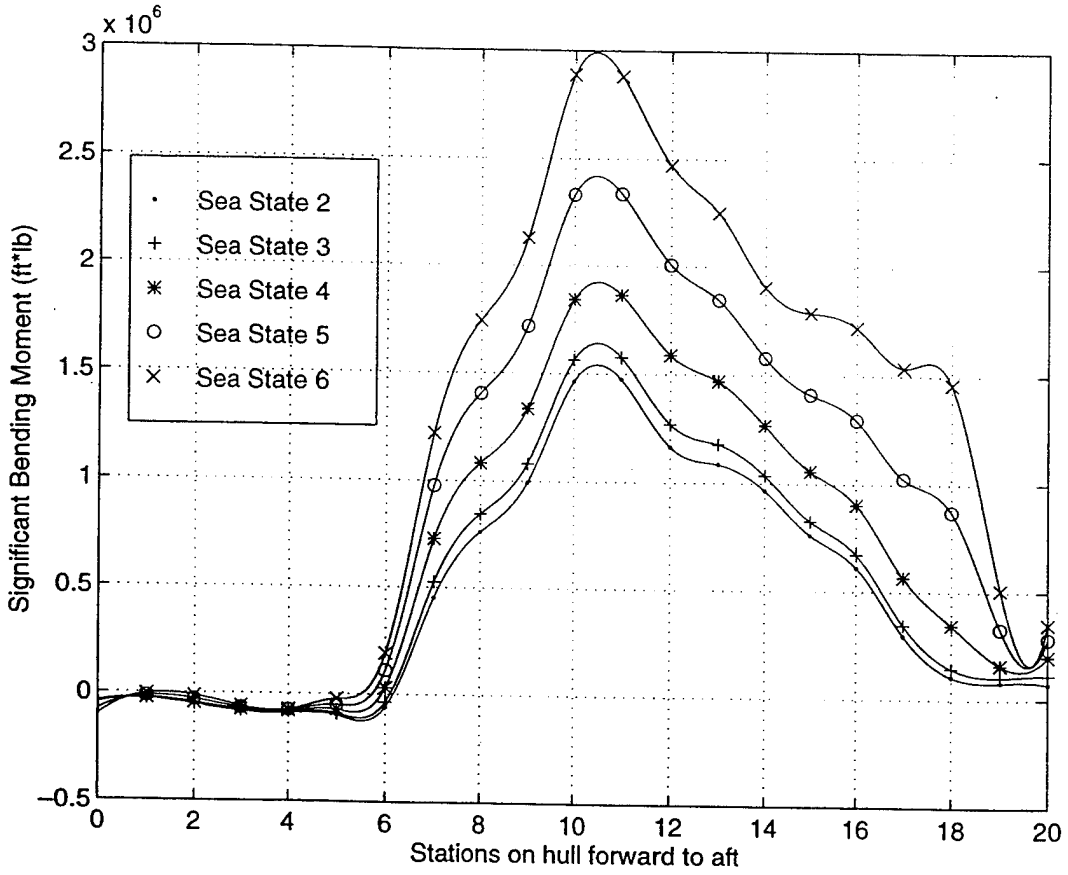

Figure (25). Dynamic Bending Moments for Head Seas and 25 Knots.

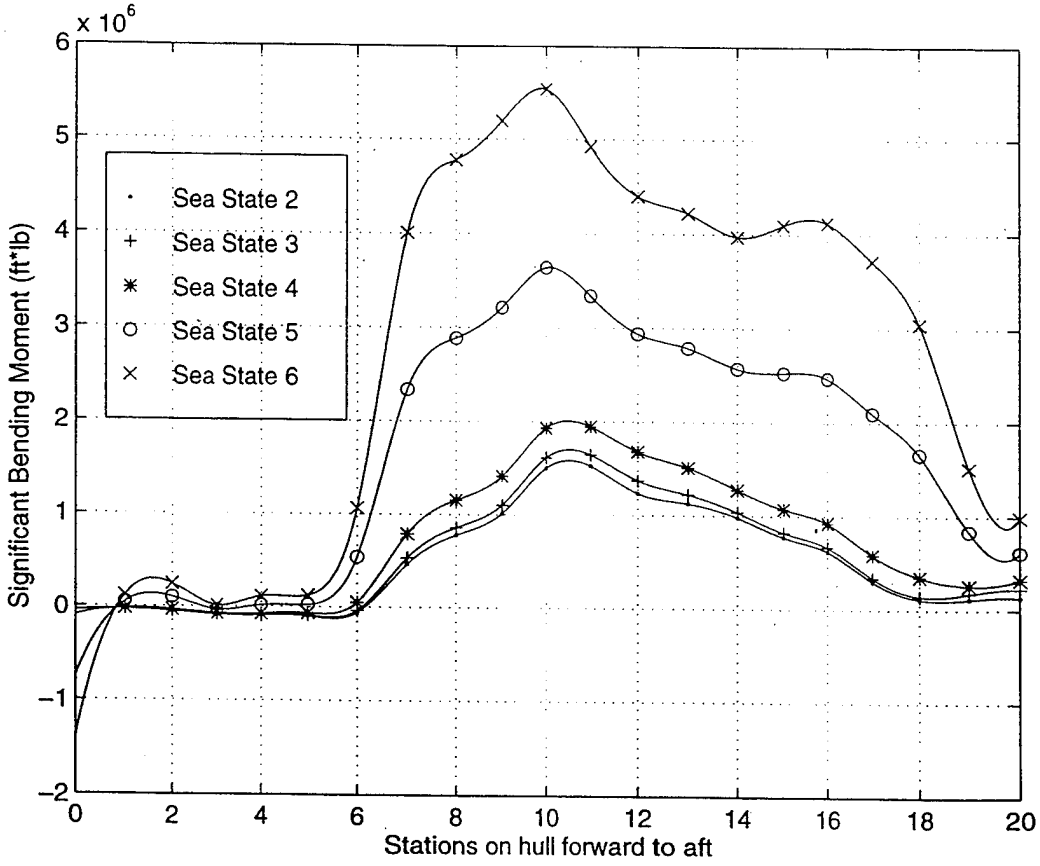

Figure (26). Dynamic Bending Moments for Head Seas and 30 Knots.

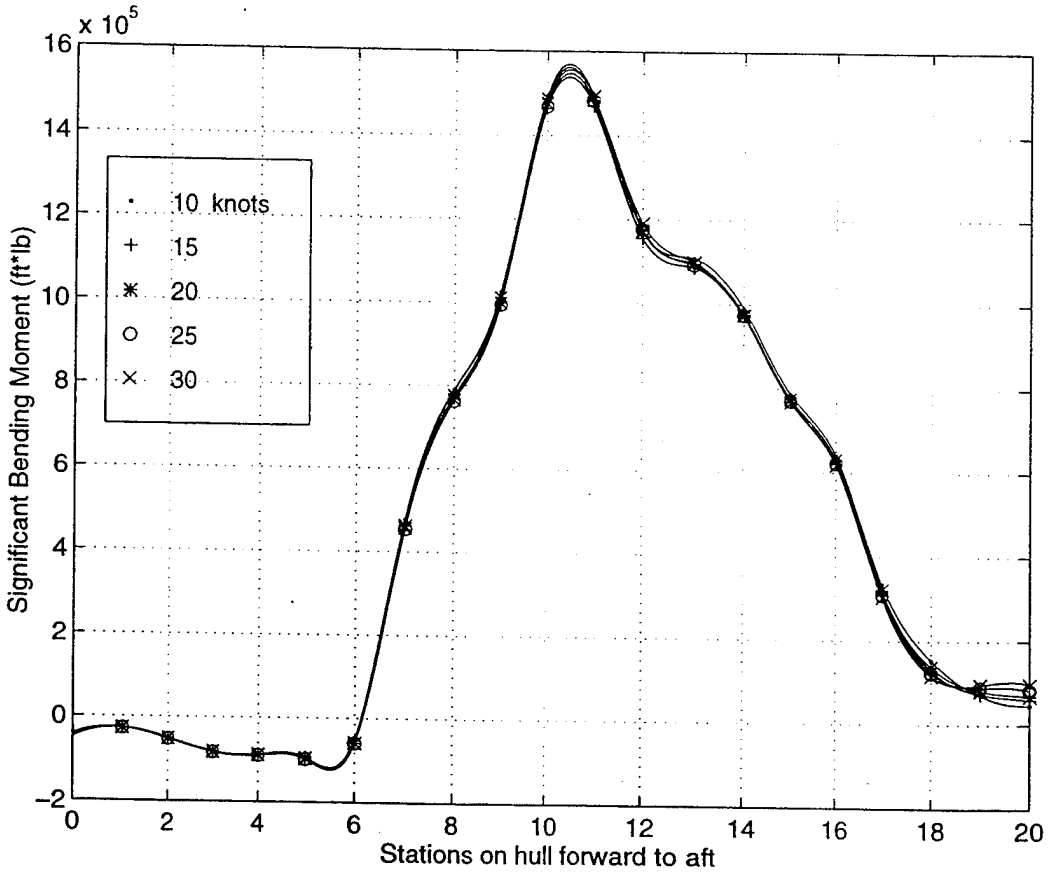

Figure (27). Dynamic Bending Moments for Sea State 2 and Following Seas.

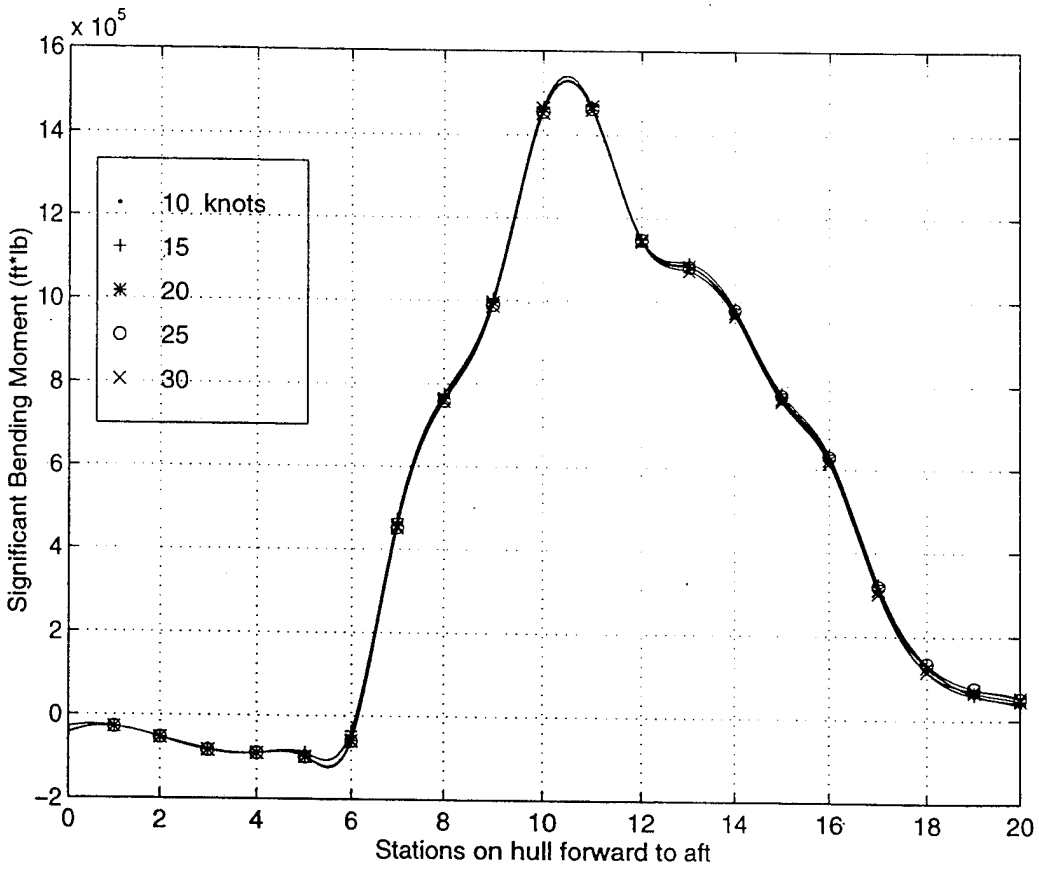

Figure (28). Dynamic Bending Moments for Sea State 2 and Quartering Seas.

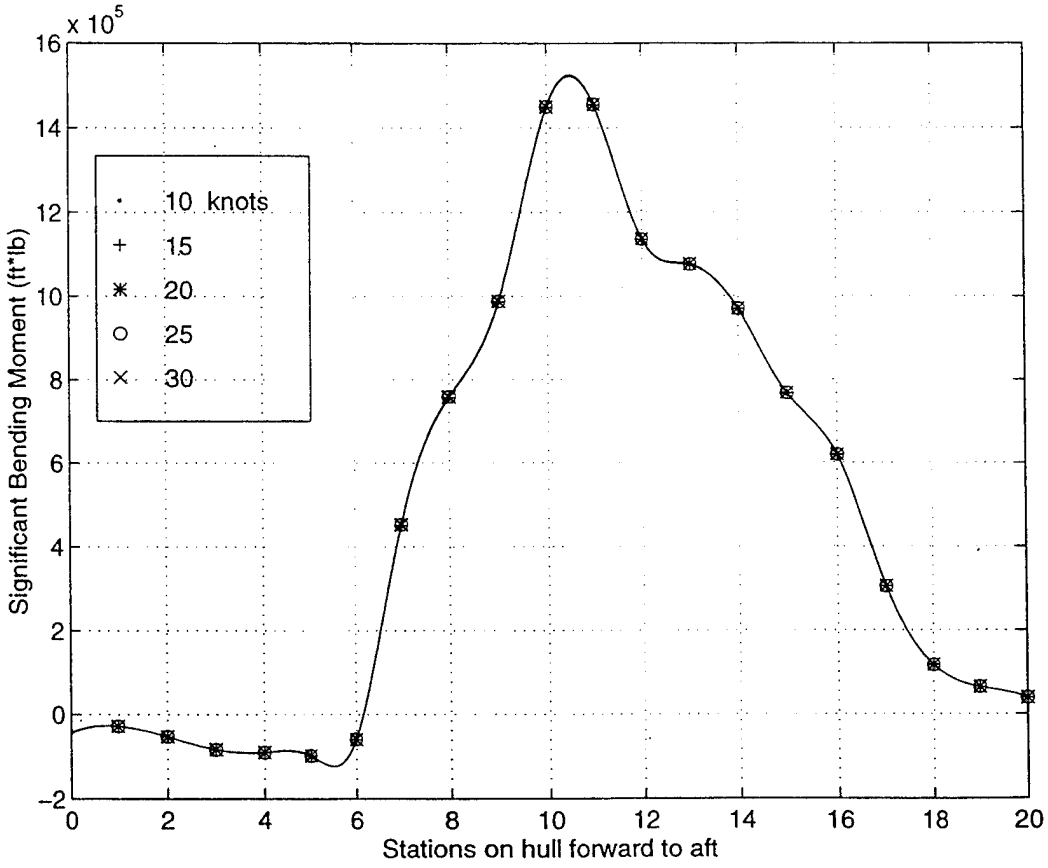

Figure (29). Dynamic Bending Moments for Sea State 2 and Beam Seas.

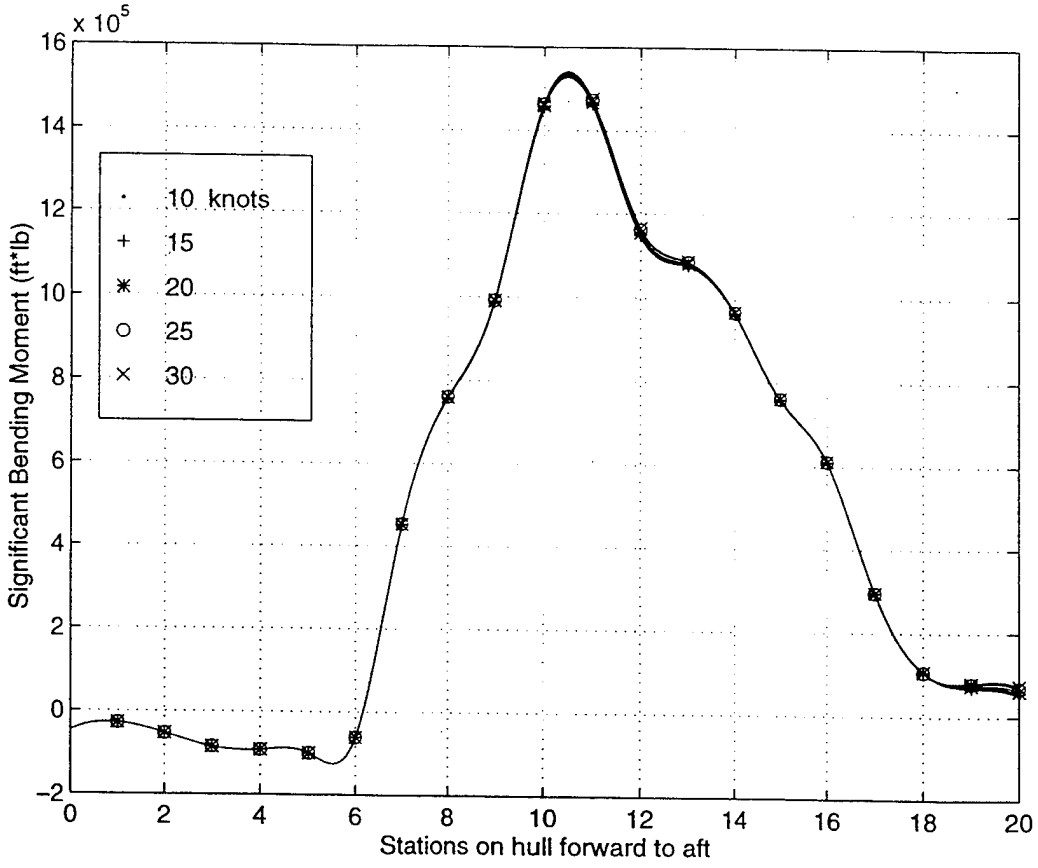

Figure (30). Dynamic Bending Moments for Sea State 2 and Bow Seas.

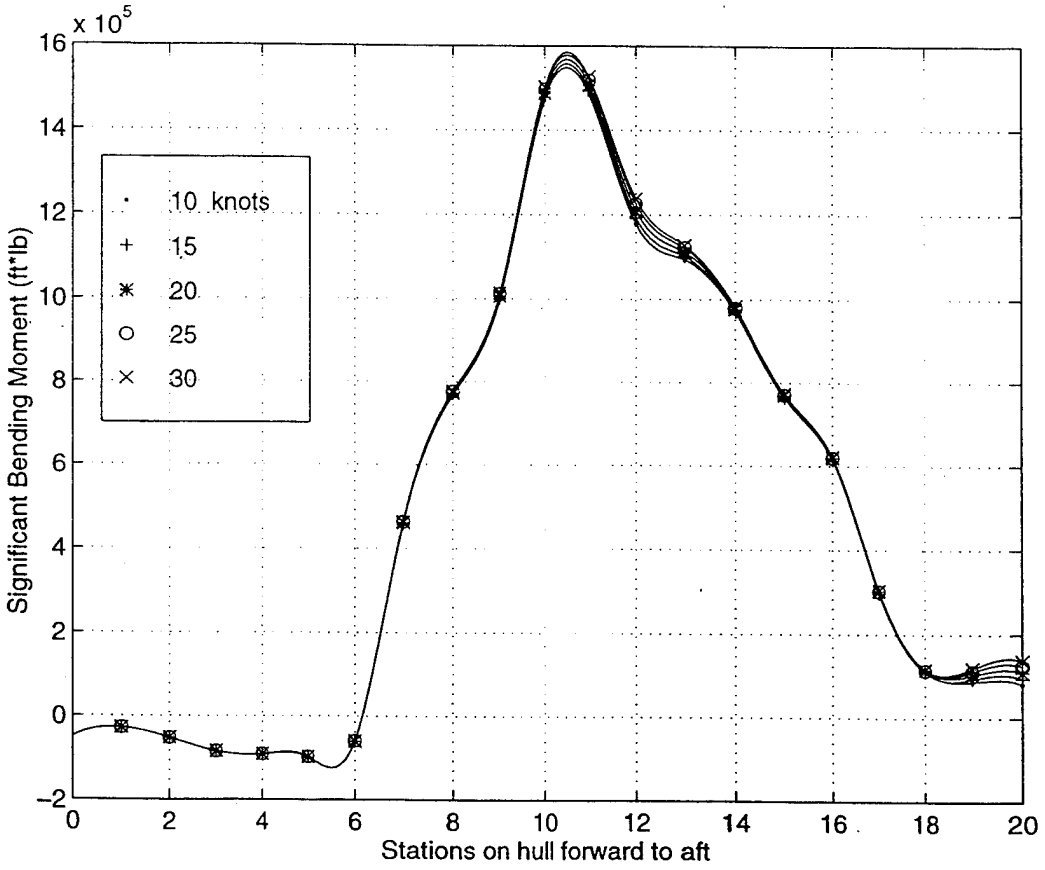

Figure (31). Dynamic Bending Moments for Sea State 2 and Head Seas.

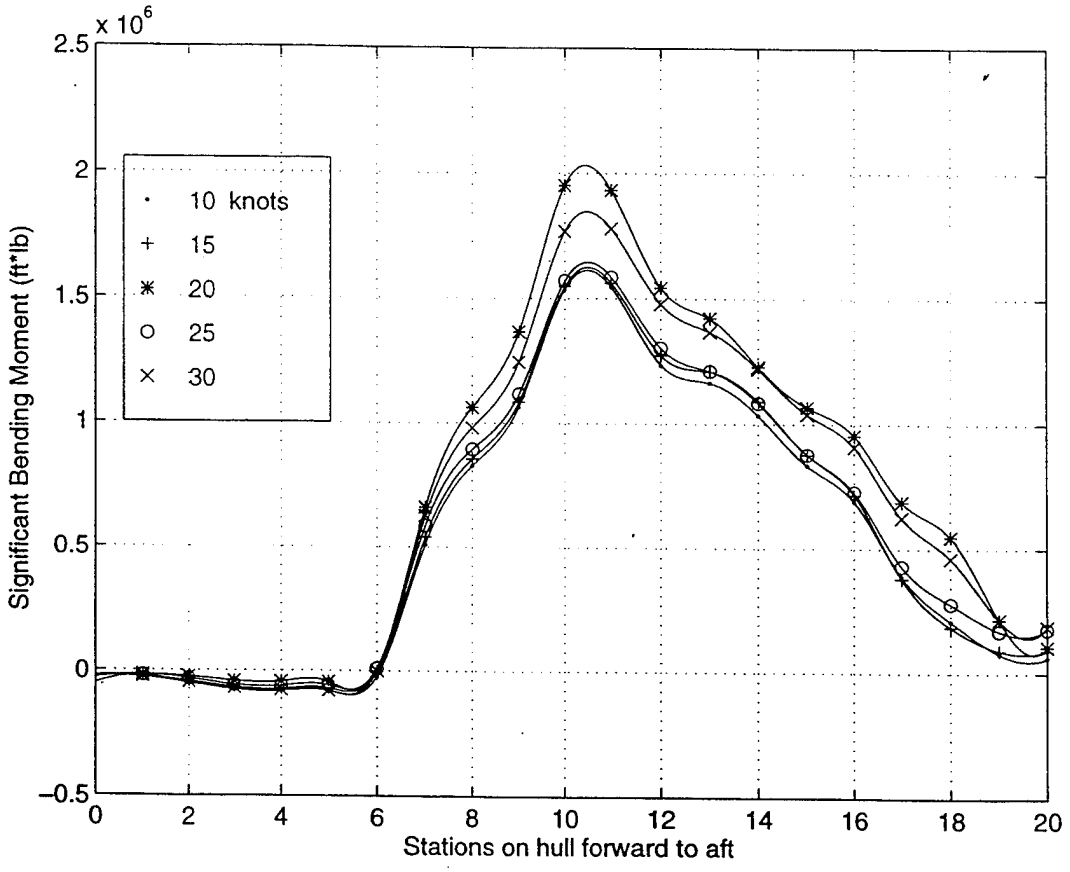

Figure (32). Dynamic Bending Moments for Sea State 3 and Following Seas.

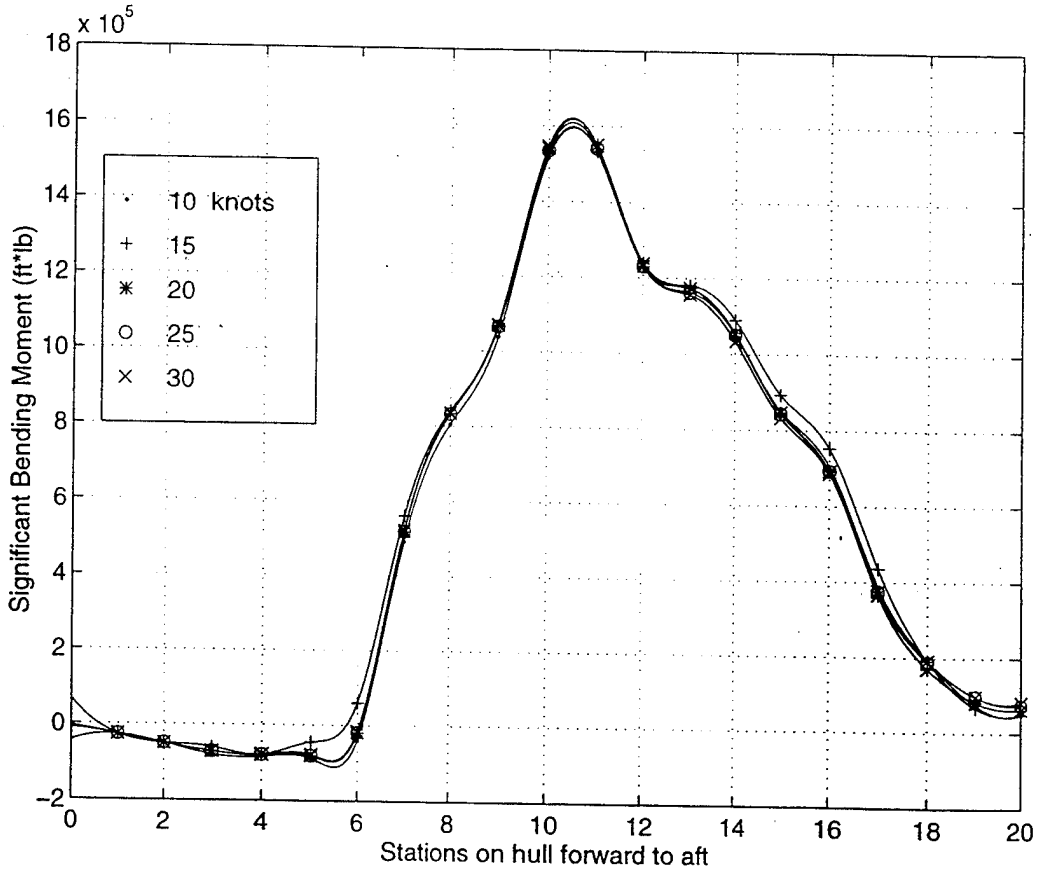

Figure (33). Dynamic Bending Moments for Sea State 3 and Quartering Seas.

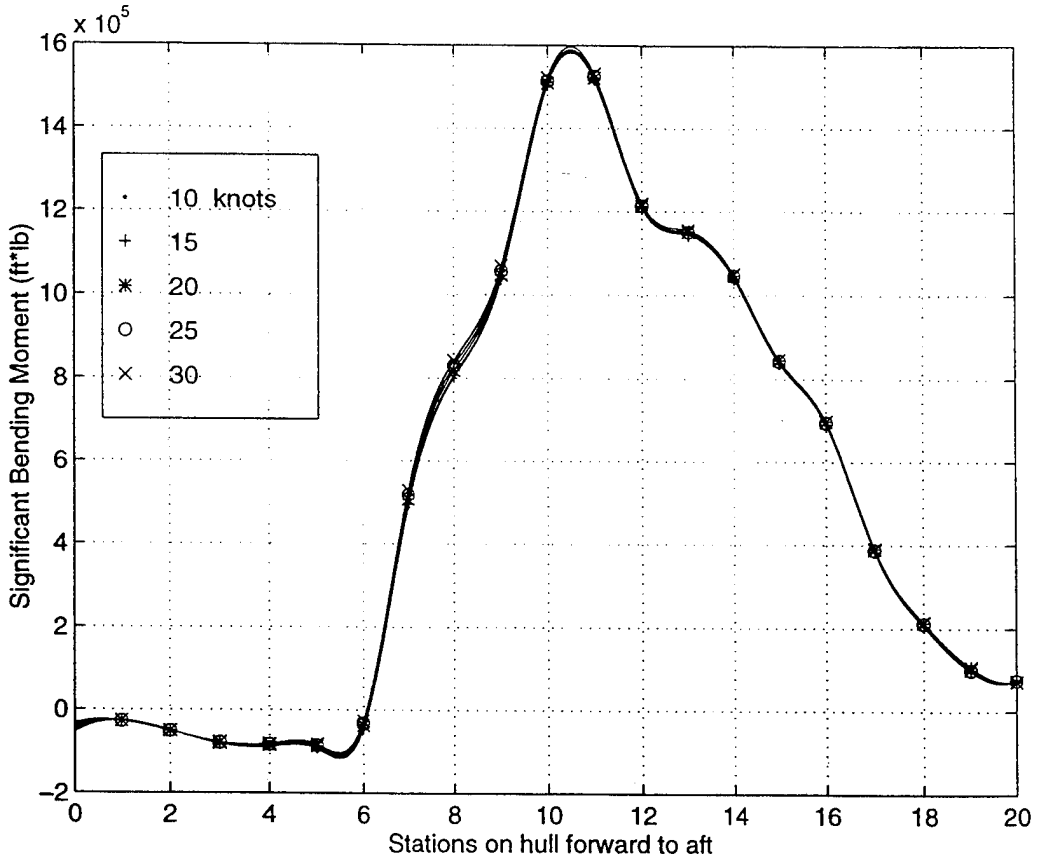

Figure (34). Dynamic Bending Moments for Sea State 3 and Beam Seas.

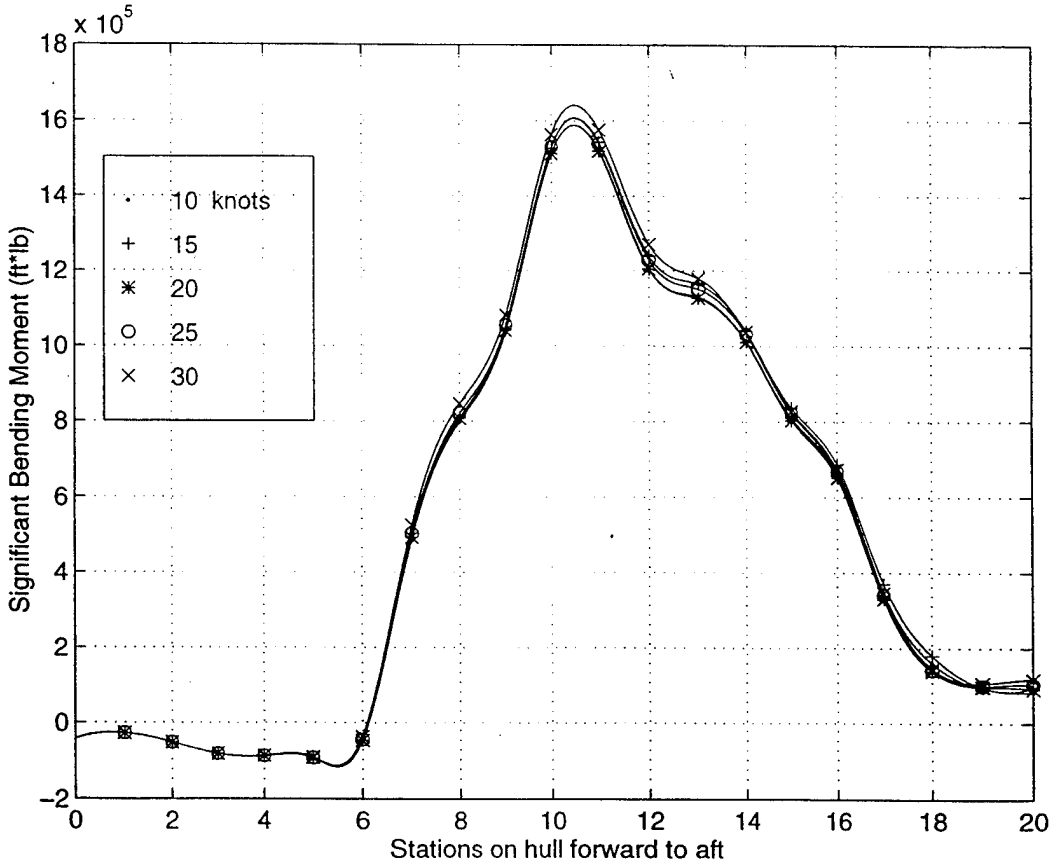

Figure (35). Dynamic Bending Moments for Sea State 3 and Bow Seas.

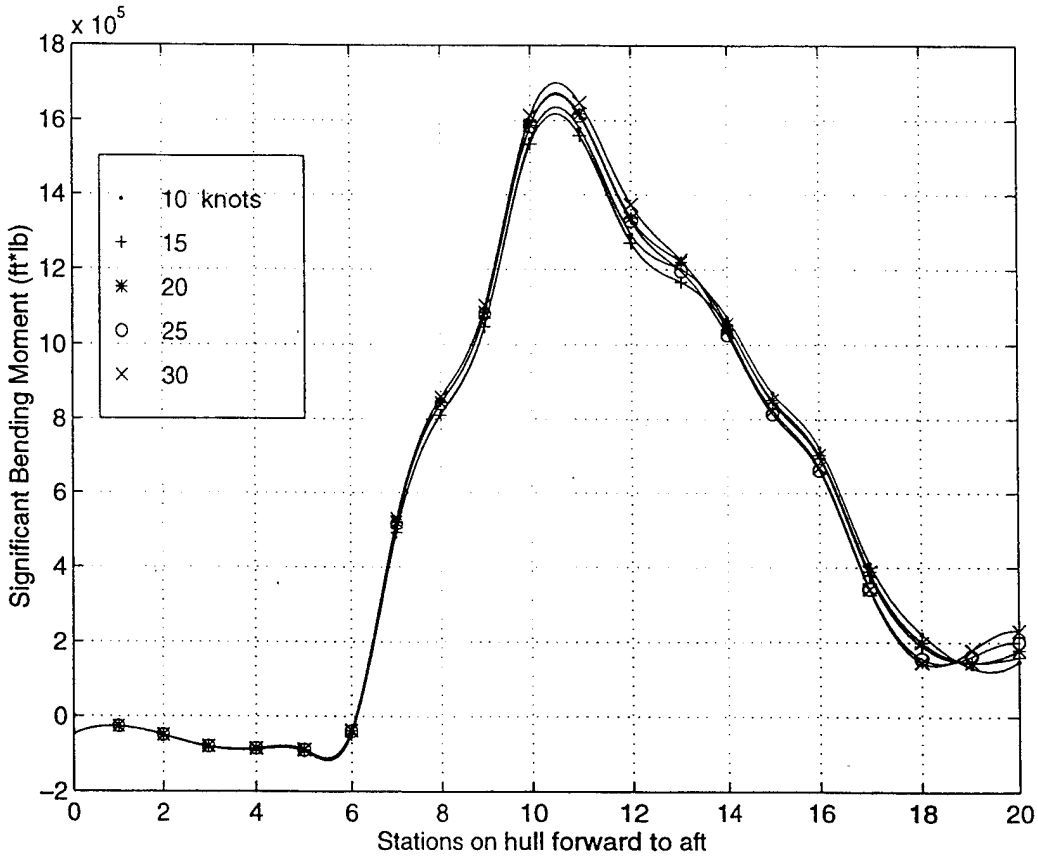

Figure (36). Dynamic Bending Moments for Sea State 3 and Head Seas.

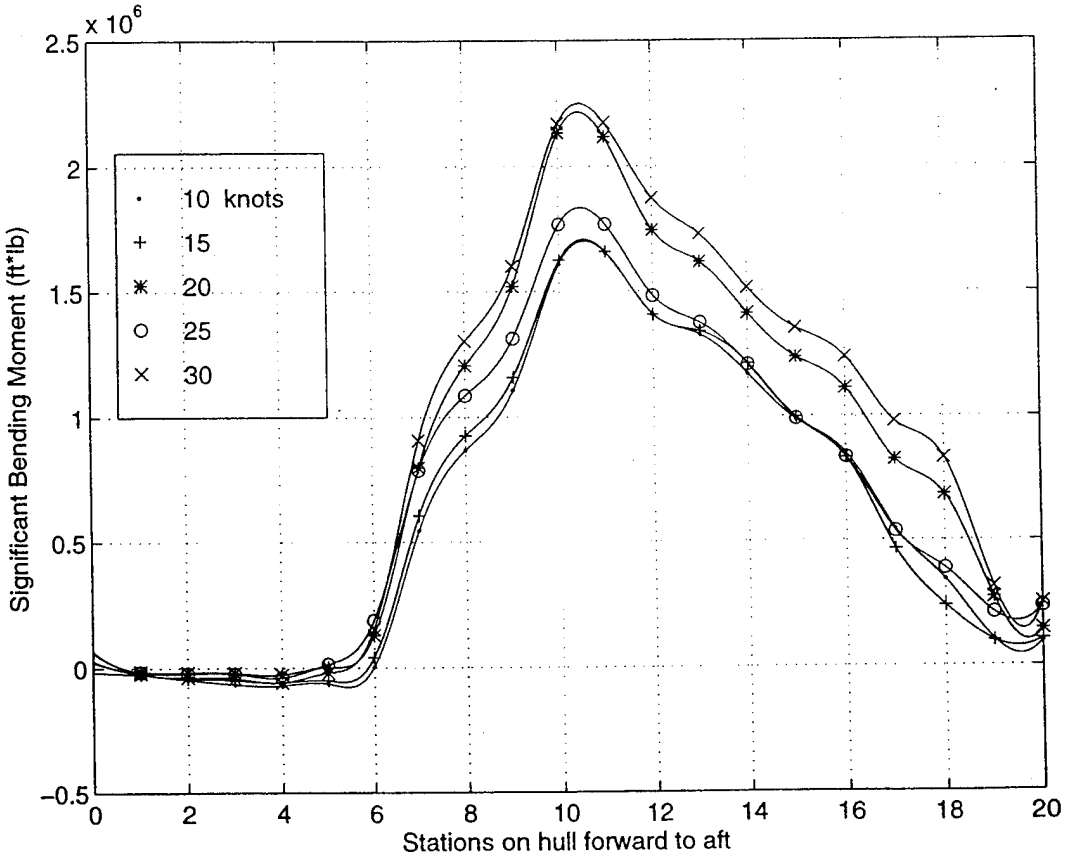

Figure (37). Dynamic Bending Moments for Sea State 4 and Following Seas.

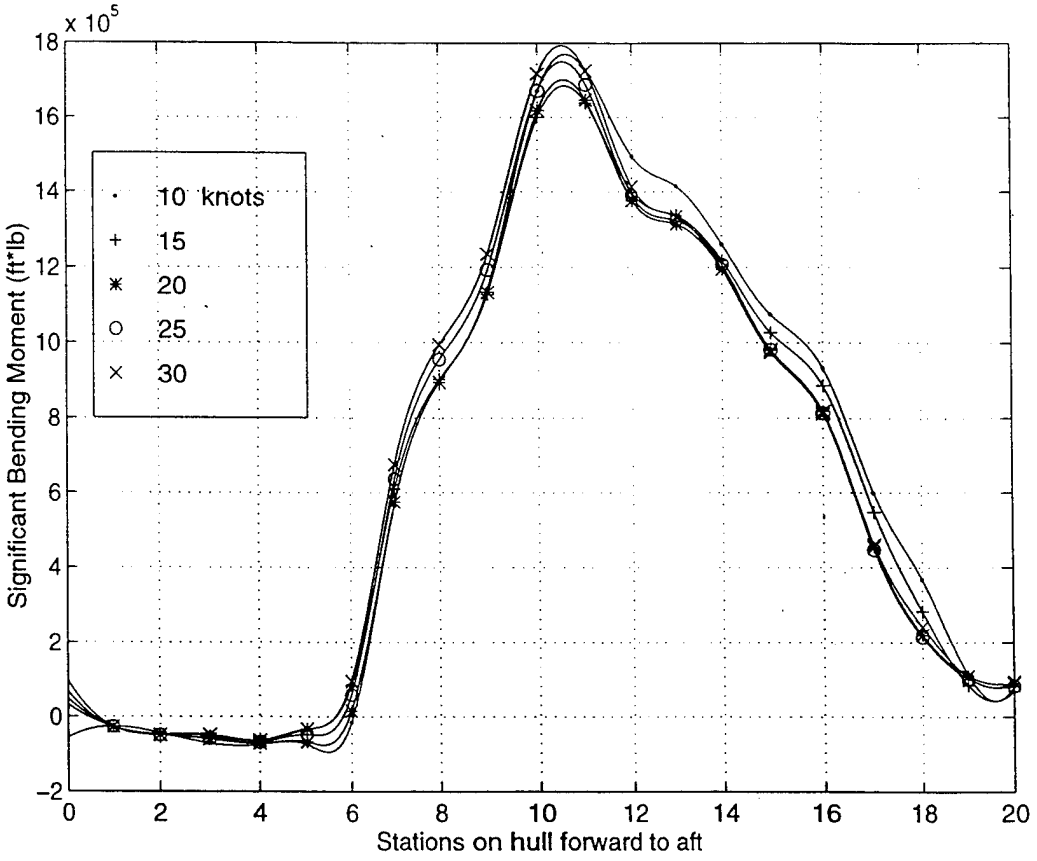

Figure (38). Dynamic Bending Moments for Sea State 4 and Quartering Seas.

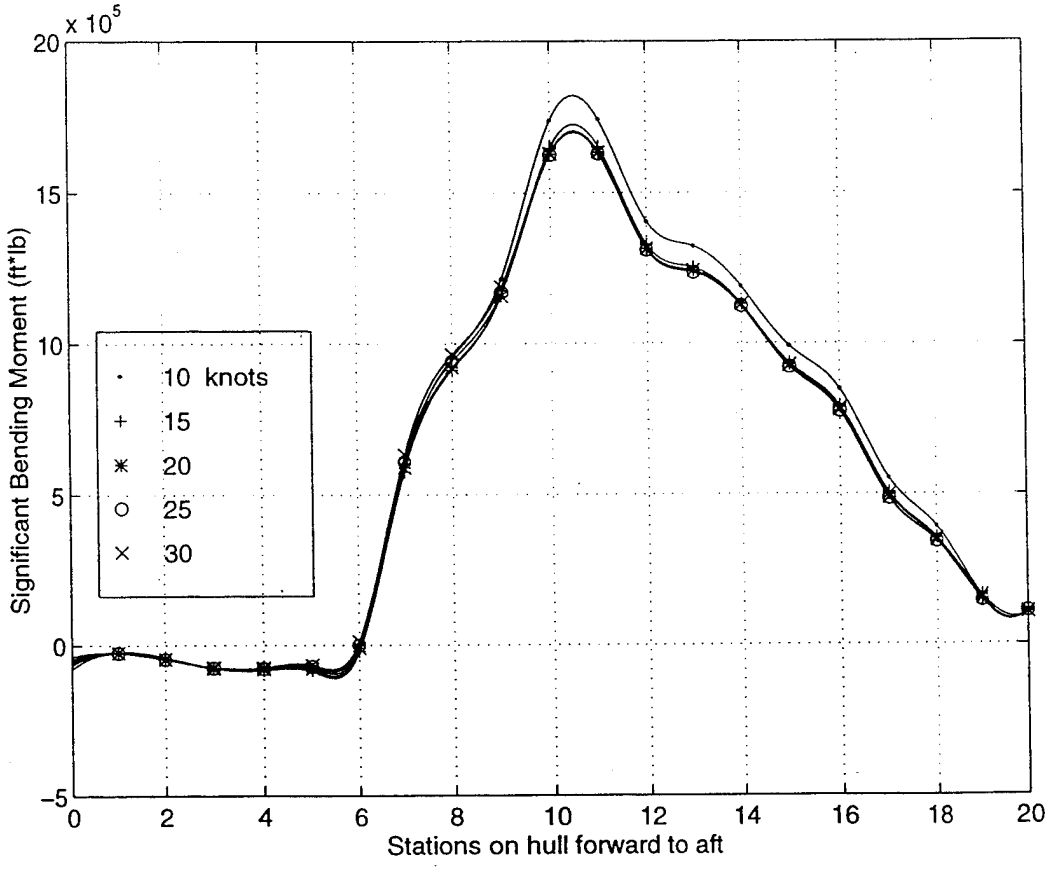

Figure (39). Dynamic Bending Moments for Sea State 4 and Beam Seas.

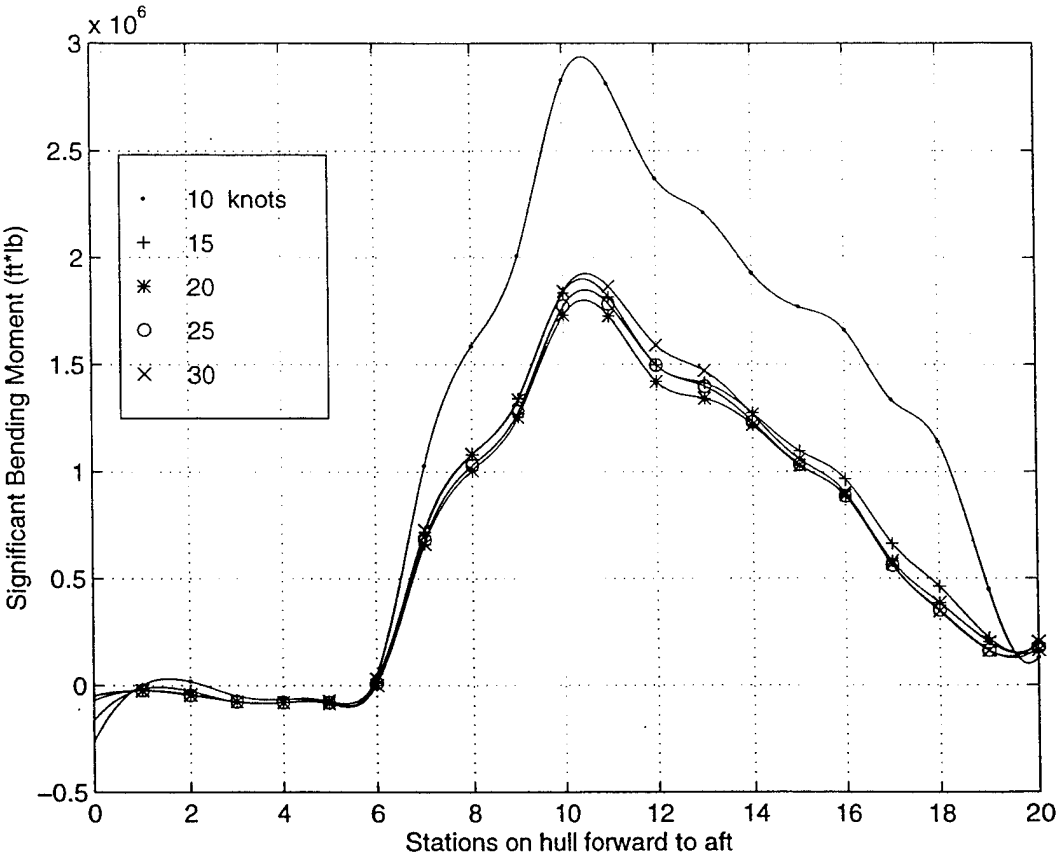

Figure (40). Dynamic Bending Moments for Sea State 4 and Bow Seas.

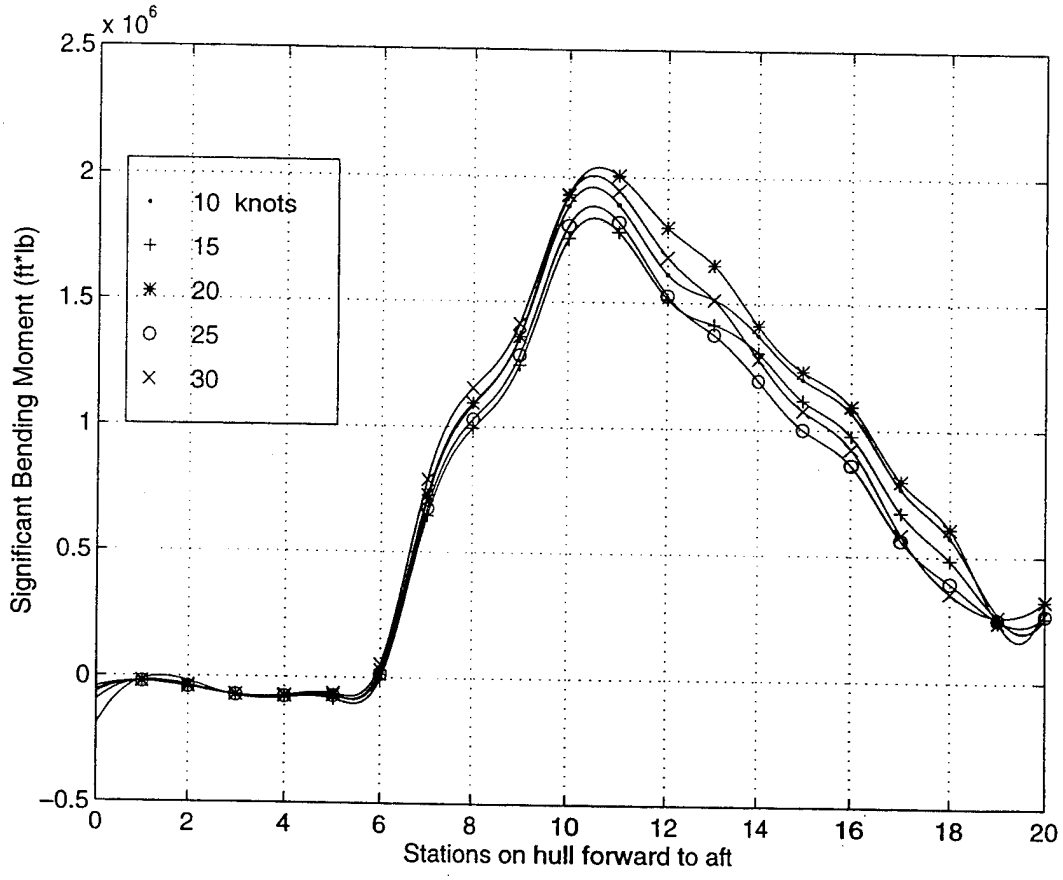

Figure (41). Dynamic Bending Moments for Sea State 4 and Head Seas.

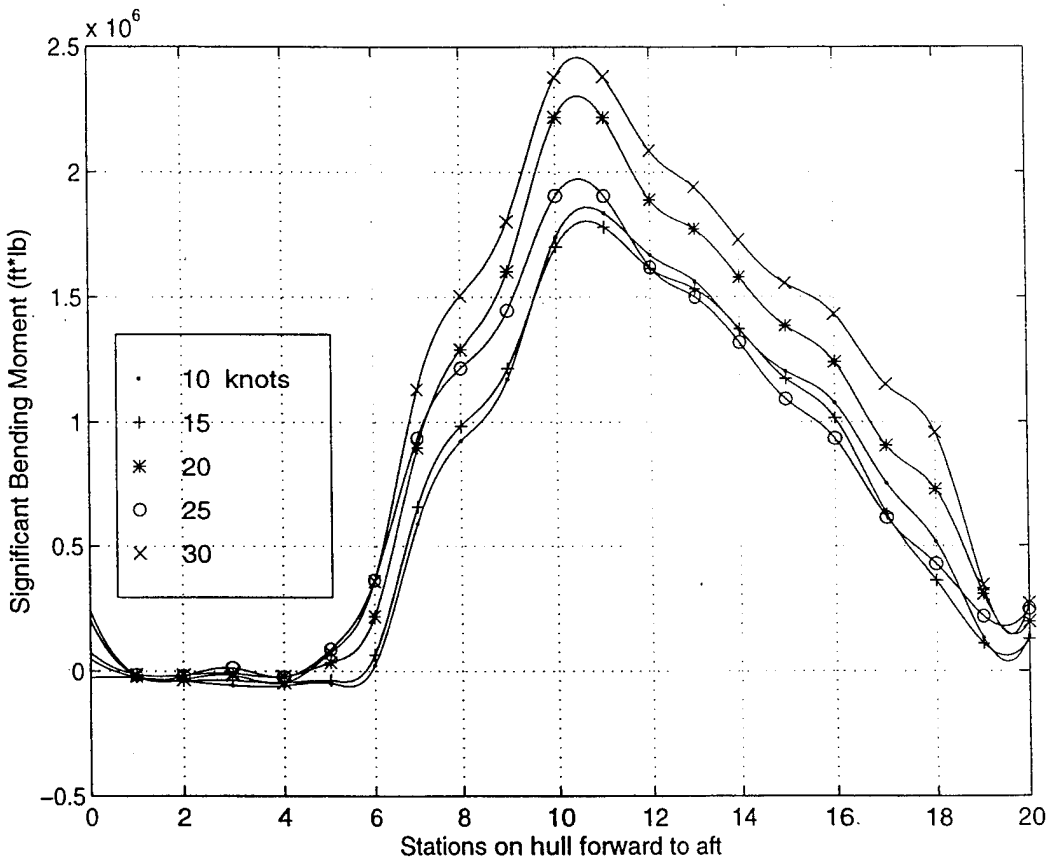

Figure (42). Dynamic Bending Moments for Sea State 5 and Following Seas.

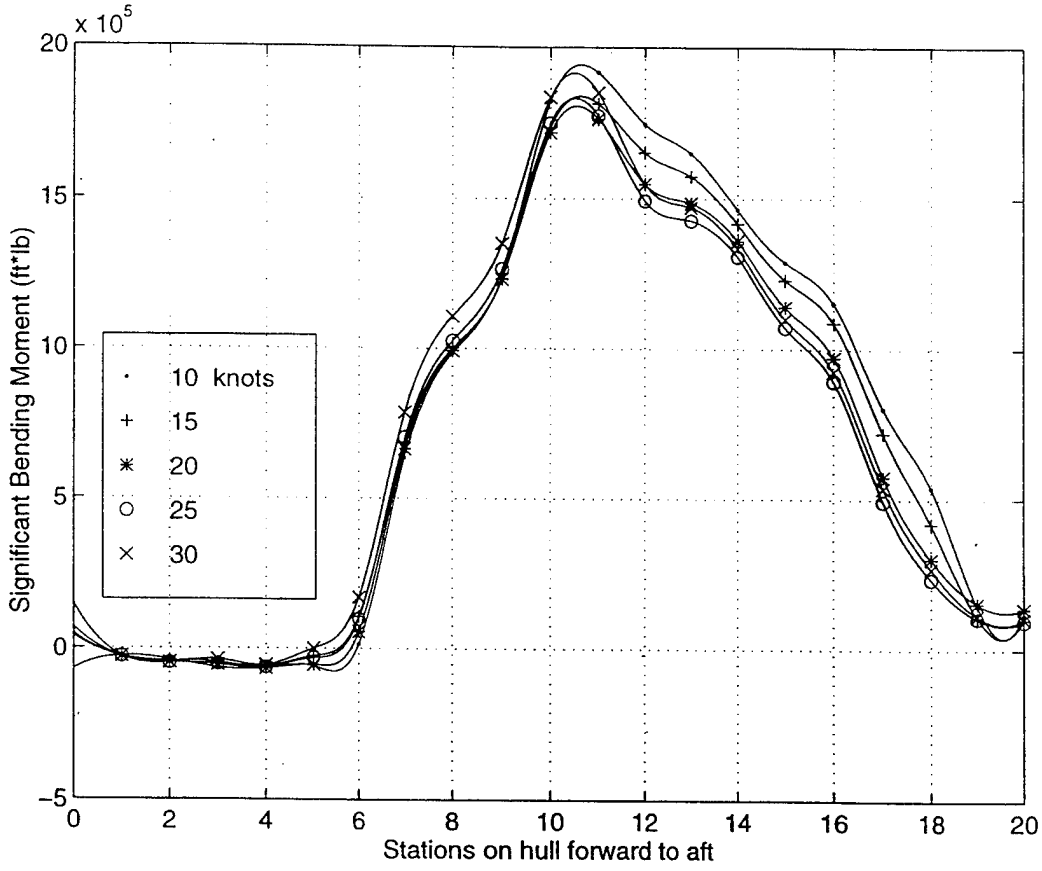

Figure (43). Dynamic Bending Moments for Sea State 5 and Quartering Seas.

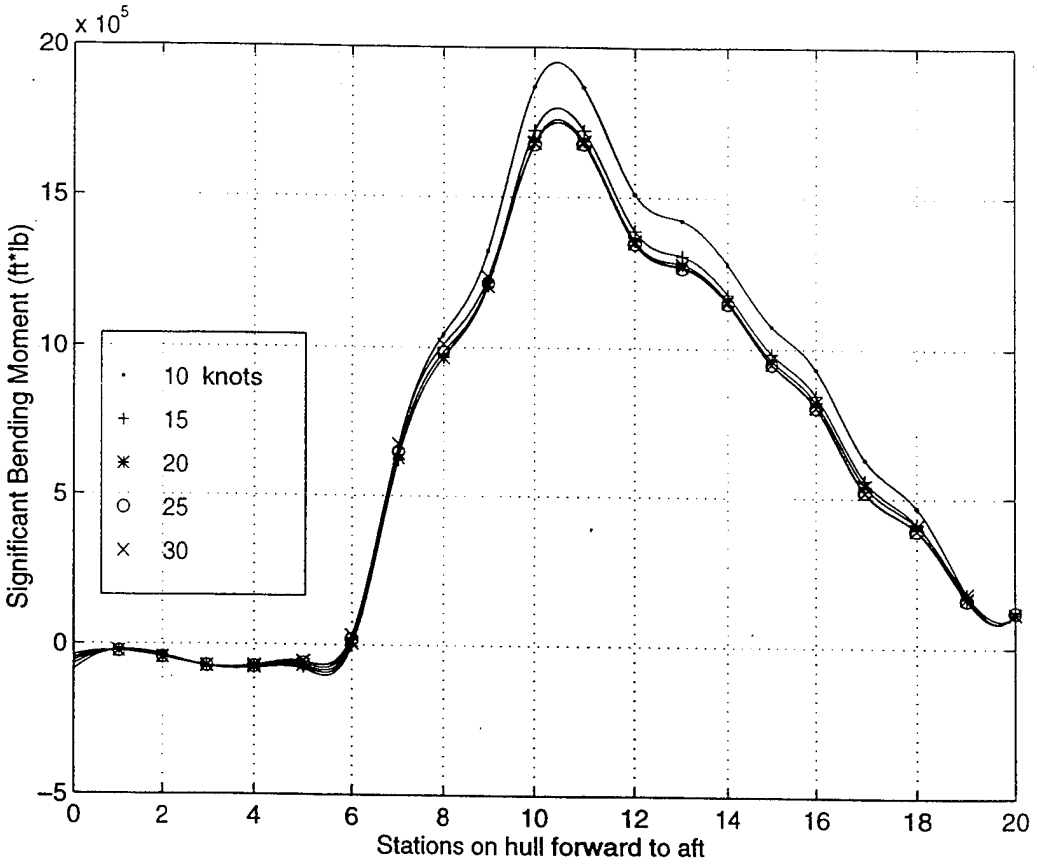

Figure (44). Dynamic Bending Moments for Sea State 5 and Beam Seas.

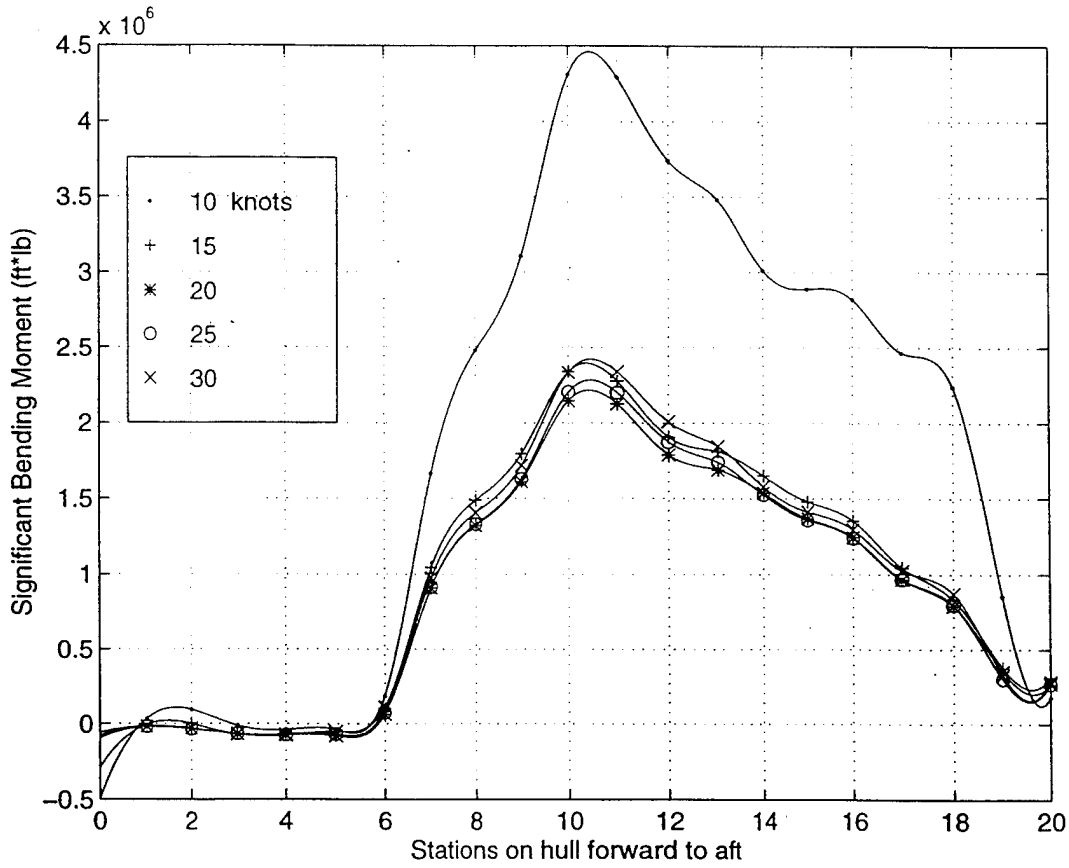

Figure (45). Dynamic Bending Moments for Sea State 5 and Bow Seas.

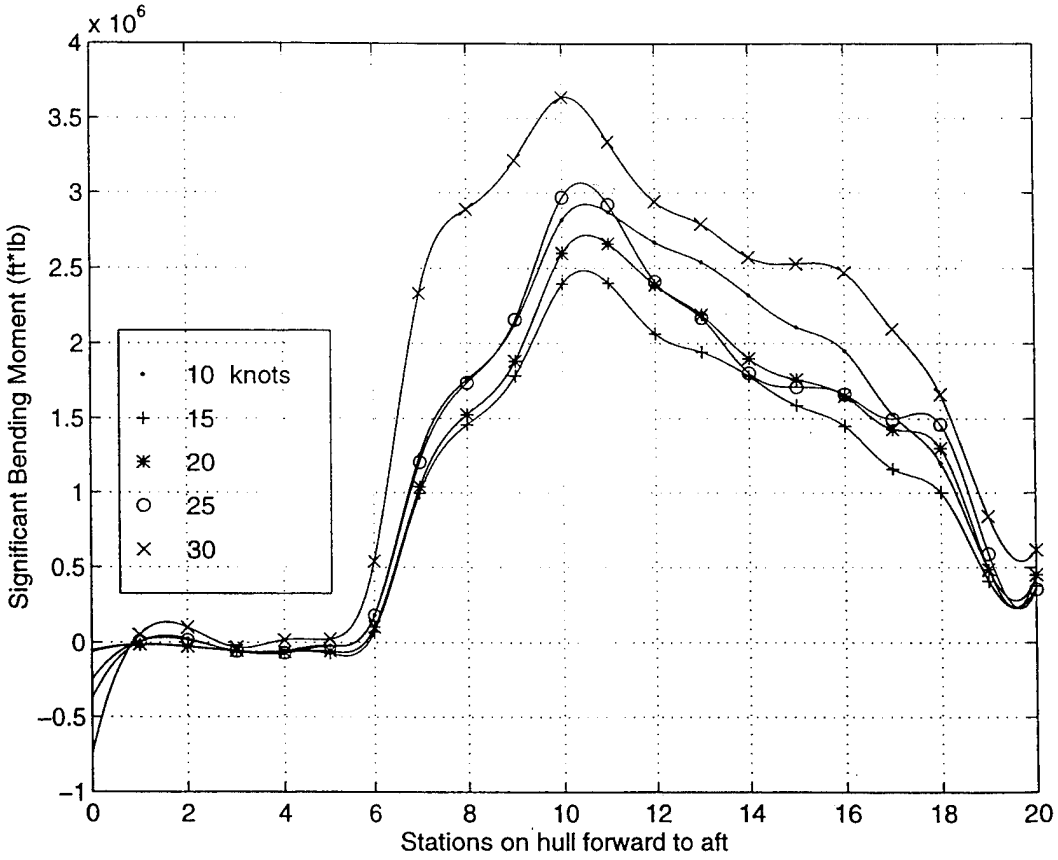

Figure (46). Dynamic Bending Moments for Sea State 5 and Head Seas.

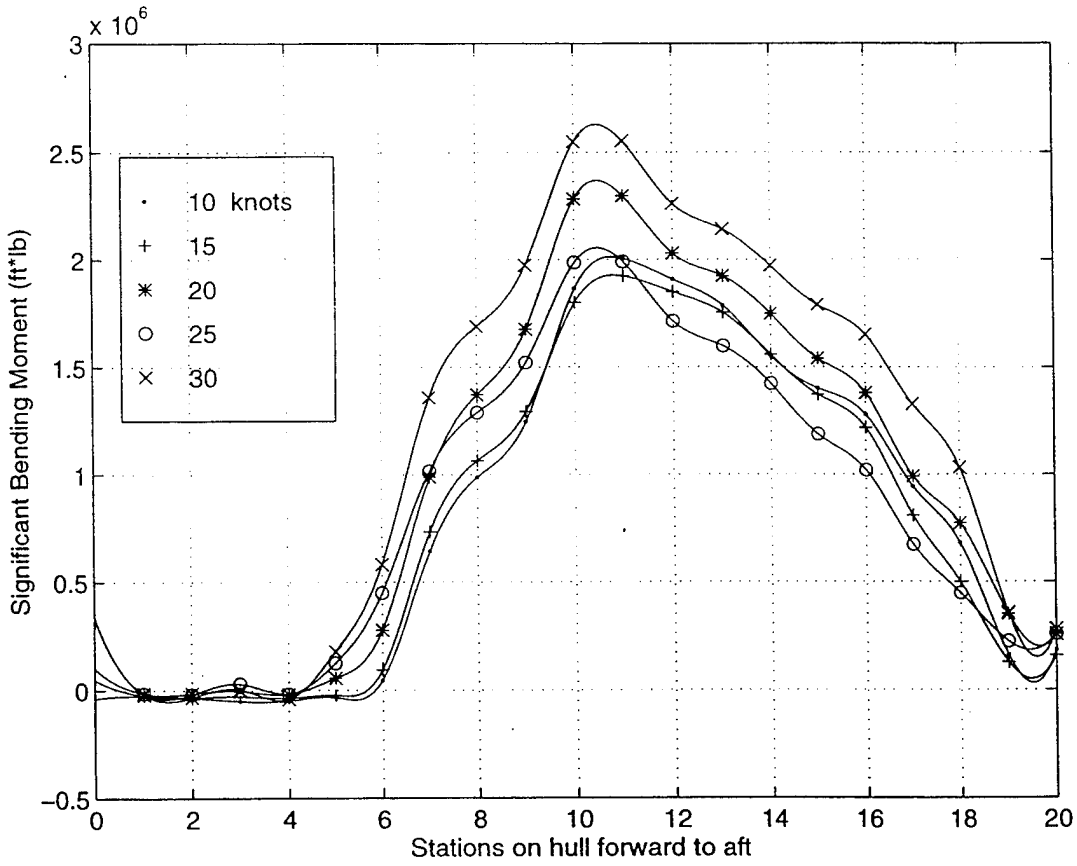

Figure (47). Dynamic Bending Moments for Sea State 6 and Following Seas.

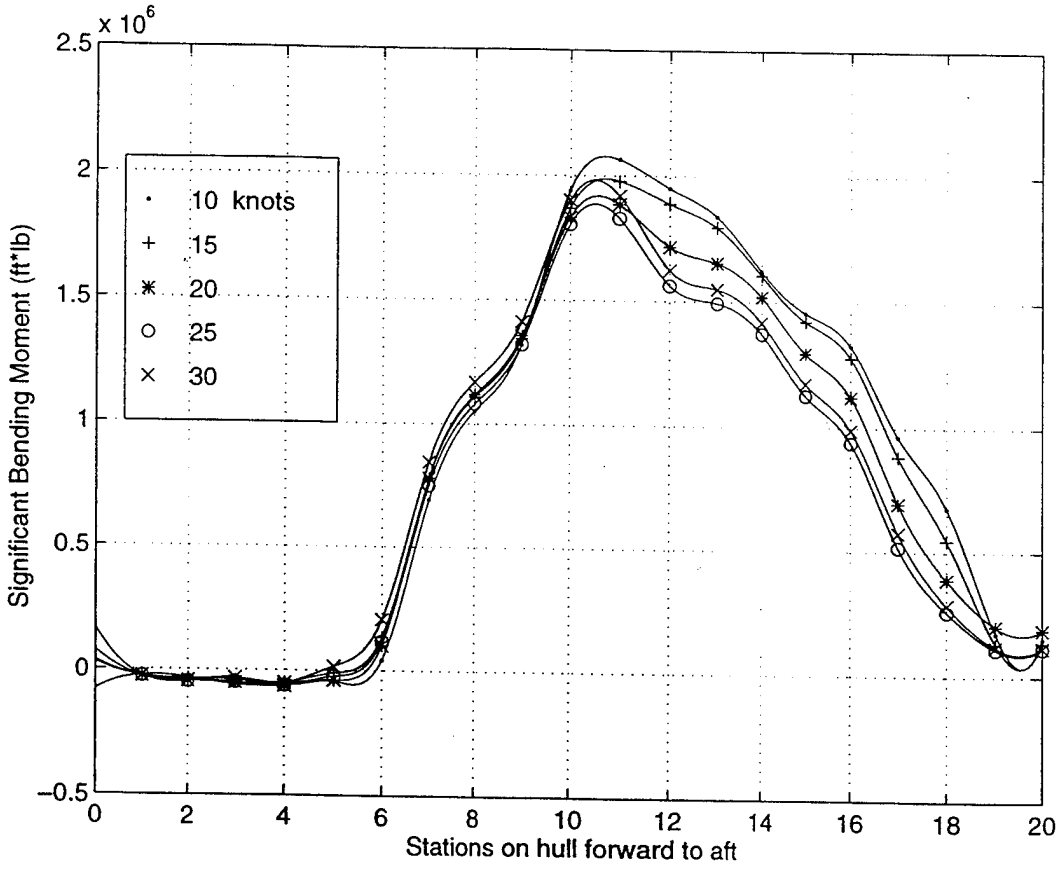

Figure (48). Dynamic Bending Moments for Sea State 6 and Quartering Seas.

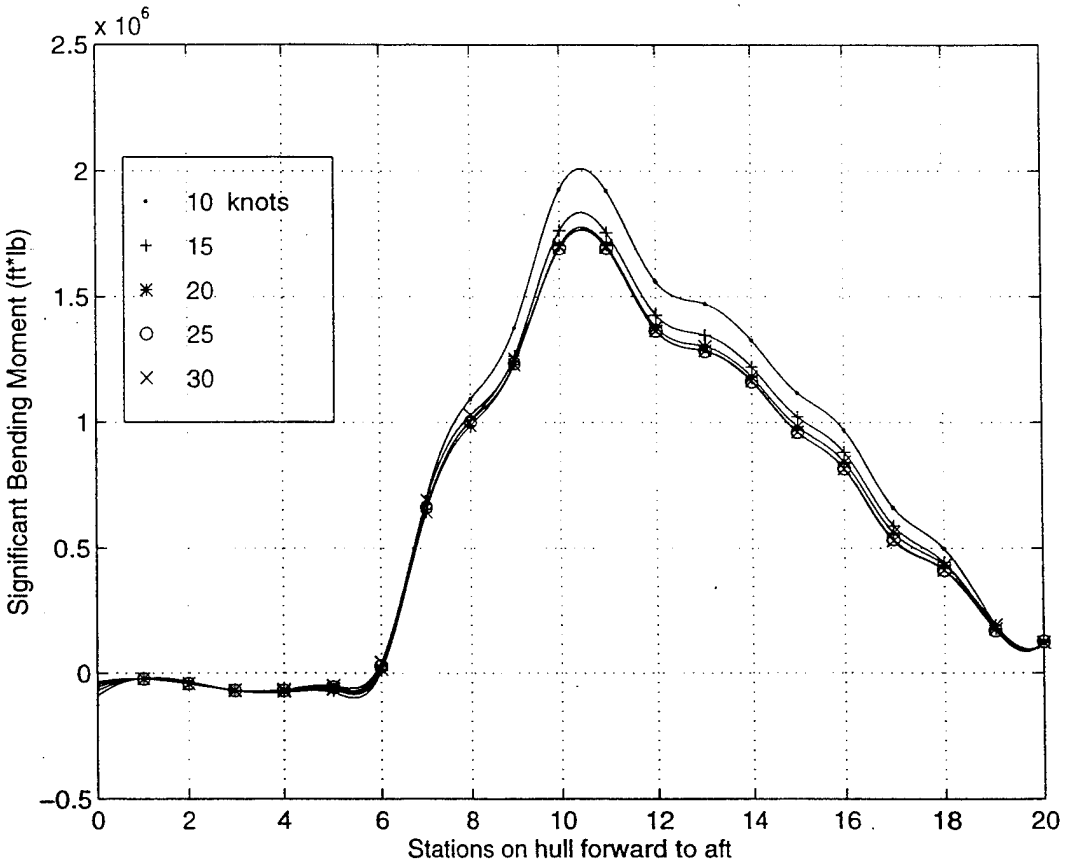

Figure (49). Dynamic Bending Moments for Sea State 6 and Beam Seas.

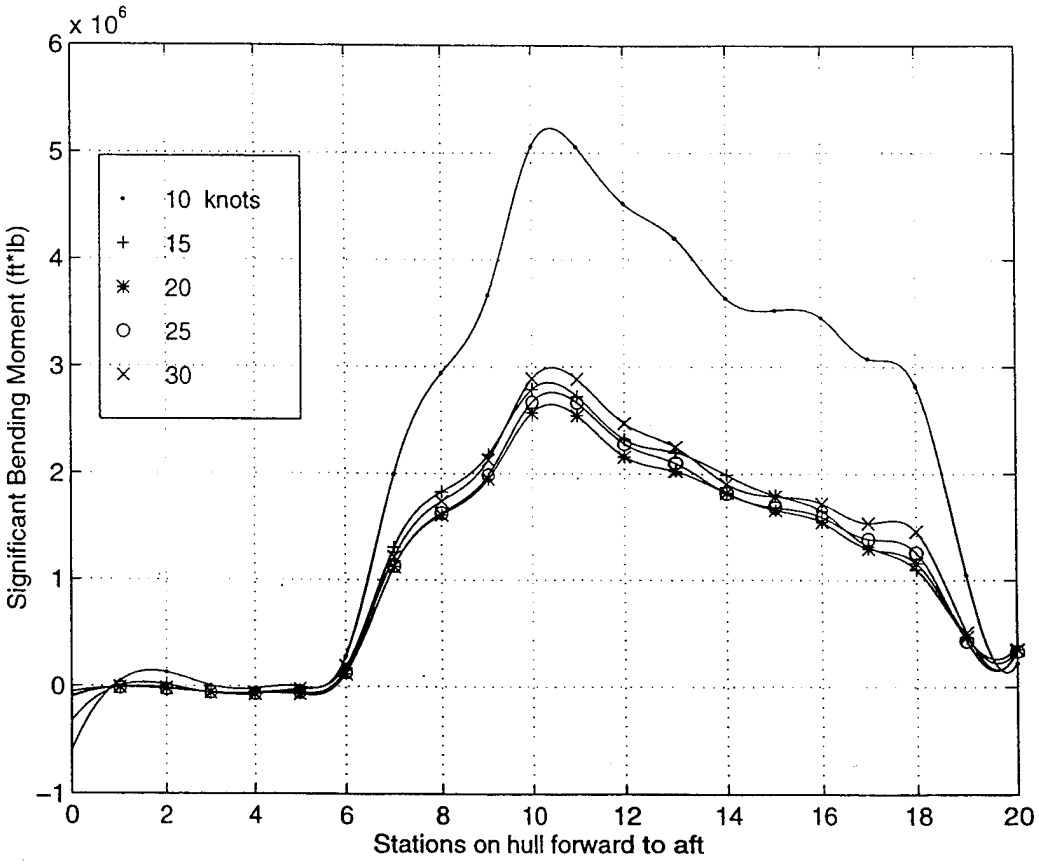

Figure (50). Dynamic Bending Moments for Sea State 6 and Bow Seas.

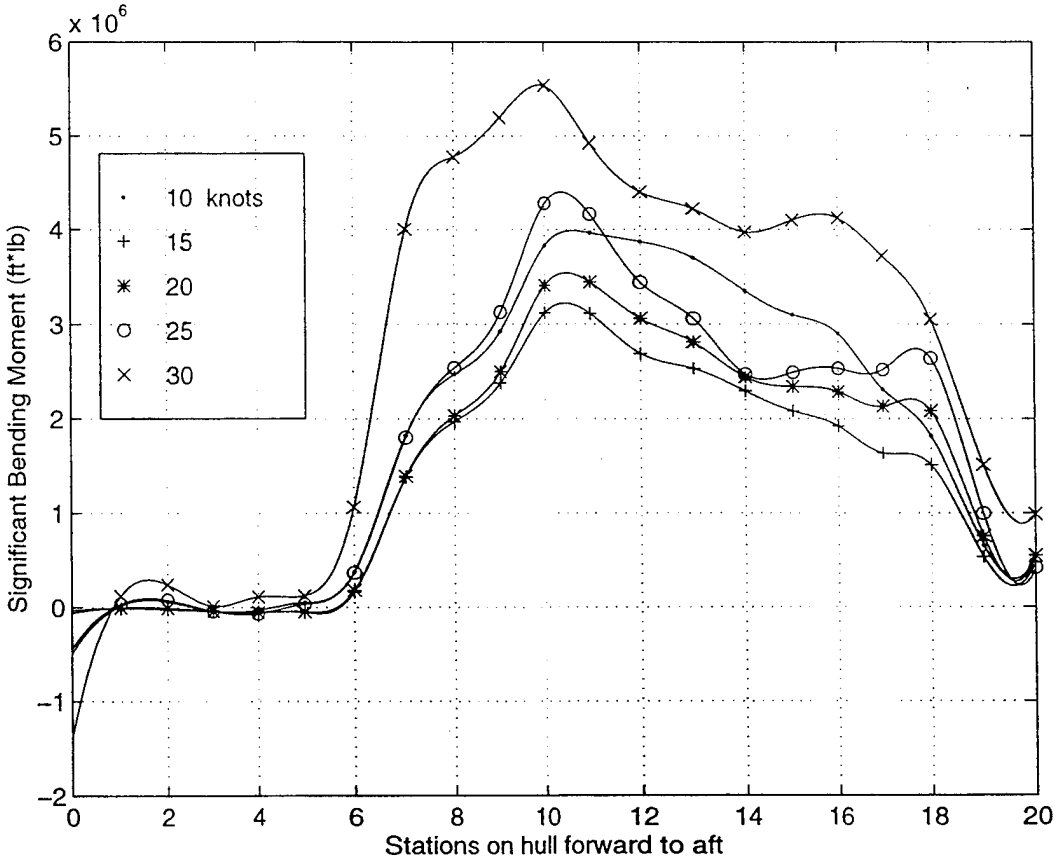

Figure (51). Dynamic Bending Moments for Sea State 6 and Head Seas.

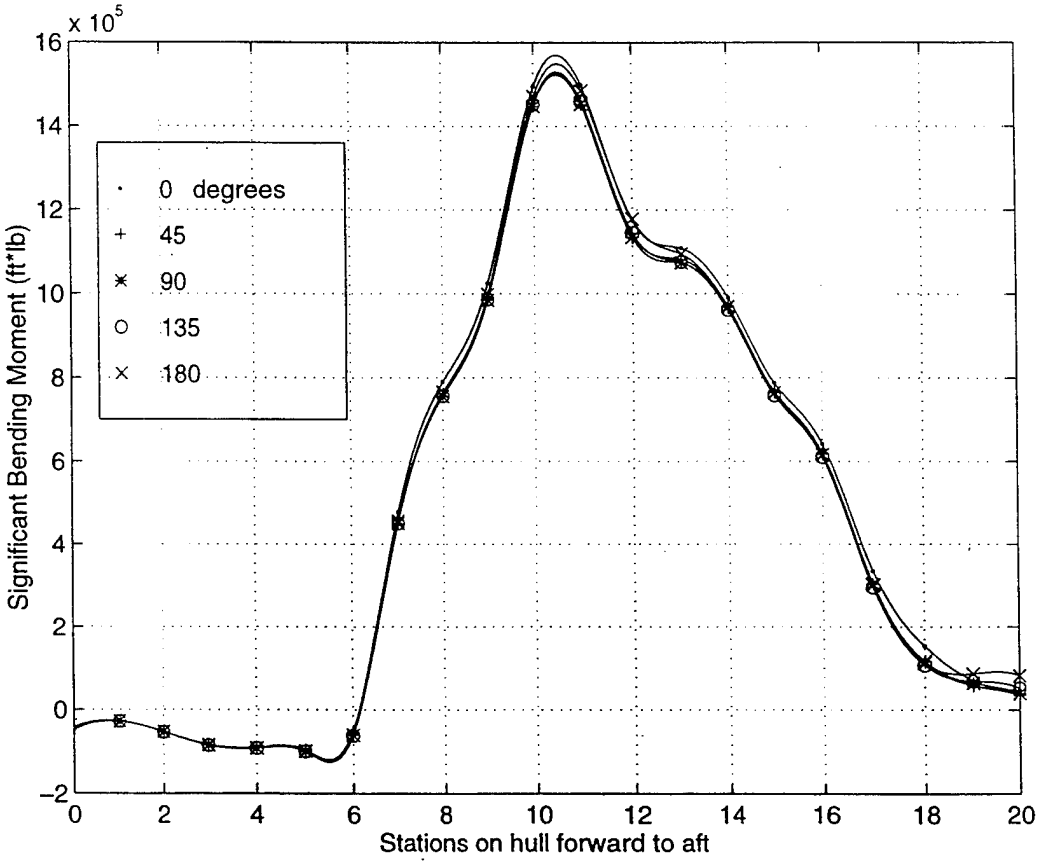

Figure (52). Dynamic Bending Moments for Sea State 2 and 10 Knots.

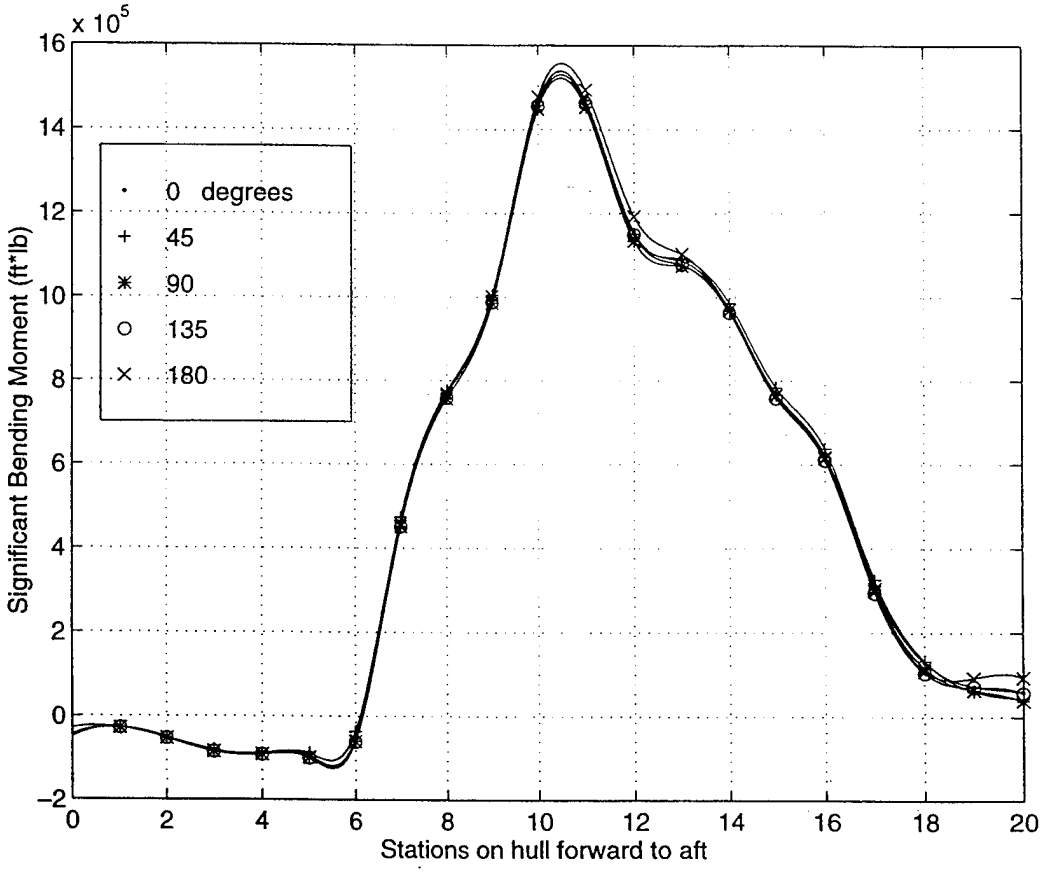

Figure (53). Dynamic Bending Moments for Sea State 2 and 15 Knots.

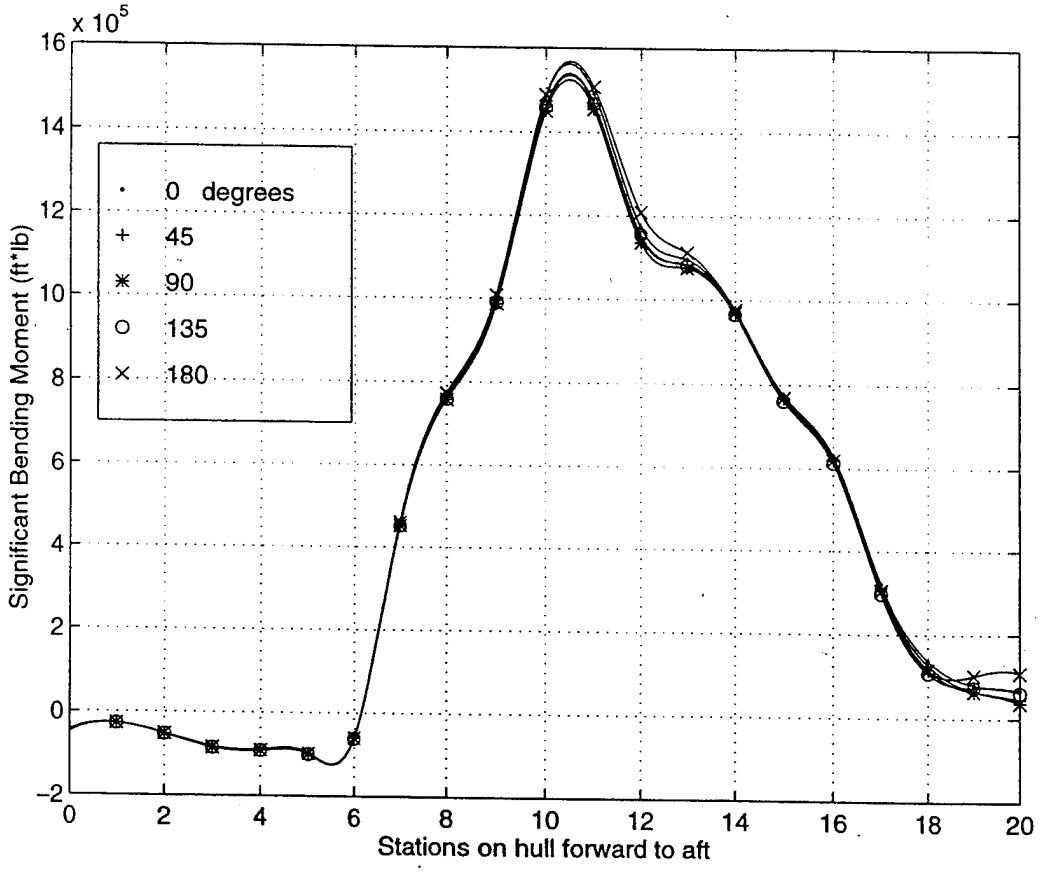

Figure (54). Dynamic Bending Moments for Sea State 2 and 20 Knots.

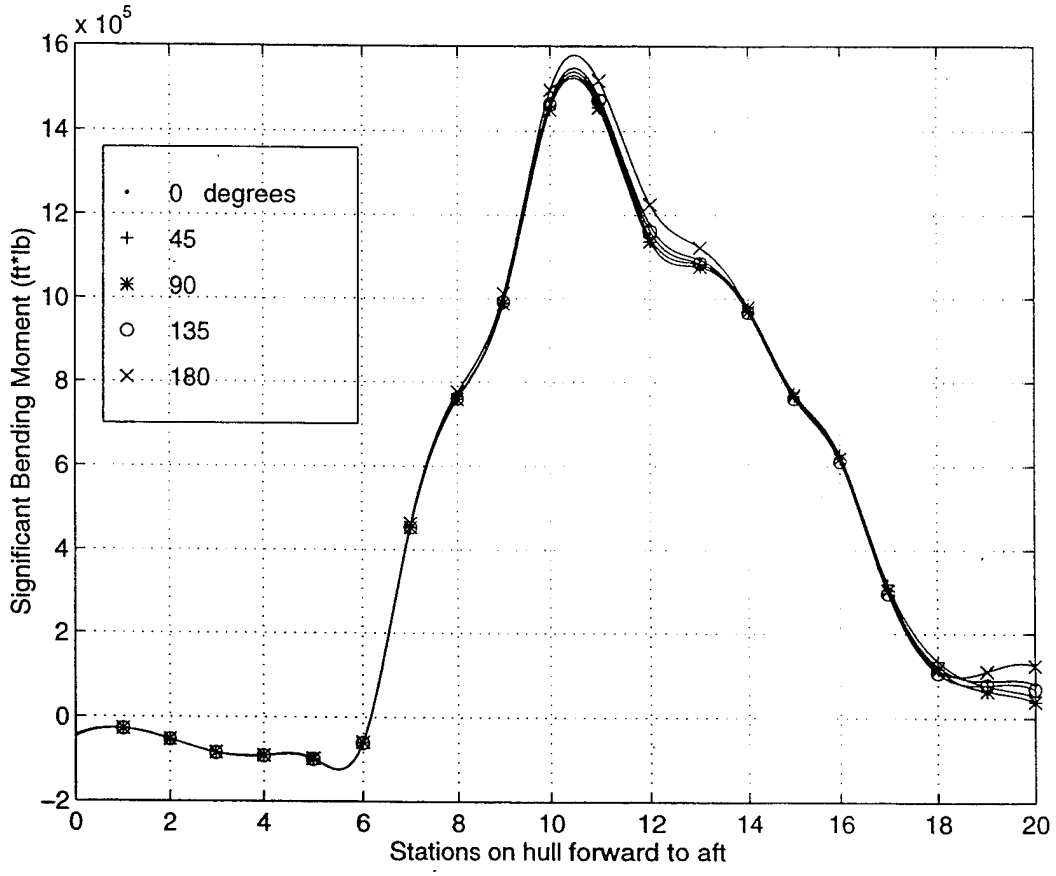

Figure (55). Dynamic Bending Moments for Sea State 2 and 25 Knots.

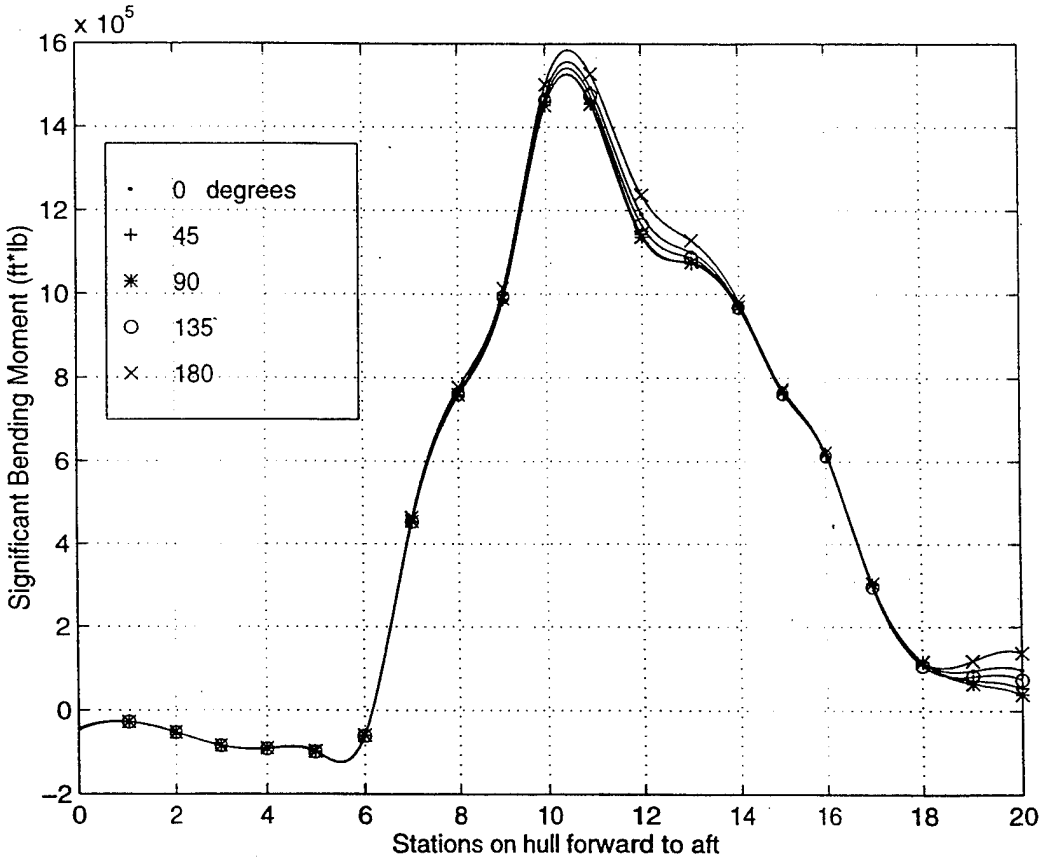

Figure (56). Dynamic Bending Moments for Sea State 2 and 30 Knots.

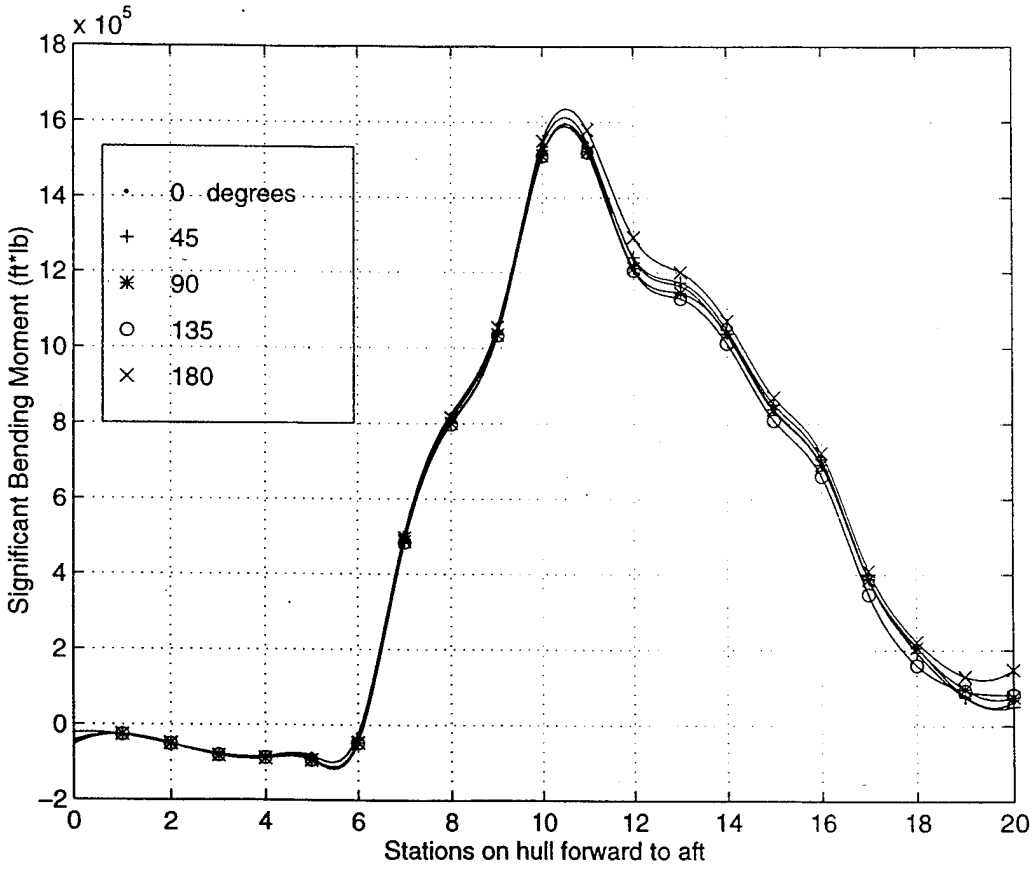

Figure (57). Dynamic Bending Moments for Sea State 3 and 10 Knots.

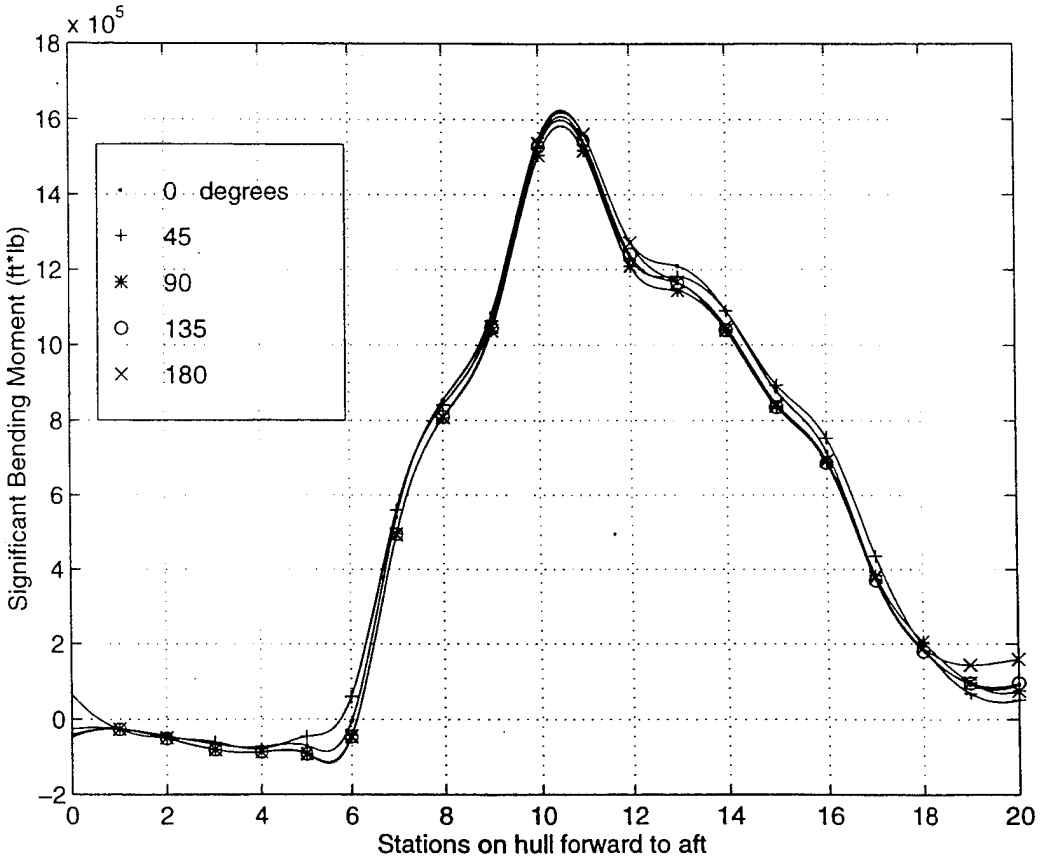

Figure (58). Dynamic Bending Moments for Sea State 3 and 15 Knots.

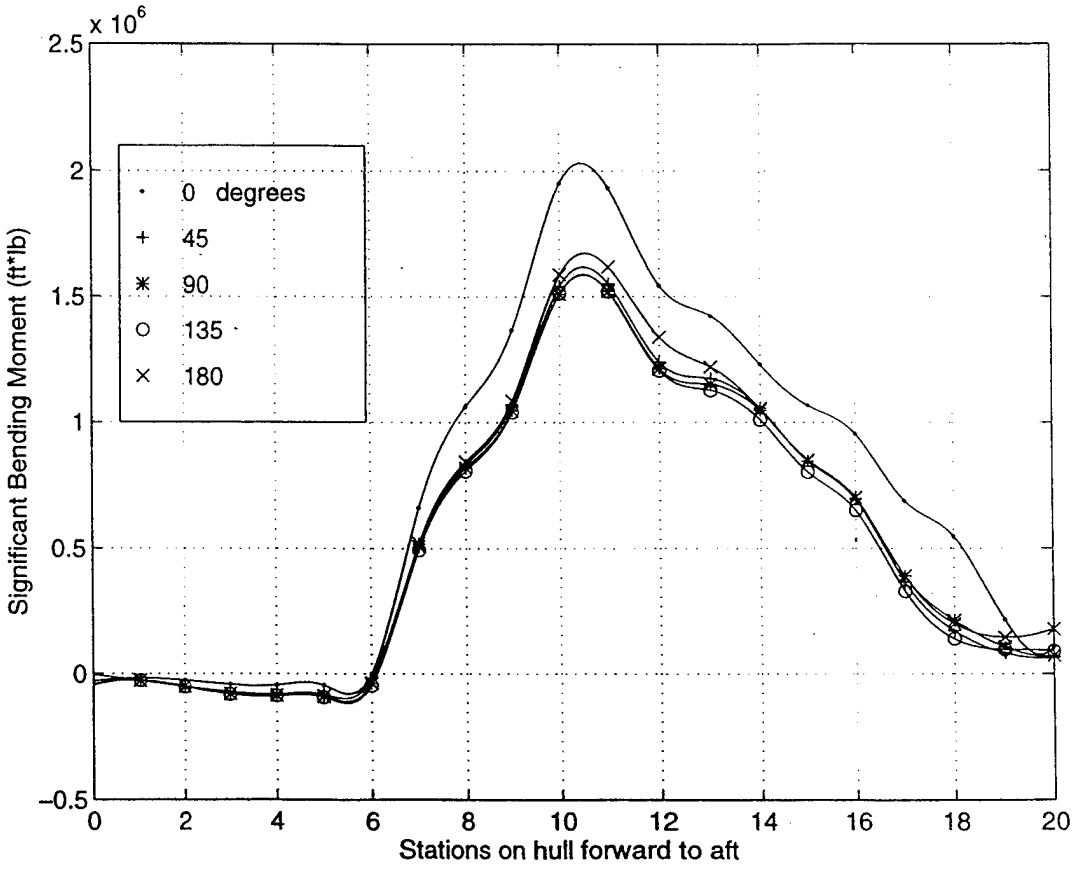

Figure (59). Dynamic Bending Moments for Sea State 3 and 20 Knots.

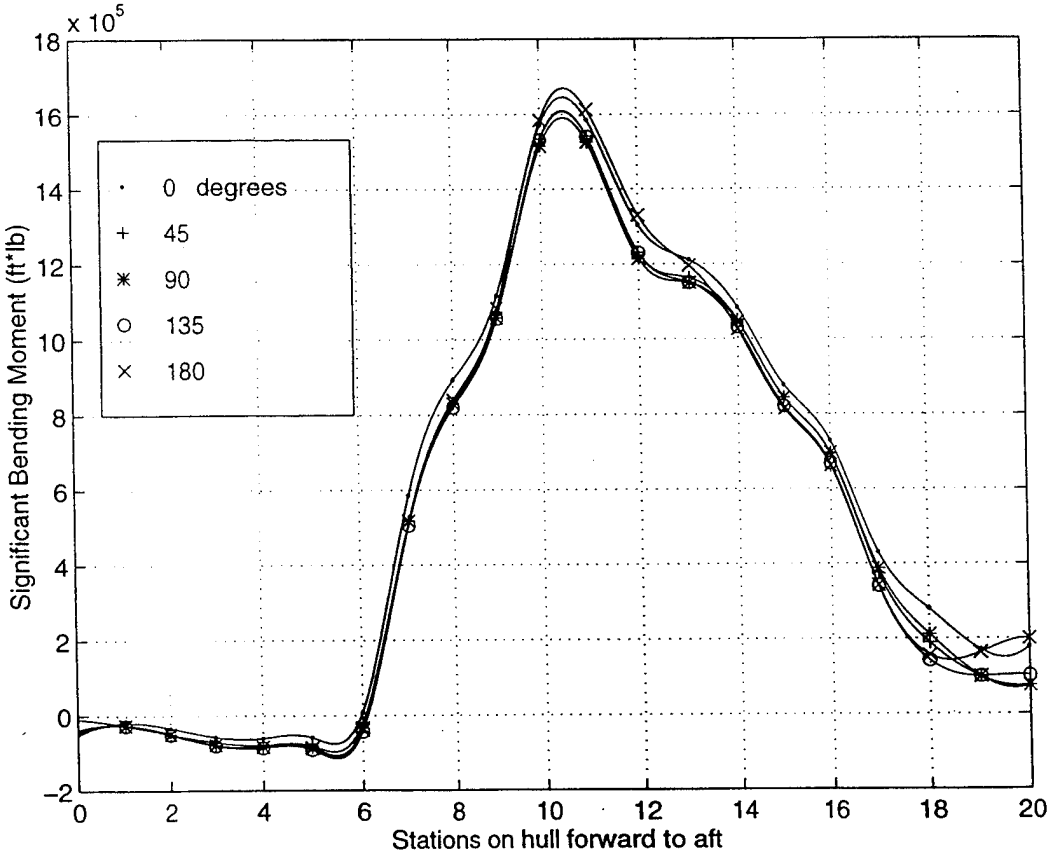

Figure (60). Dynamic Bending Moments for Sea State 3 and 25 Knots.

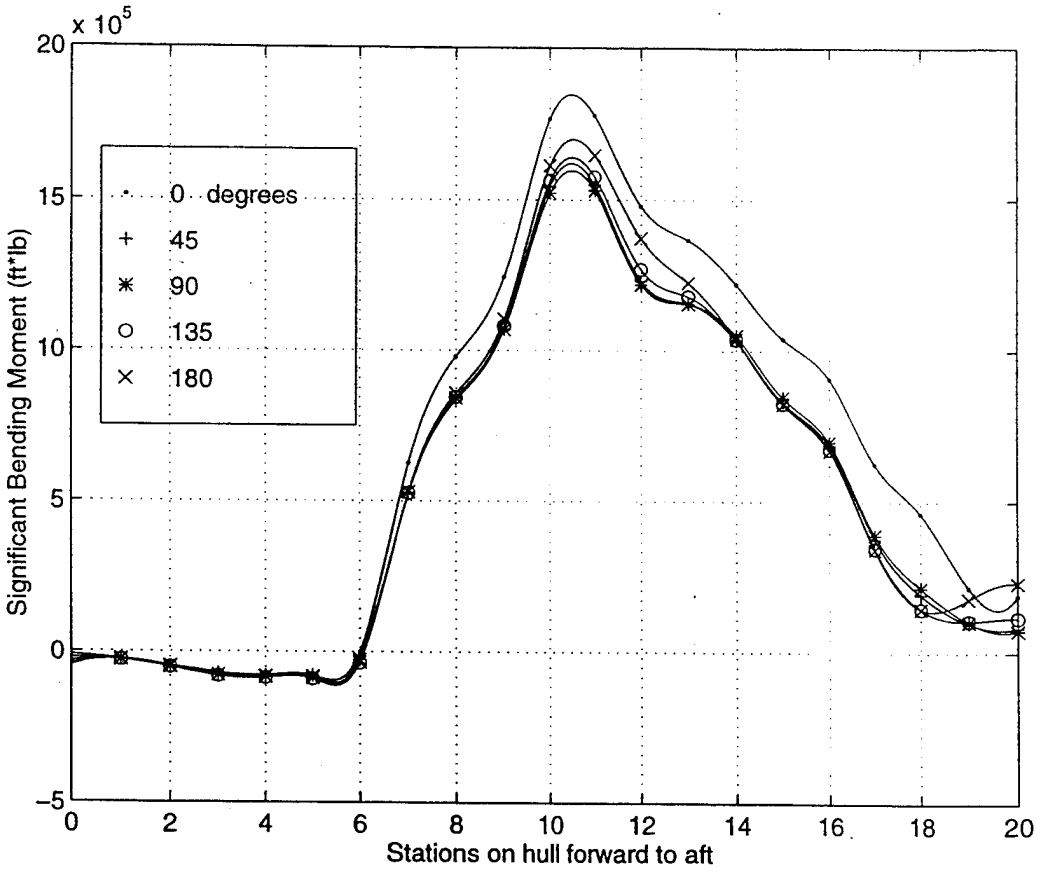

Figure (61). Dynamic Bending Moments for Sea State 3 and 30 Knots.

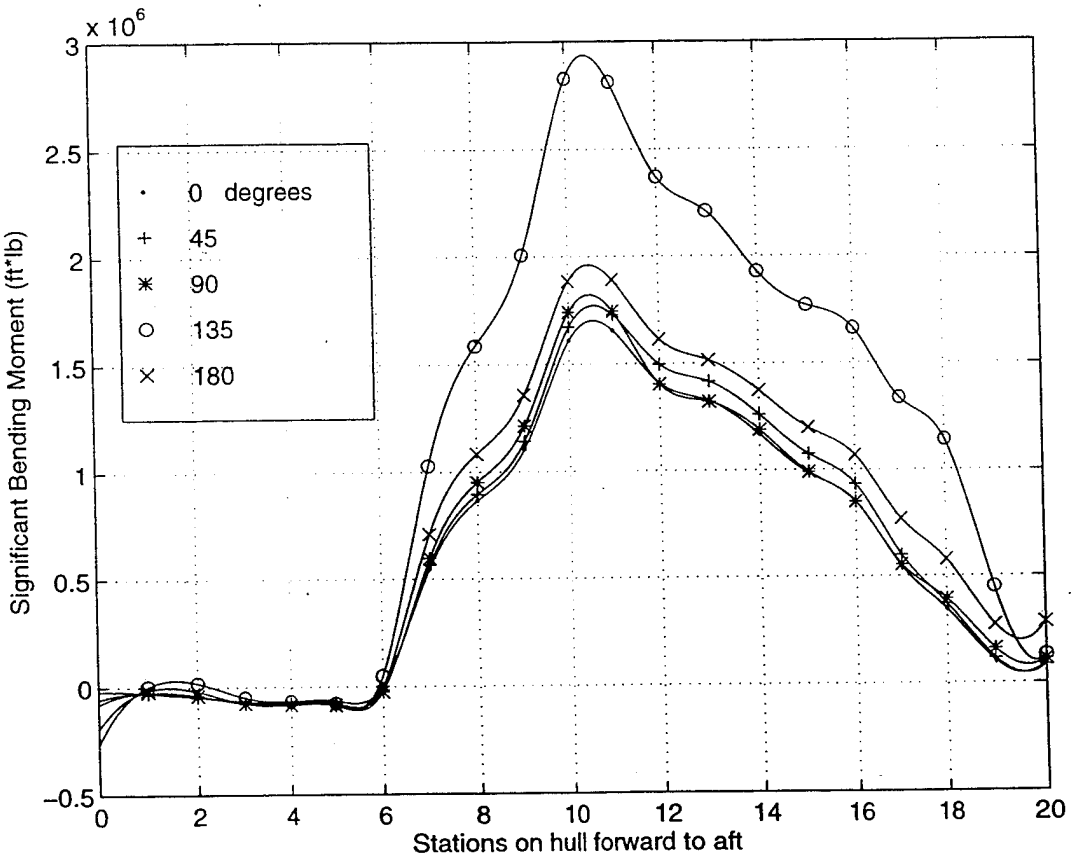

Figure (62). Dynamic Bending Moments for Sea State 4 and 10 Knots.

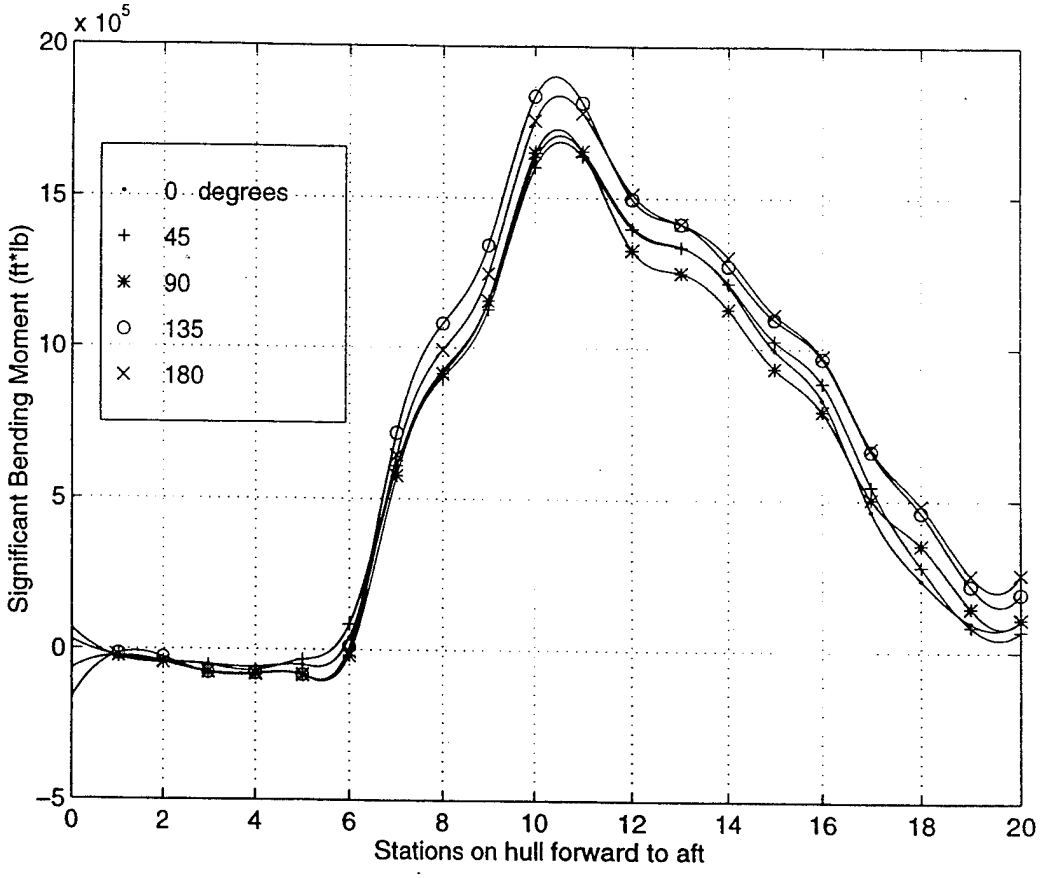

Figure (63). Dynamic Bending Moments for Sea State 4 and 15 Knots.

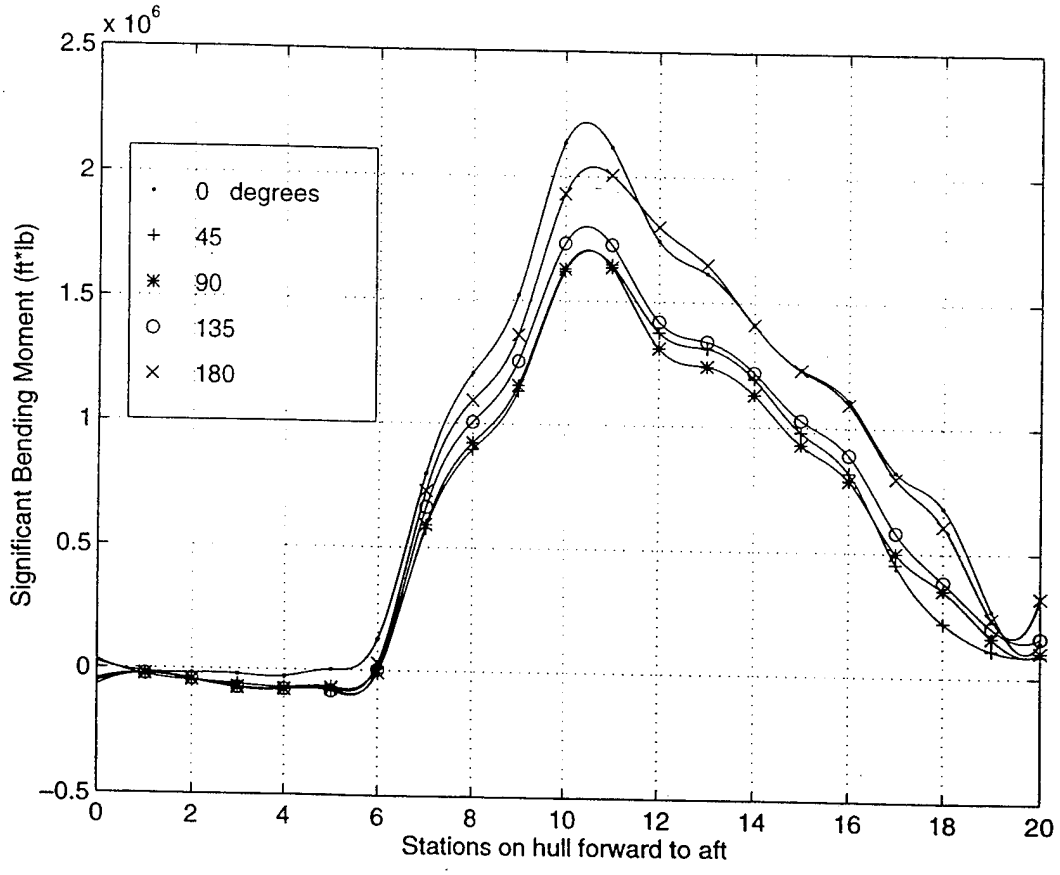

Figure (64). Dynamic Bending Moments for Sea State 4 and 20 Knots.

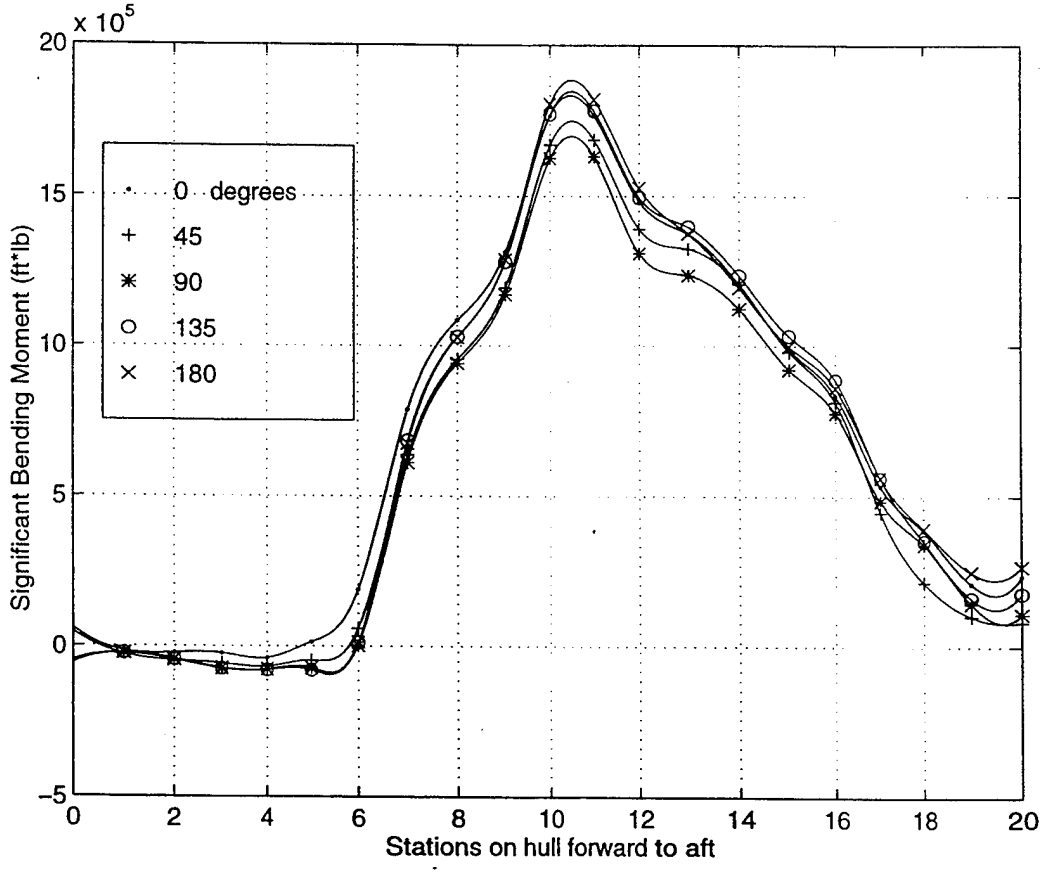

Figure (65). Dynamic Bending Moments for Sea State 4 and 25 Knots.

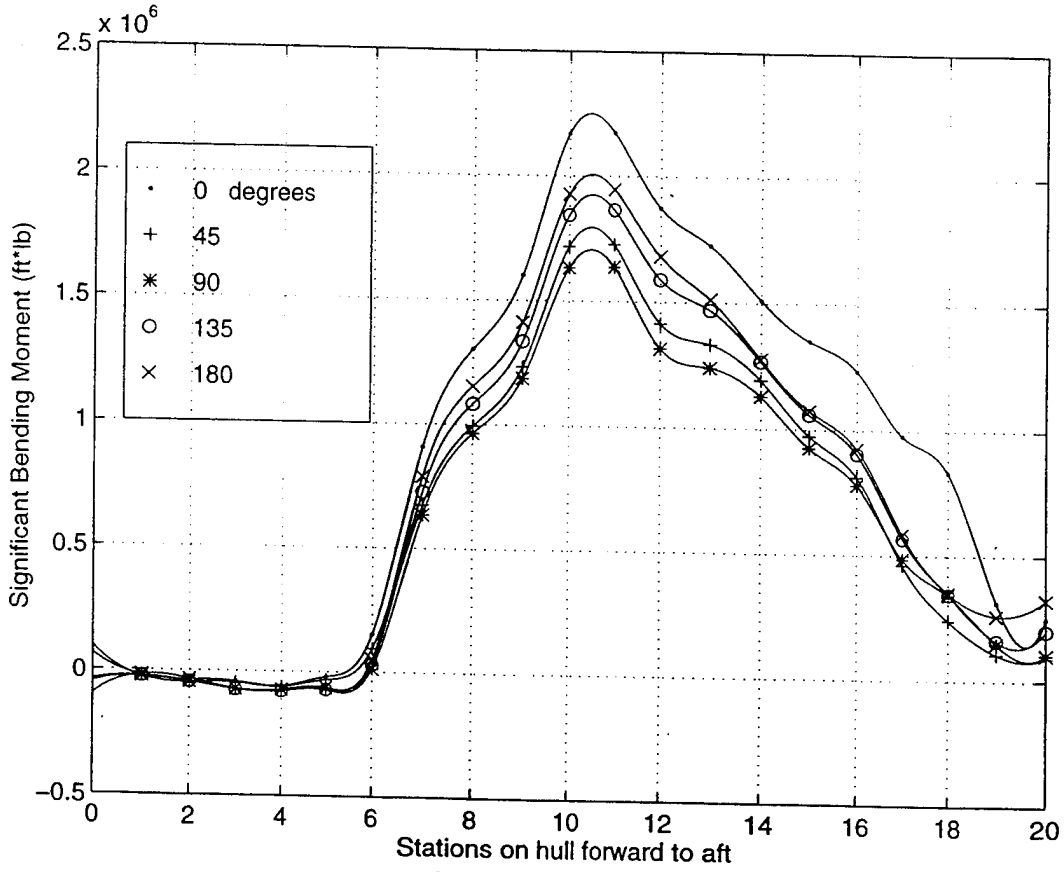

Figure (66). Dynamic Bending Moments for Sea State 4 and 30 Knots.

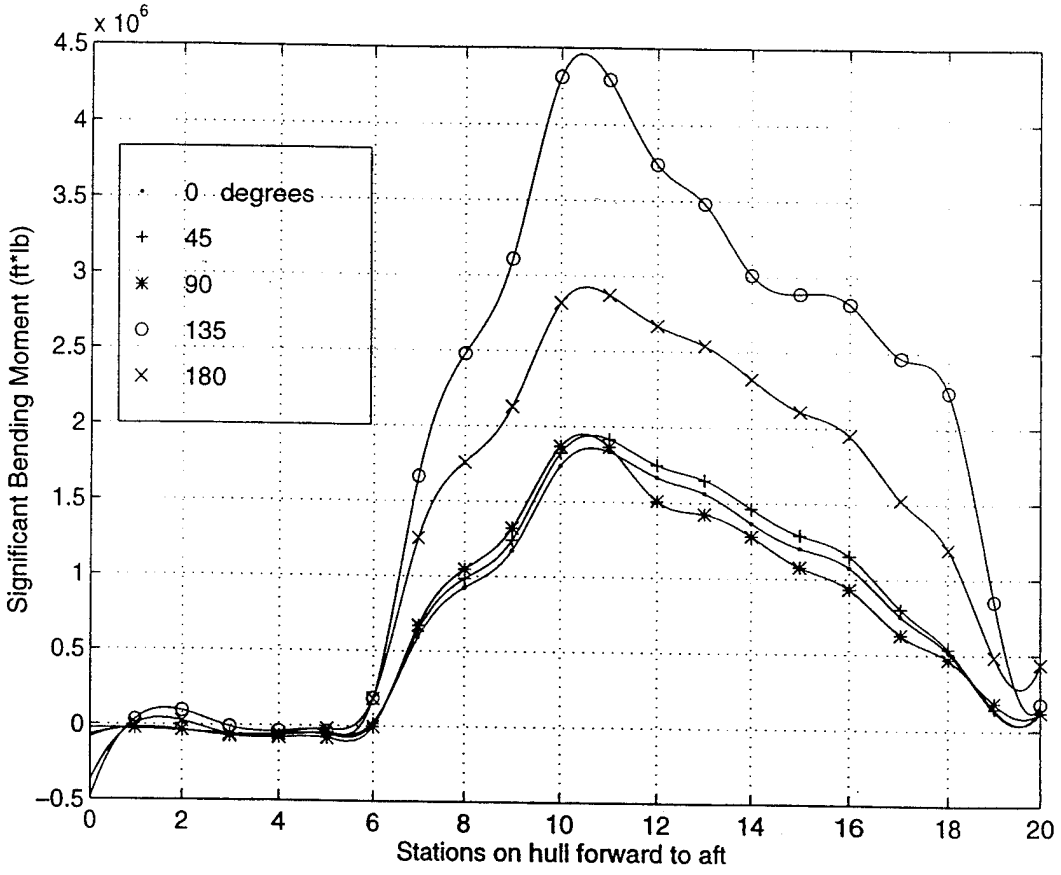

Figure (67). Dynamic Bending Moments for Sea State 5 and 10 Knots.

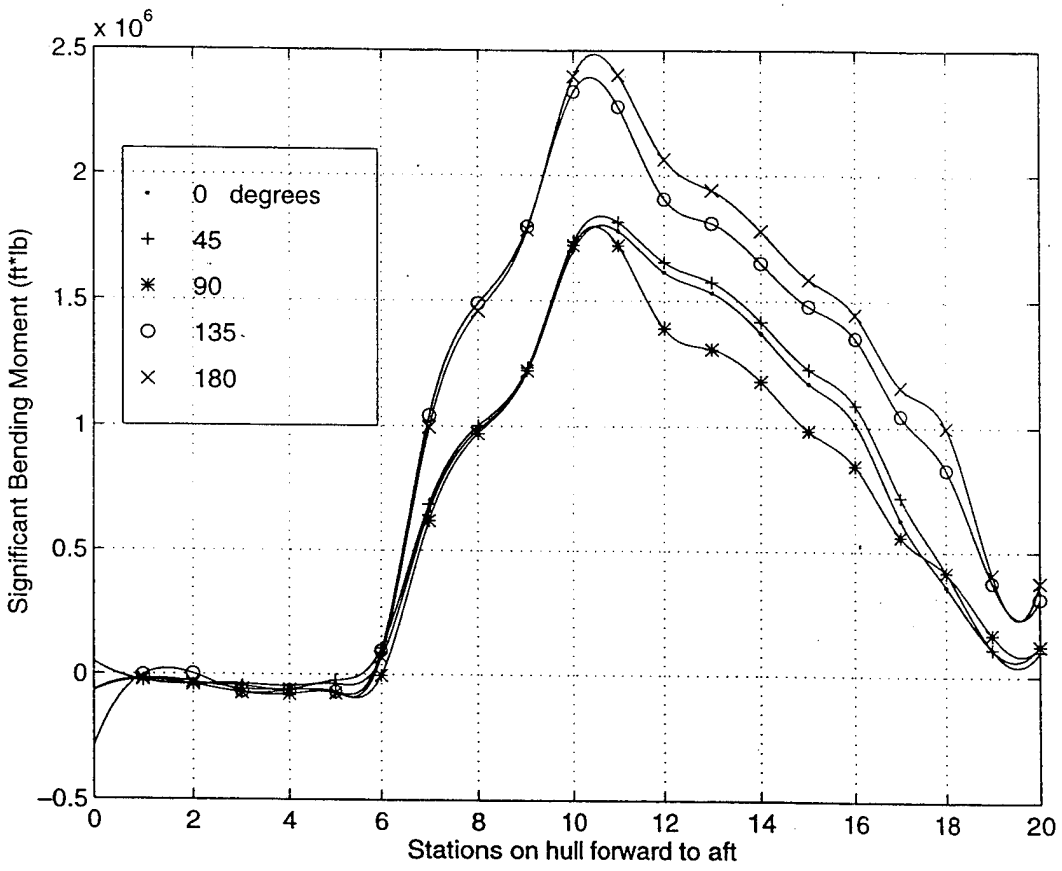

Figure (68). Dynamic Bending Moments for Sea State 5 and 15 Knots.

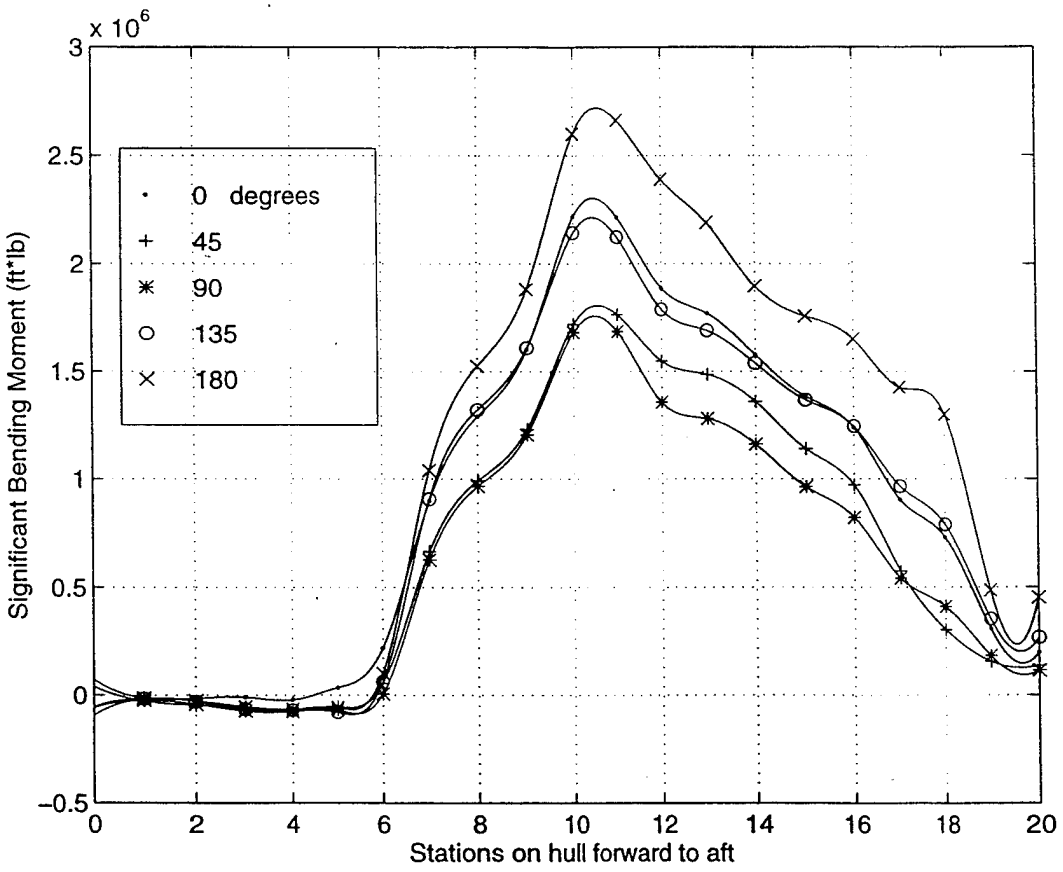

Figure (69). Dynamic Bending Moments for Sea State 5 and 20 Knots.

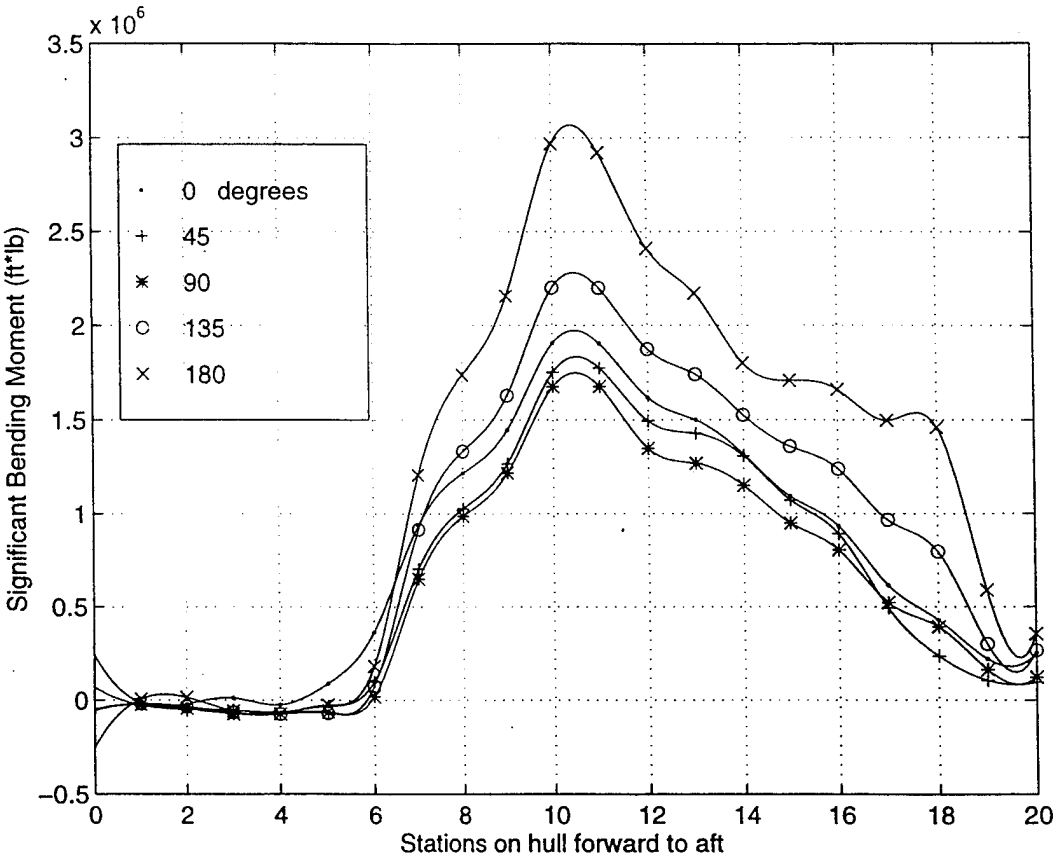

Figure (70). Dynamic Bending Moments for Sea State 5 and 25 Knots.

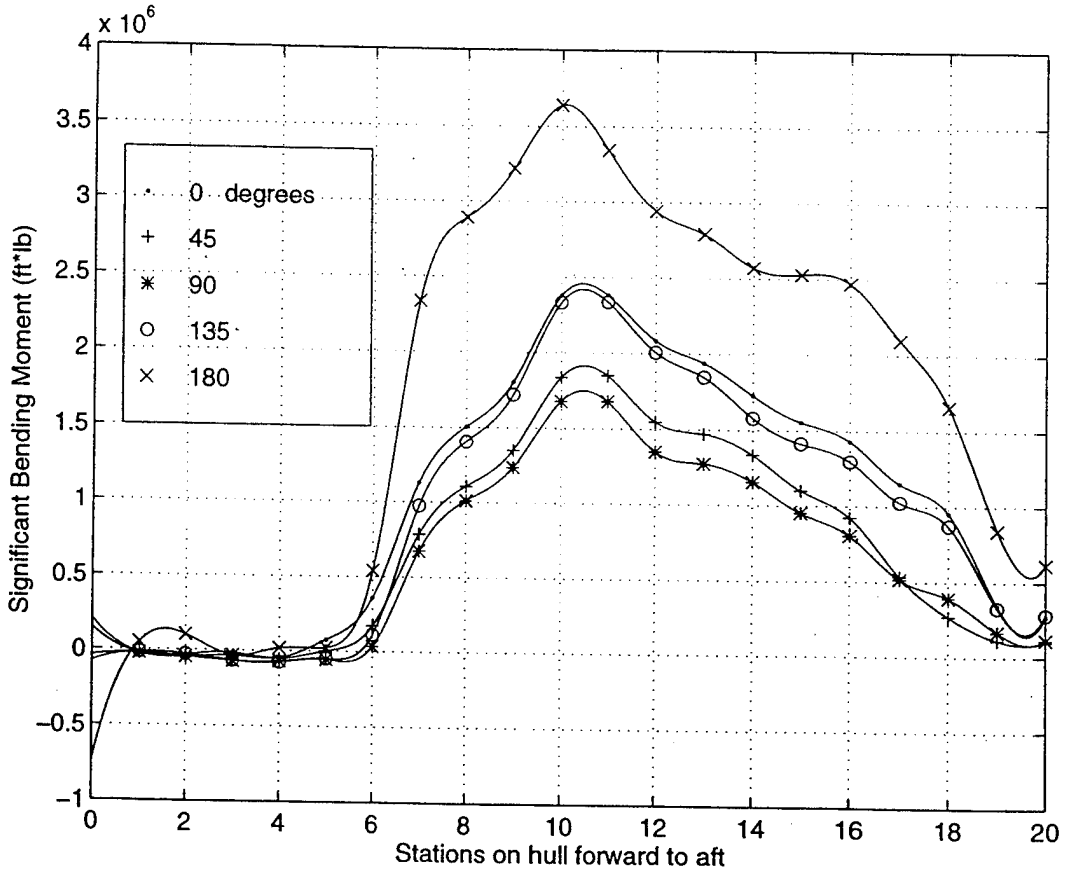

Figure (71). Dynamic Bending Moments for Sea State 5 and 30 Knots.

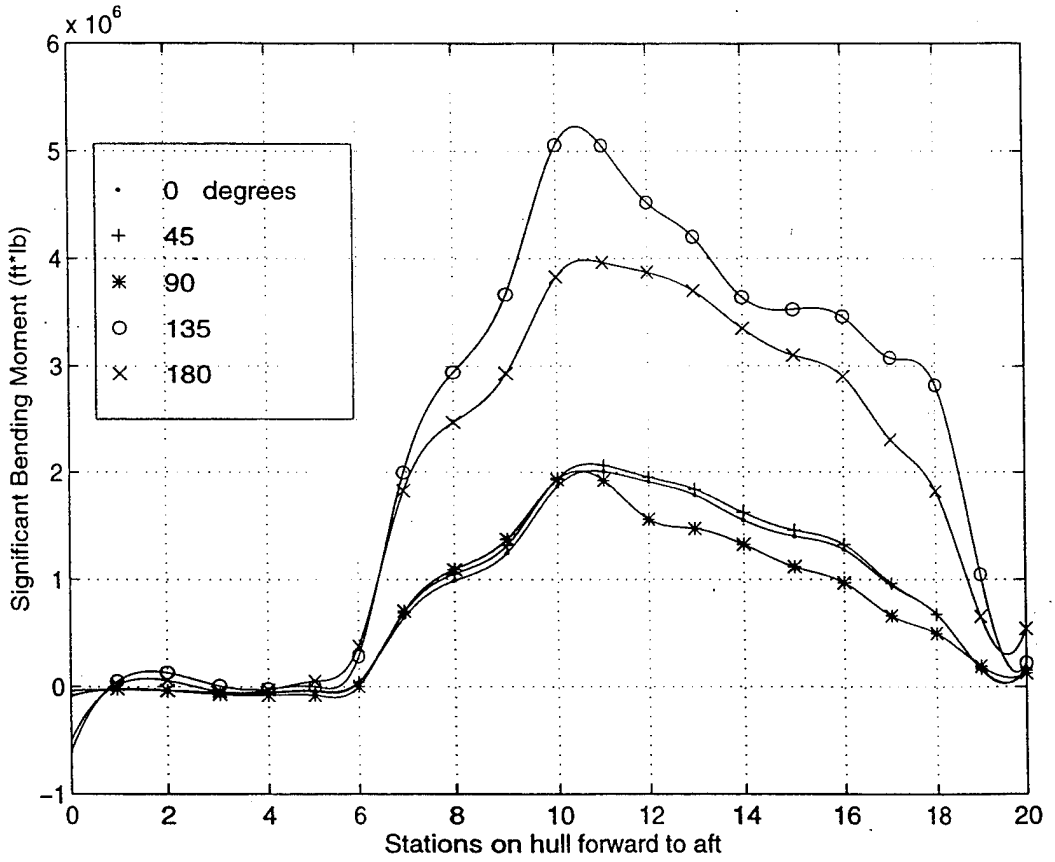

Figure (72). Dynamic Bending Moments for Sea State 6 and 10 Knots.

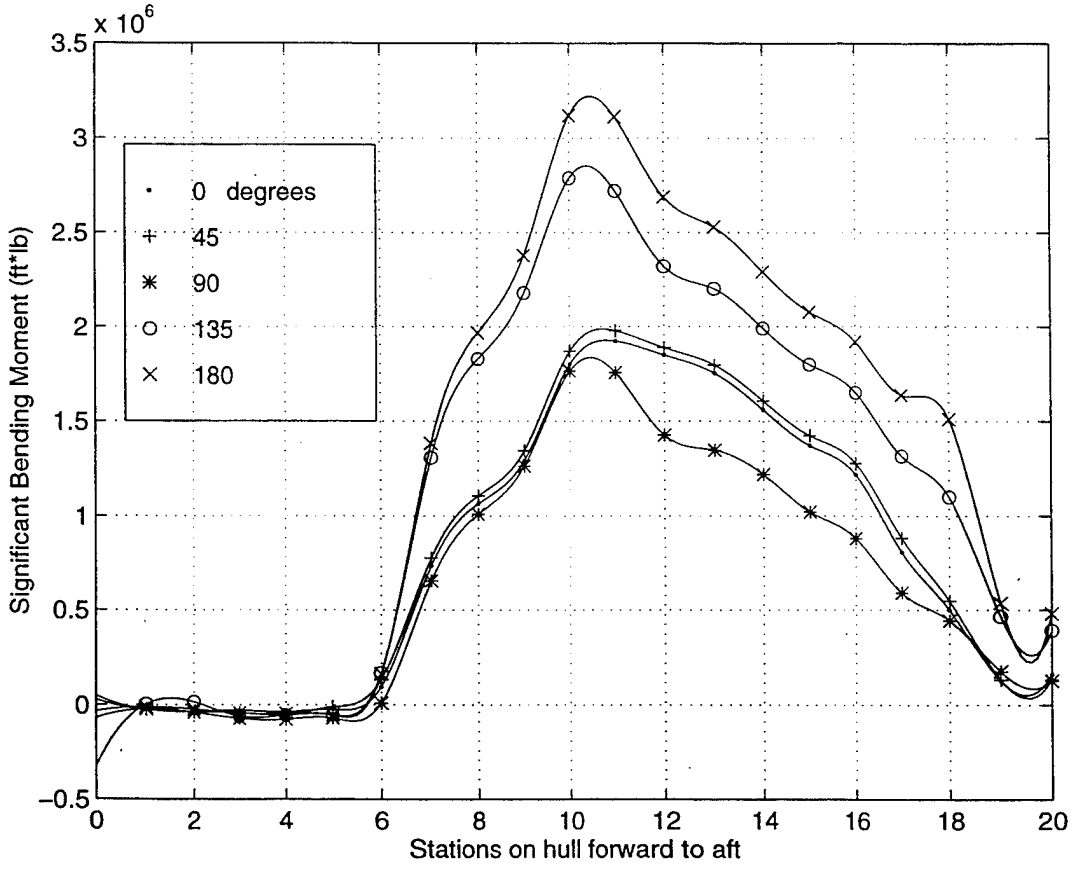

Figure (73). Dynamic Bending Moments for Sea State 6 and 15 Knots.

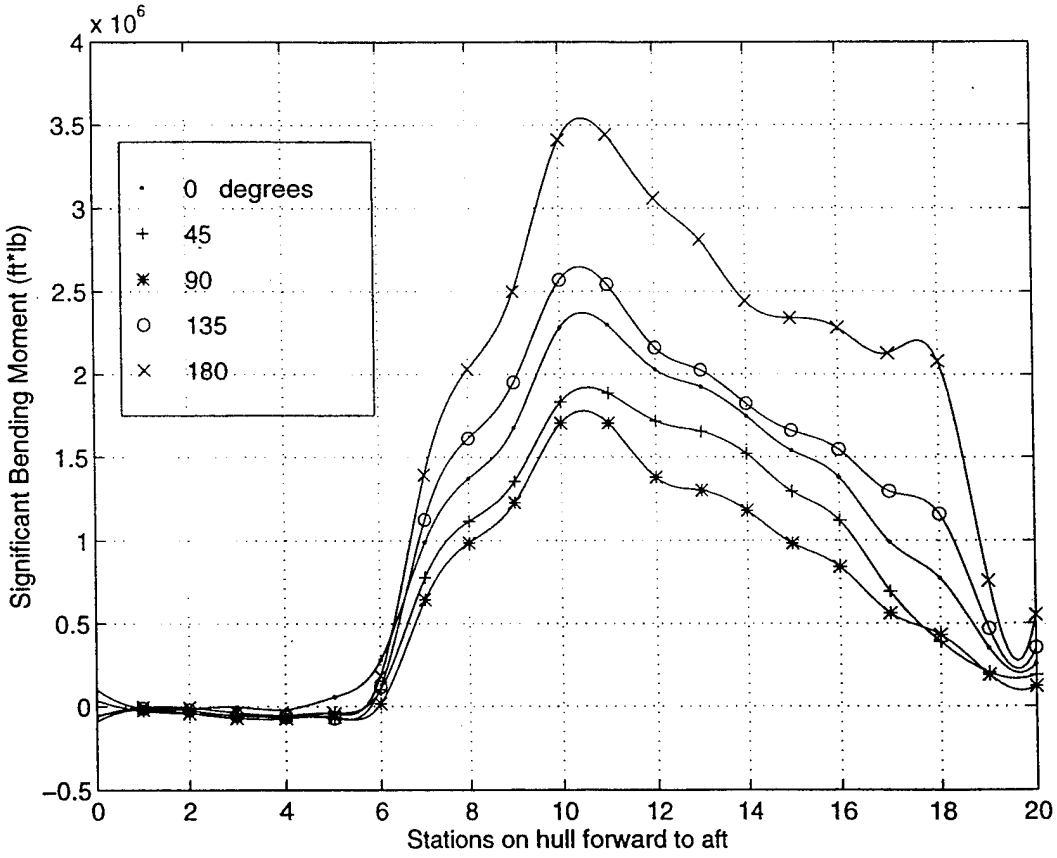

Figure (74). Dynamic Bending Moments for Sea State 6 and 20 Knots.

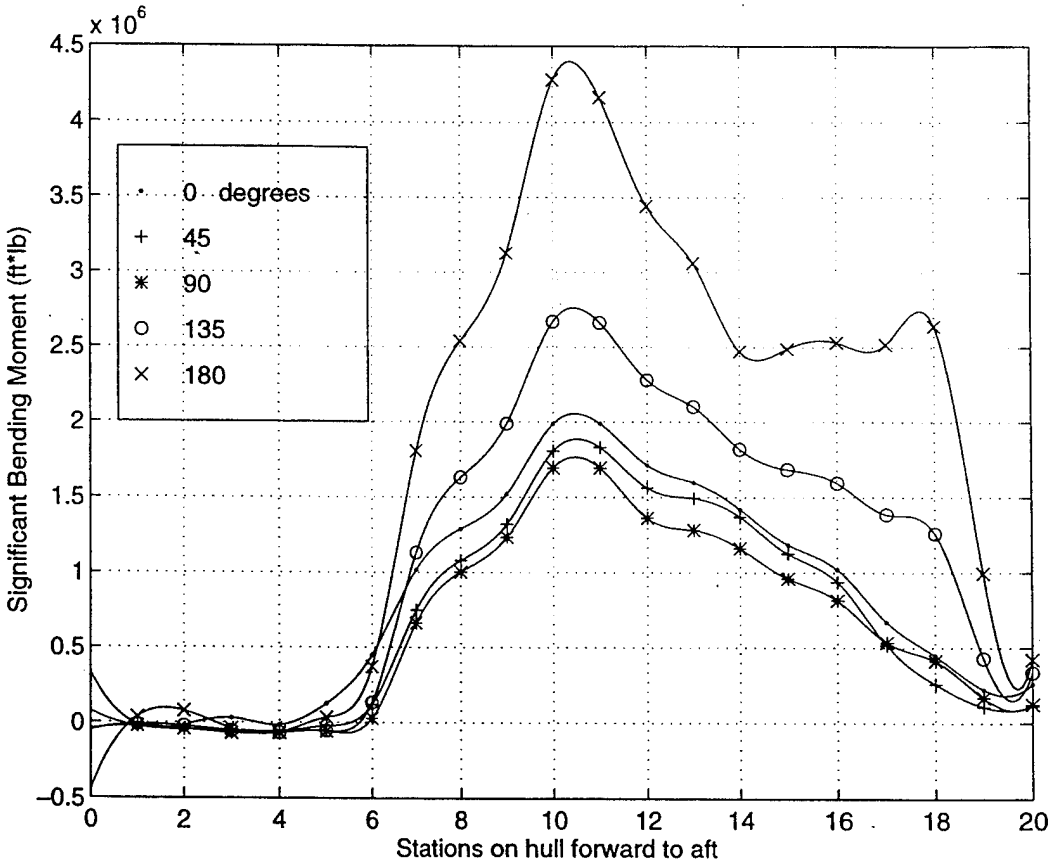

Figure (75). Dynamic Bending Moments for Sea State 6 and 25 Knots.

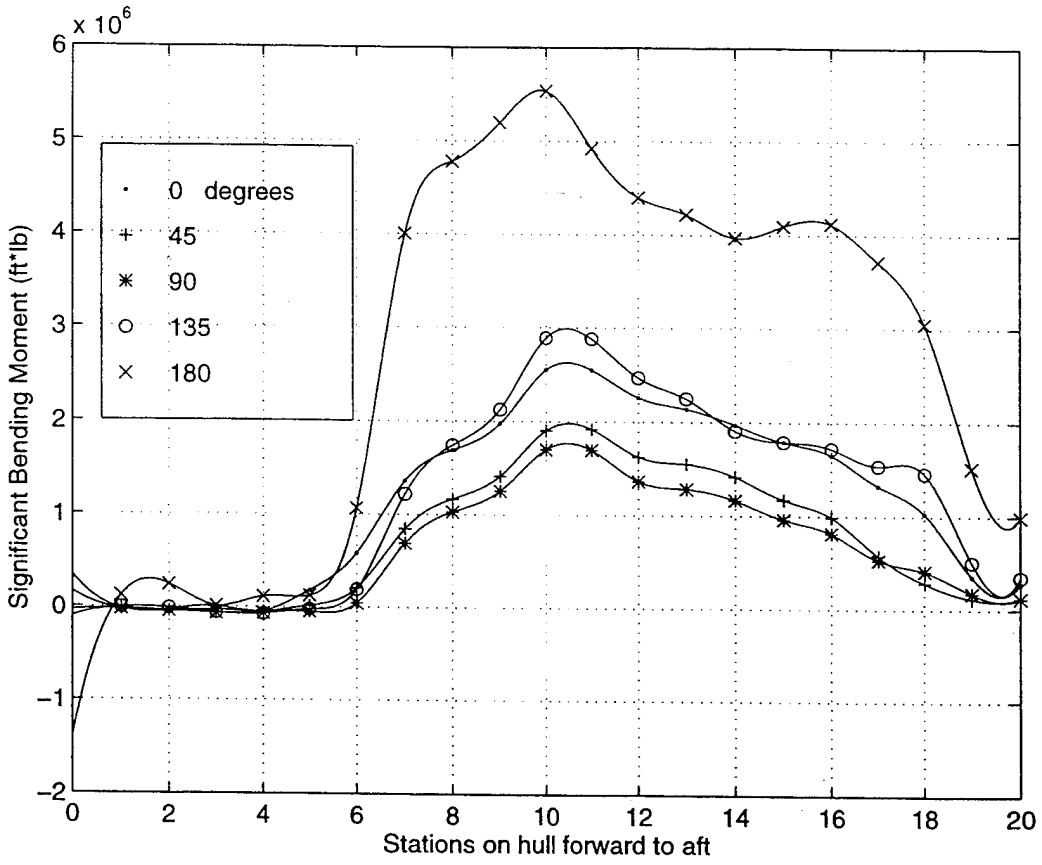

Figure (76). Dynamic Bending Moments for Sea State 6 and 30 Knots.

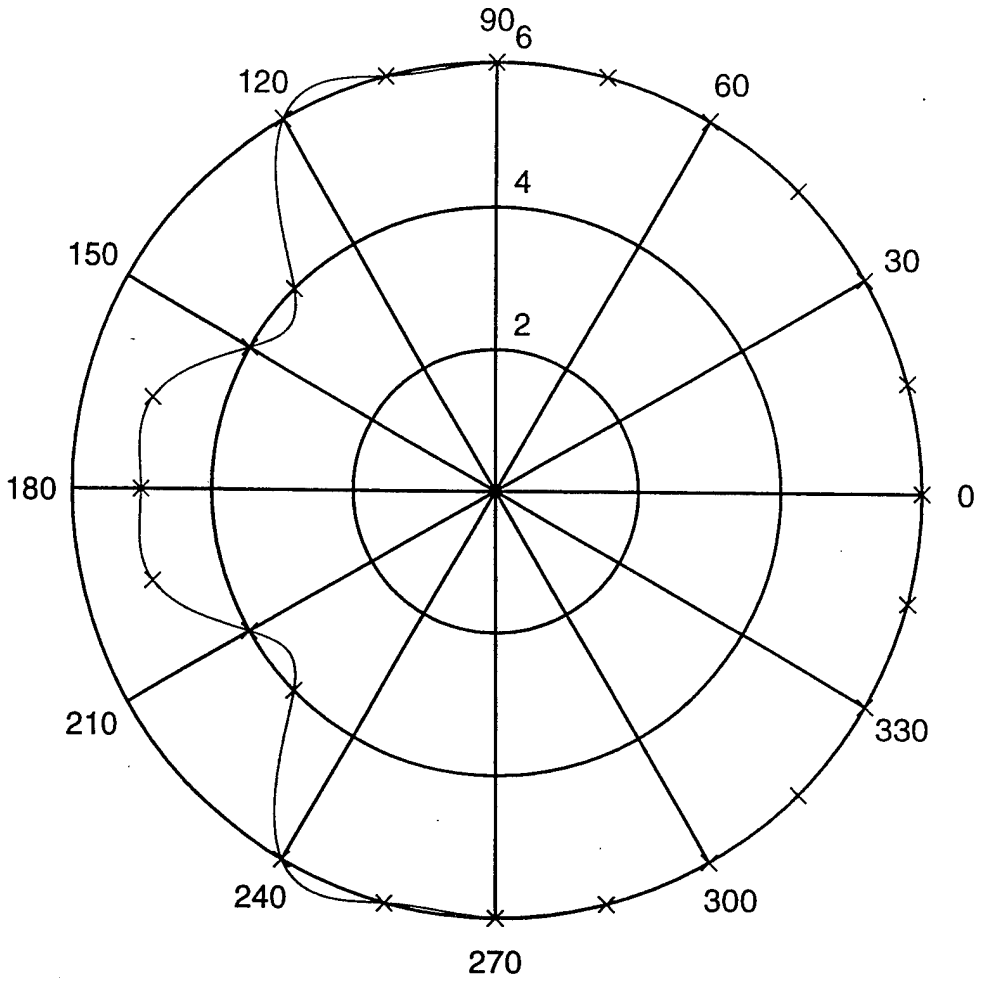

Figure (77). Operability at 10 kts, Sea State Versus Heading.

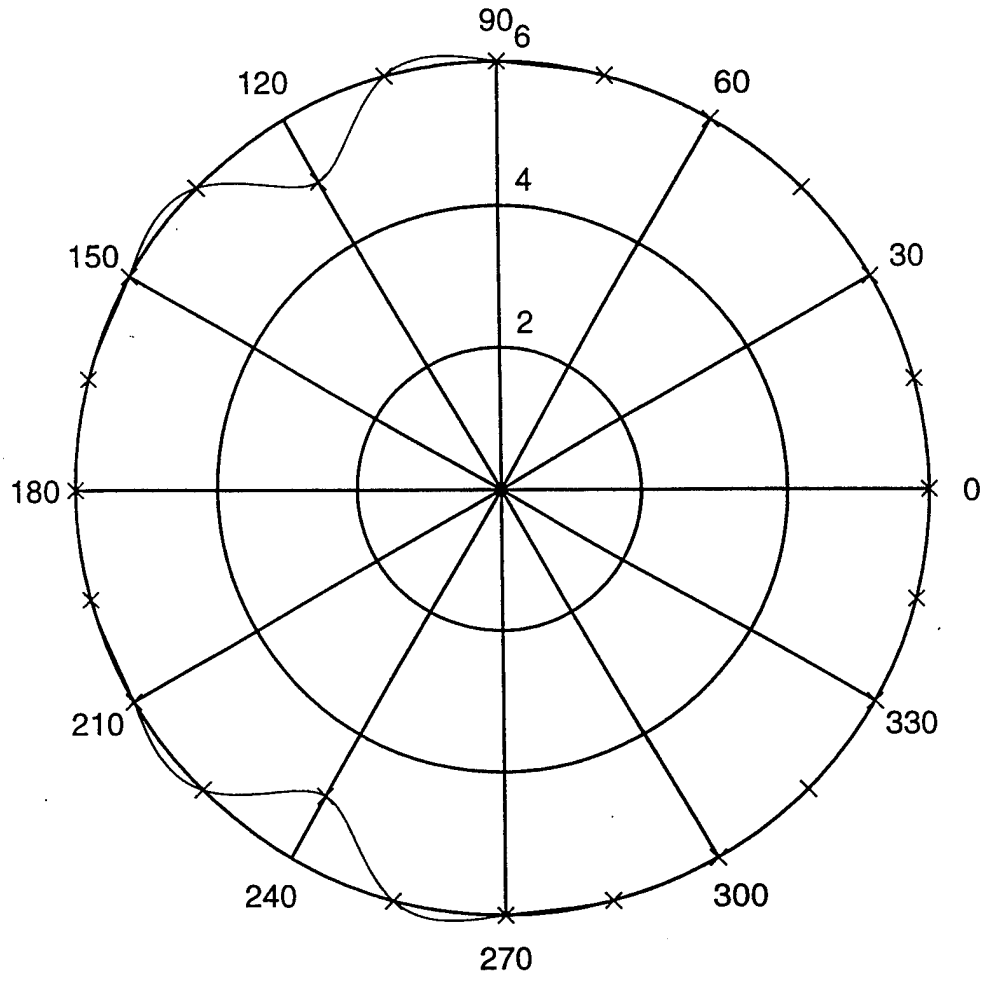

Figure (78). Operability at 15 kts, Sea State Versus Heading.

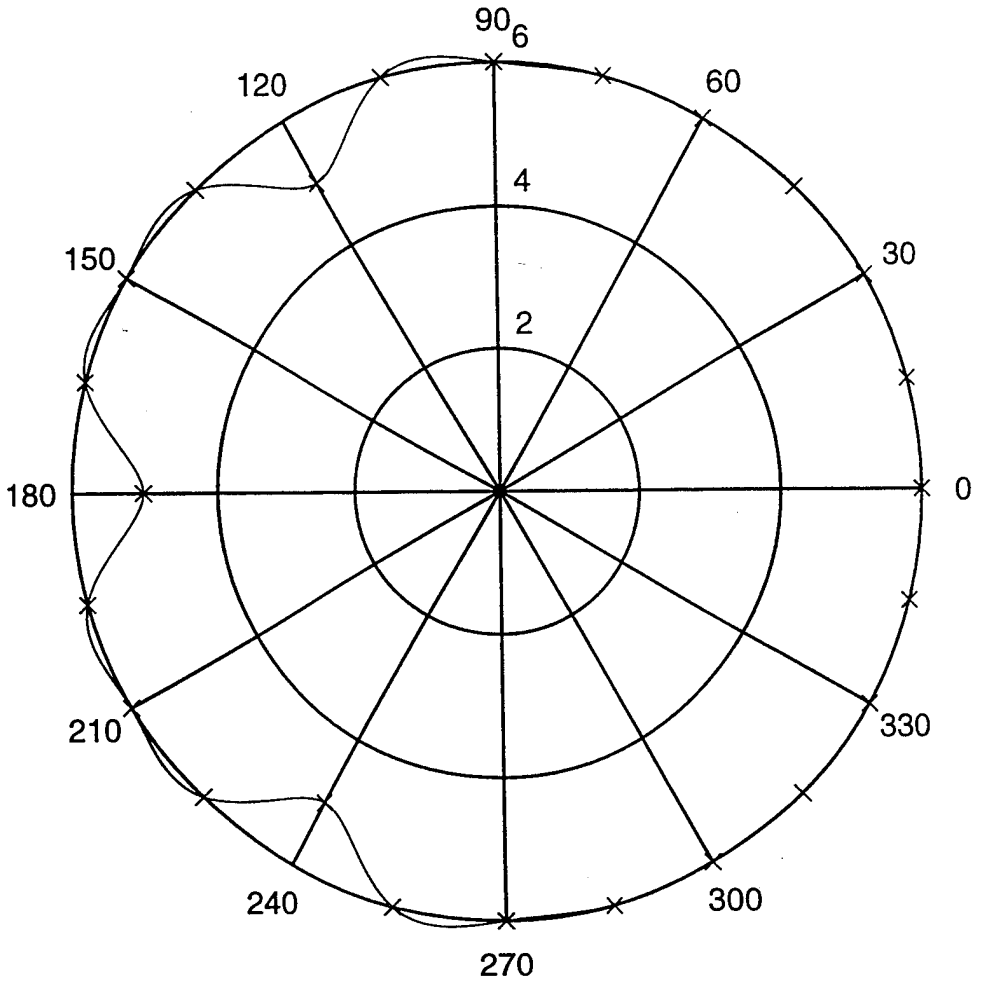

Figure (79). Operability at 20 kts, Sea State Versus Heading.

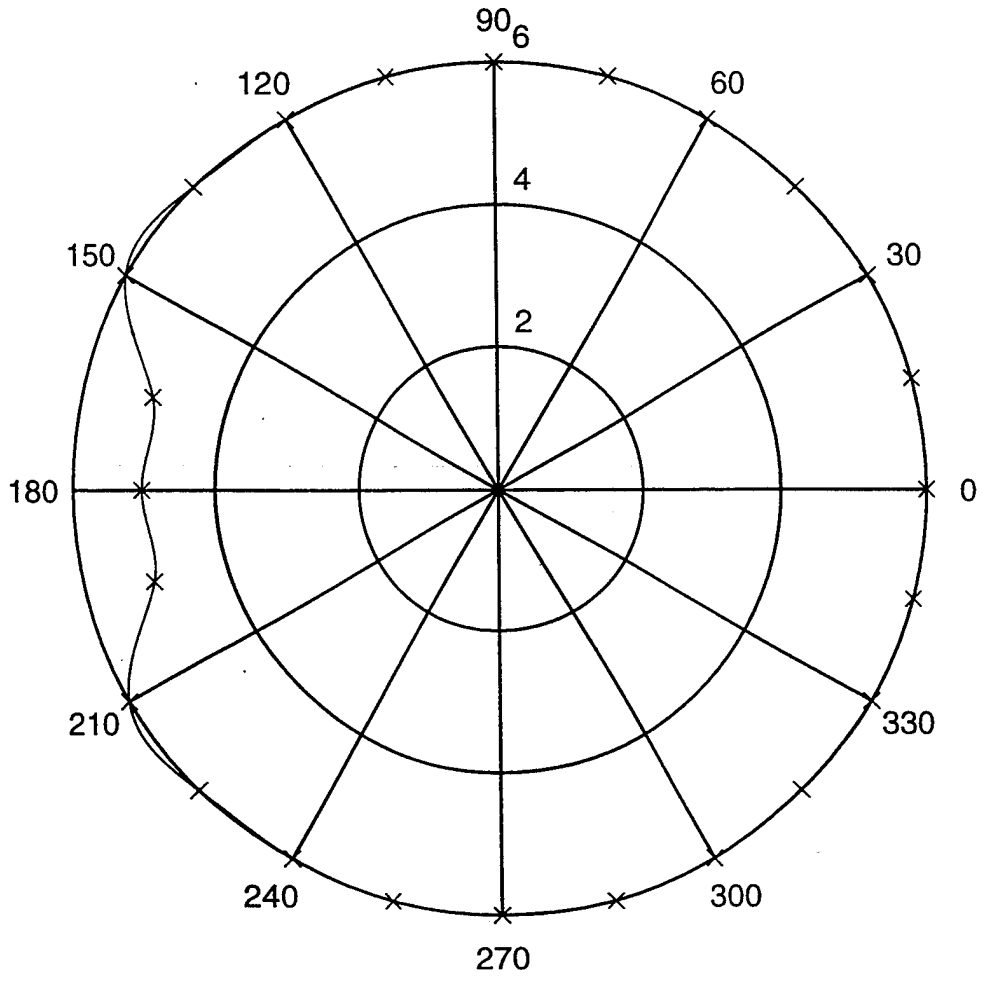

Figure (80). Operability at 25 kts, Sea State Versus Heading.

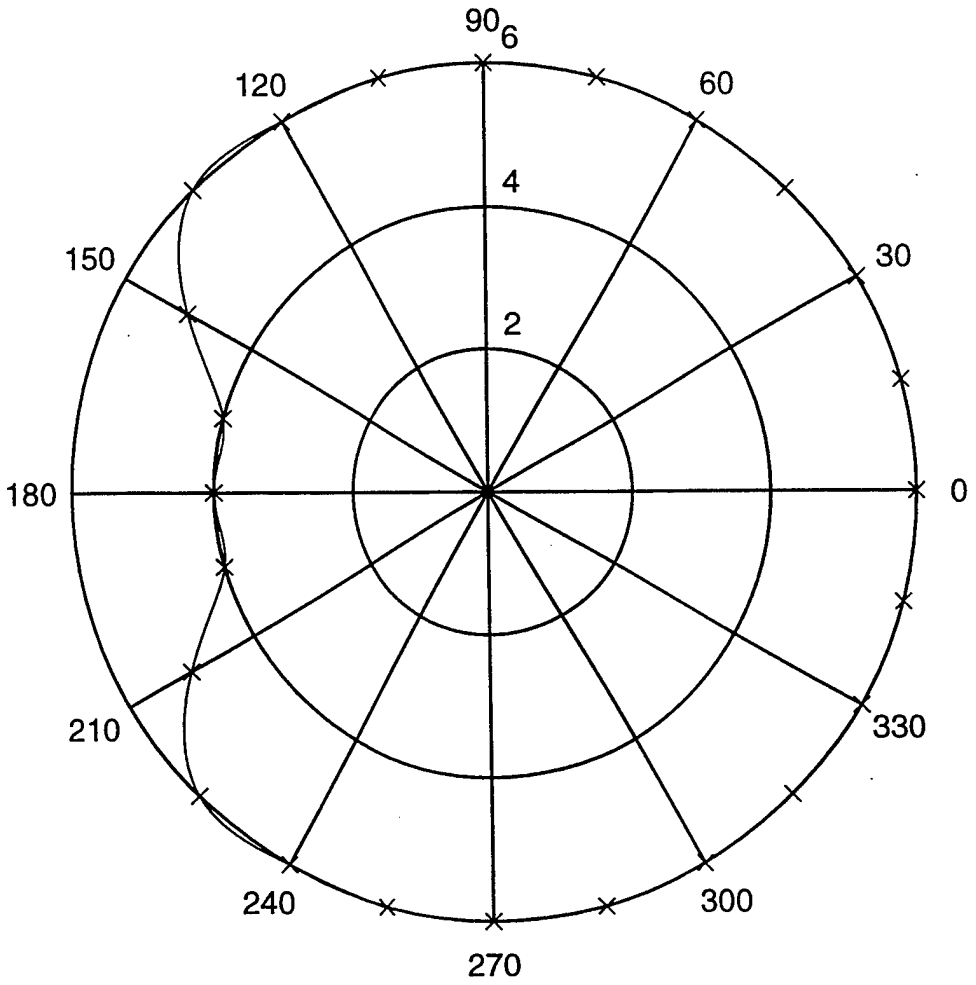

Operability at 30 kts, Sea State Versus Heading.

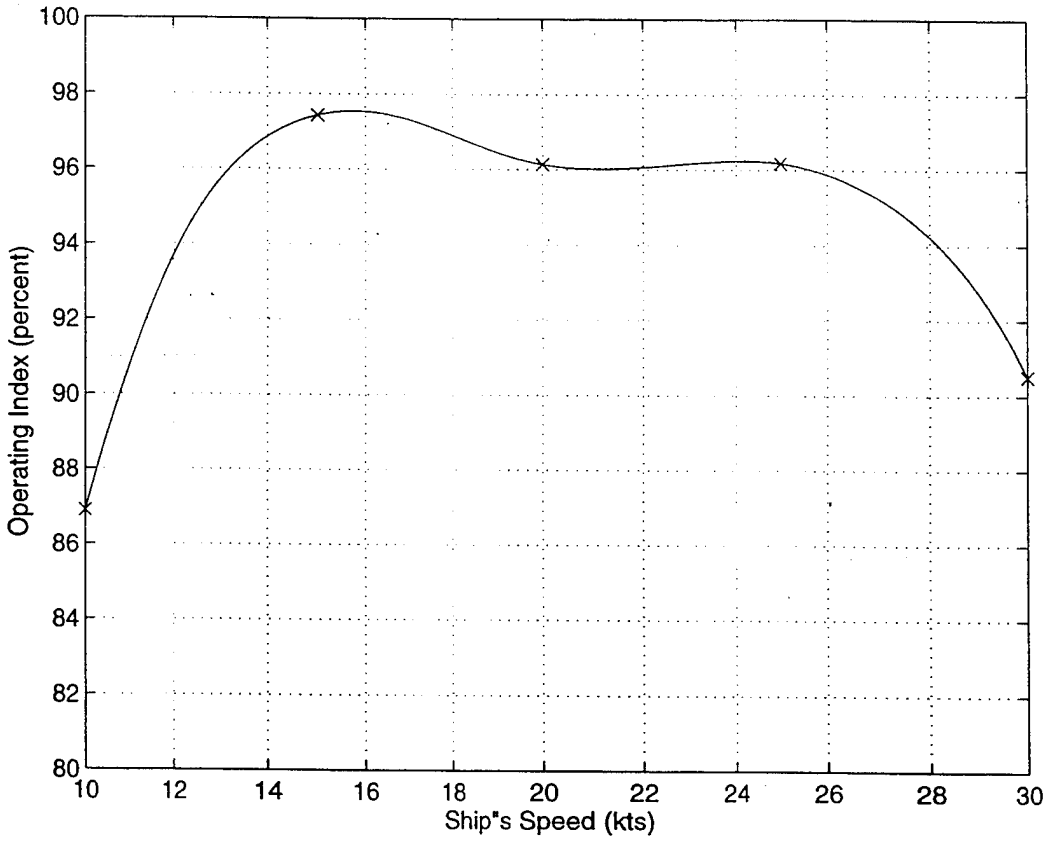

Figure (82). Normalized Operability, Sea State Versus Heading.

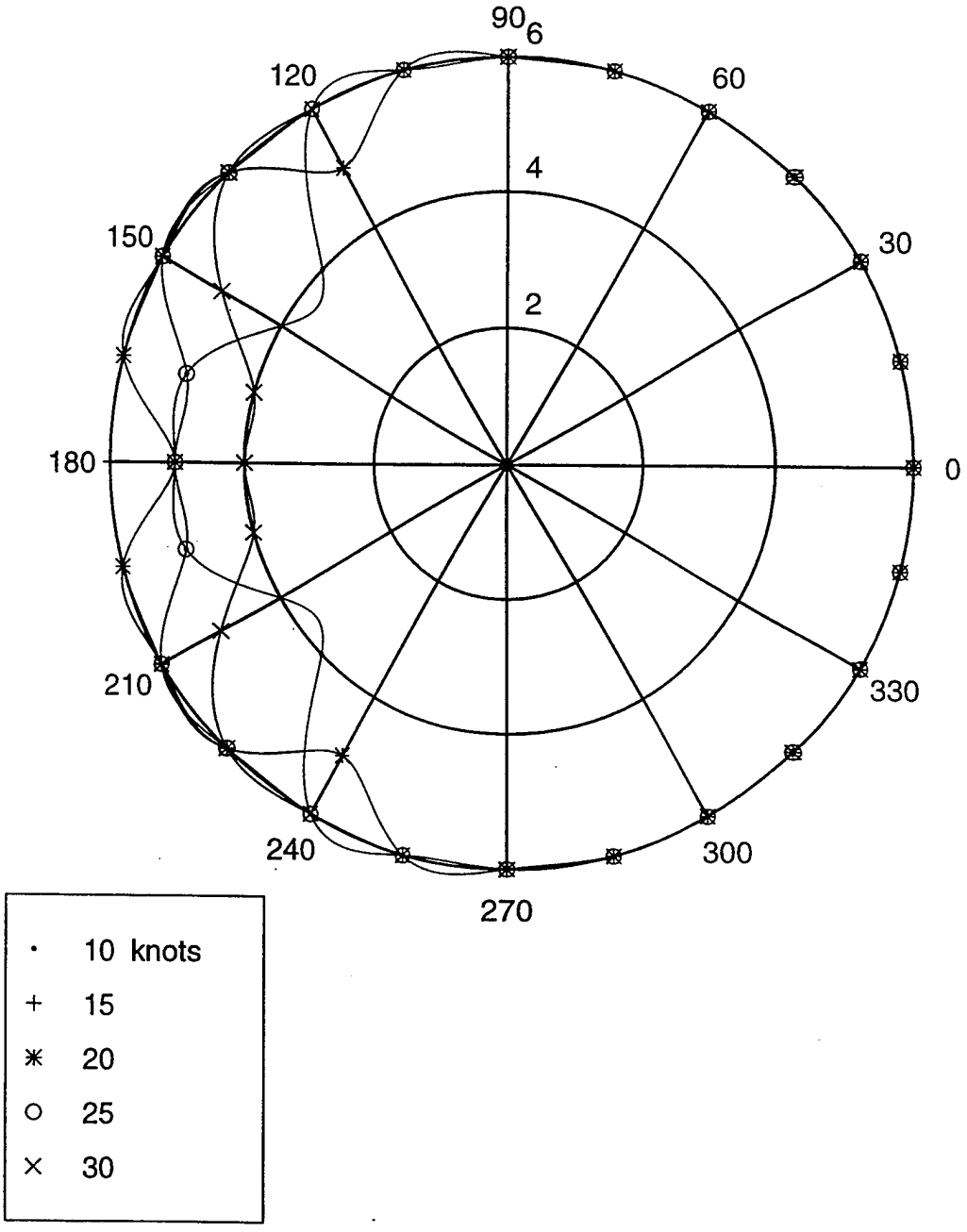

Figure (83). Operability for Family of Speeds, Sea State Versus Heading.

APPENDIX C. CROSS SECTIONAL PROPERTIES CALCULATIONS

A. INTRODUCTION

The limiting cross section of the SLICE hull is characterized by two properties a relatively large bending moment and a small second area moment or moment of inertia. Based on these aspects the area near frame 18 or station 10 was identified as the limiting cross section of the hull. Figure (1) shows views of the SLICE with the limiting cross section marked. Figure (2) shows a view of the limiting cross section in the transverse plane. The cross section is made up of two pentagram shapes spaced 31 feet apart. The structural plates are 0.25 in thick. Figure (3) is an enlarged view of one side of the cross section, the three stiffeners shown are bulb plate stiffeners. Equations for the second moment of inertial and the parallel axis theorem are used to determine the half section properties which is then doubled for the total second moment of inertia. Data for these calculations are displayed in Table (1). The end results of the calculations is a second moment of inertial I_{xx} = 201,312 in^4 and the neutral axis is located 38.4 in below plate number 1 or the main deck.

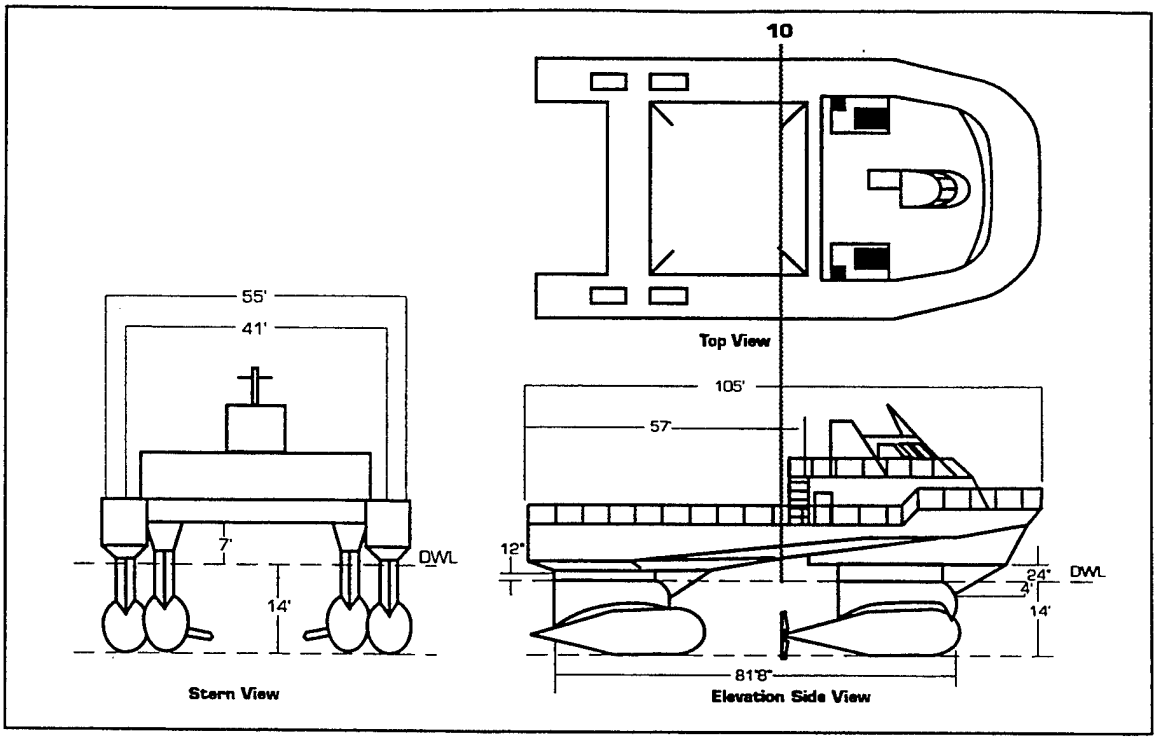

Figure 1. SLICE Hull with Limiting Cross Section, After LMSC, 1994.

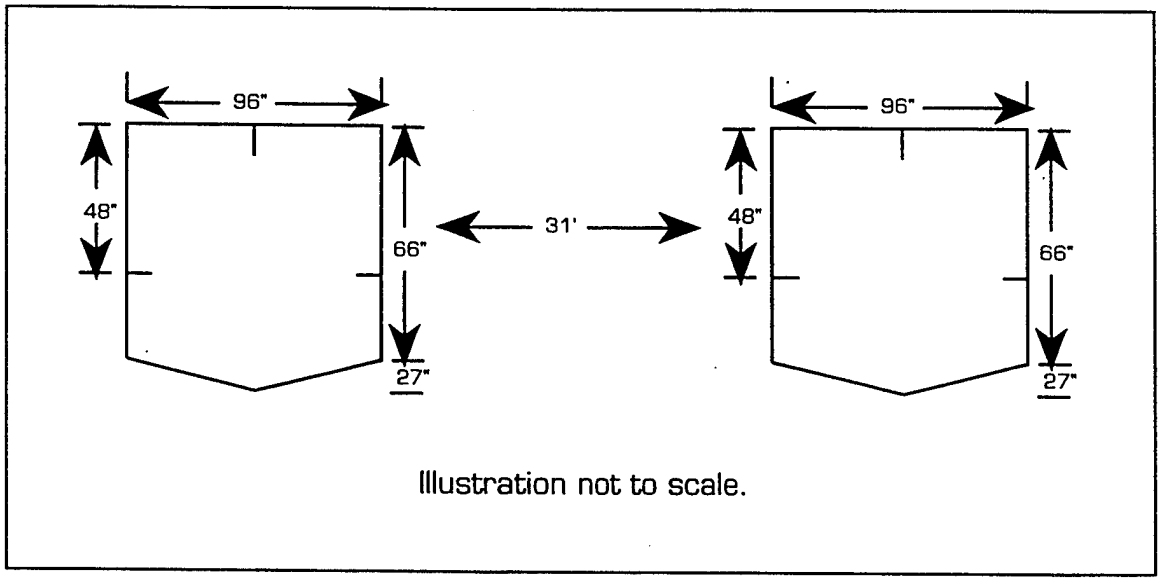

Figure 2. Limiting Cross Section at station 10.

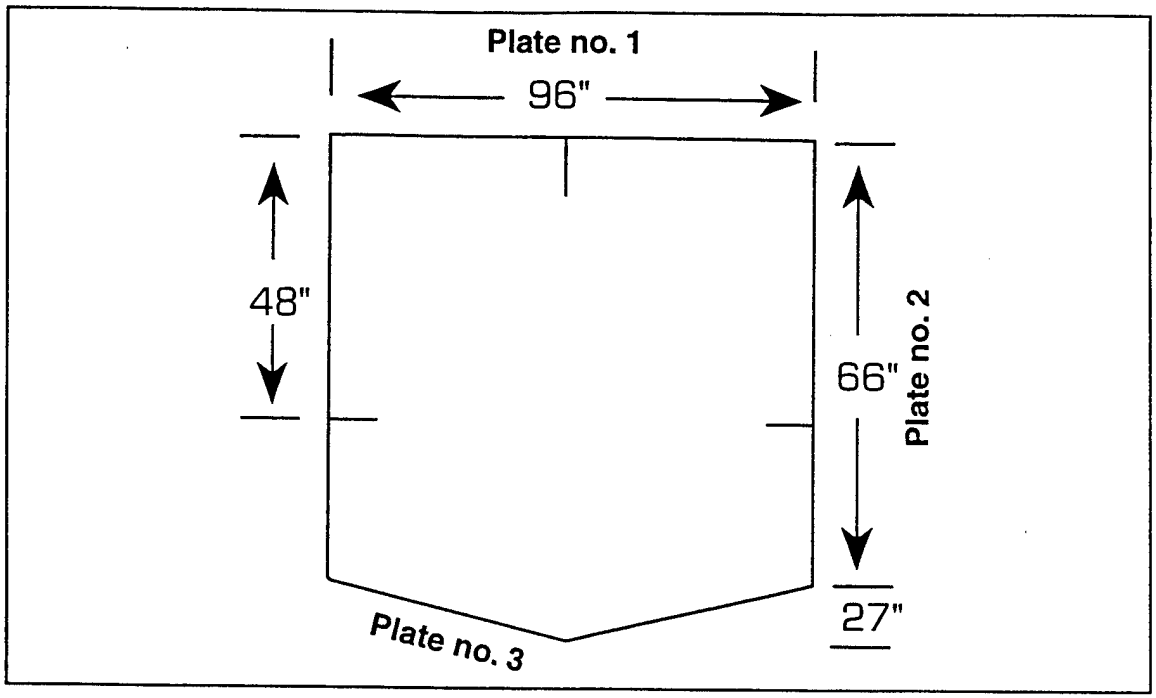

Figure 3. One Side of Limiting Cross Section

Piece	Length l in	Area A in^2	D in	D*a in^3	D^2*A in^3	Ixx in^4	#
Plate 1	.25	24	0	0	0	0.125	1
Plate 2	66	16.5	33	544.5	17,968.5	5989.5	2
Plate 3	55.1	13.8	na	*1094.6	*87,843	*836.3	2
Stiffener 1	3 1	0.75 1	1.5 3.5	1.125 3.5	1069 12.25	0.5625 0.0833	1 1
Stiffener 2	0.25 1.0	0.75 1.0	48 48	36 48	1728 2304	0.0039 0.0833	2 2
Totals		89.85		3451	219,701	13,651.5	

Table (1). Data for One Half Limiting Cross Section.

B. CALCULATIONS

The calculations for the sectional property contribution for plate numbers 1, 2 and the bulb plate stiffeners are fairly straight forward and are based on the equation for the second moment for a rectangle.

$$I_{xx} = \frac{bh^3}{12} \qquad (1)$$

where b = length of base of plate

h = height of plate.

Equation (1) is used to determine the second moment of inertial about the centroid of each of these pieces. Figure (4) shows diagrams that approximate the bulb plate stiffeners. Because of the orientation of plate number 3 the values of D*A, D2*A and the second moment of inertia about the plates centroid must be solved with integration. Figure (5a) shows plate number 3 offset from the x axis which runs along plate number 1 and Figure (5b) shows a differential element of the plate.

$$dA = \frac{0.25}{\cos\theta}\, dx \qquad (2)$$

$$d = 66 + \frac{27}{48}x \quad for\ 0 \le x \le 48 \qquad (3)$$

Figure (5) shows plate number 3 with the coordinate system located at its centroid.

$$D*A = \int d * da = \int (66 + \frac{27}{48}x) * \frac{0.25}{\cos\theta}\, dx = 1094.6\ in^3 \quad \textbf{(4)}$$

$$D^2*A = \int d^2 * da = \int (66 + \frac{27}{48}x)^2 * \frac{0.25}{\cos\theta}\, dx = 63,711\ in^4 \quad \textbf{(5)}$$

$$I_{xx} = \int y^2 da \quad \textbf{(6)}$$

$$y = \frac{27}{48}x \quad for\ -24 \le x \le +24 \quad \textbf{(7)}$$

$$I_{xx} = \int (\frac{27}{48}x)^2 * \frac{0.25}{\cos\theta}x\, dx = 1475.5\ in^4 \quad \textbf{(8)}$$

The neutral axis of the section is determined

$$NA = \frac{\sum D*A}{\sum A} = \frac{3451}{89.85} = 38.43\ in \quad \textbf{(9)}$$

The second moment of inertia about the neutral axis is determined by correcting the second moment of inertia about plate number 1 using the parallel axis theorem.

$$I_{xx} = \sum I_{xxcent.} + \sum D^2 * A - (\sum A * NA^2) \quad \textbf{(10)}$$

$$I_{xx} = 219,701 + 13,651.5 - 89.85 * 38.4^2 = 100,656\ in^4 \quad \textbf{(11)}$$

$$I_{total} = 2I_{xx} = 201,312\ in^4 \quad \textbf{(12)}$$

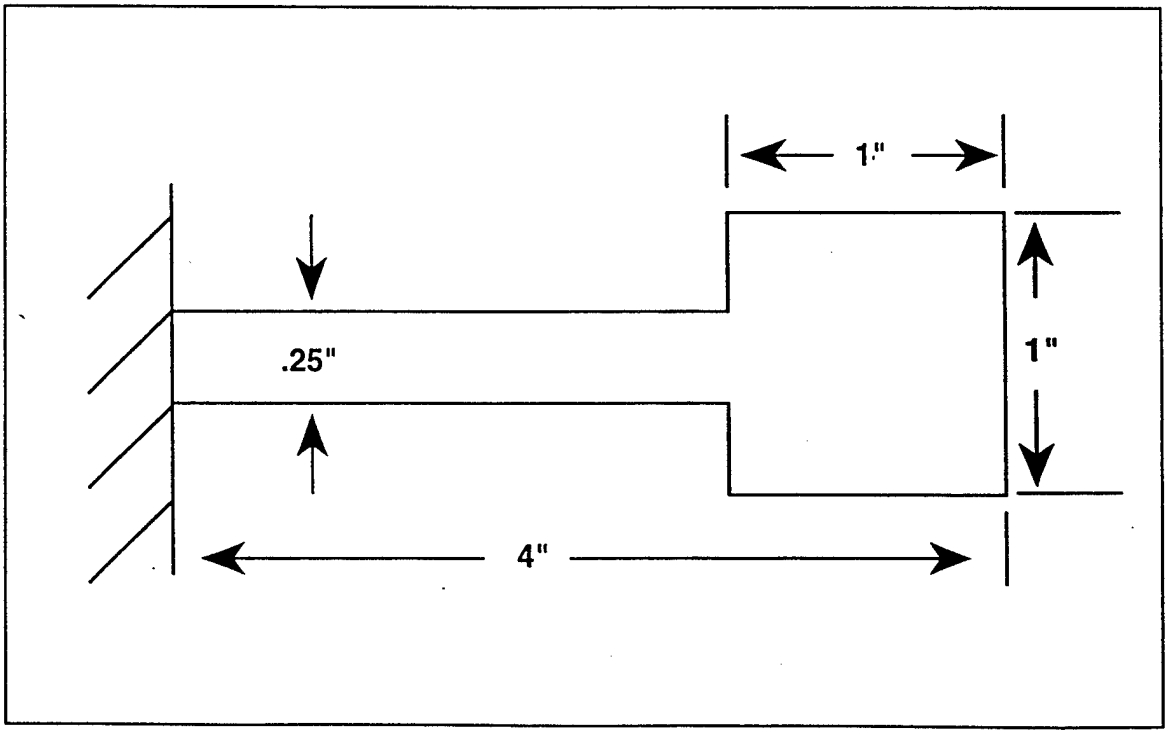

Figure 4. Bulb Plate Stiffener Approximation

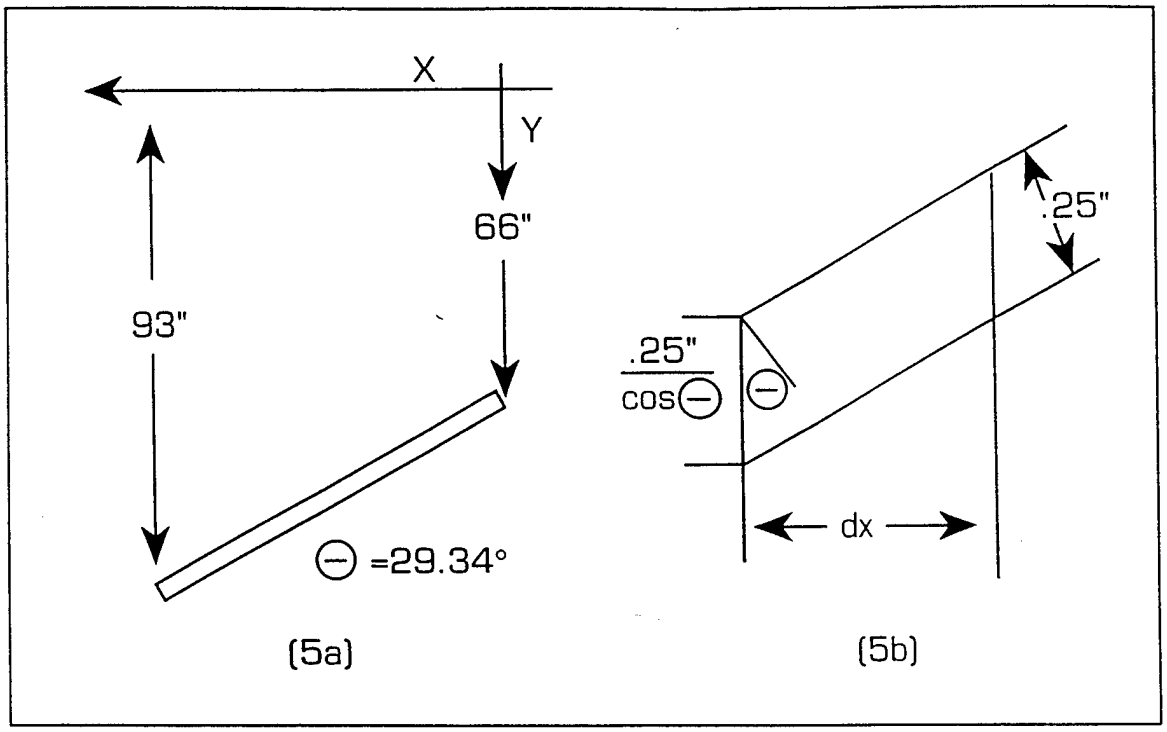

Figure 5. Plate no. 3 and Differential element of Plate no. 3.

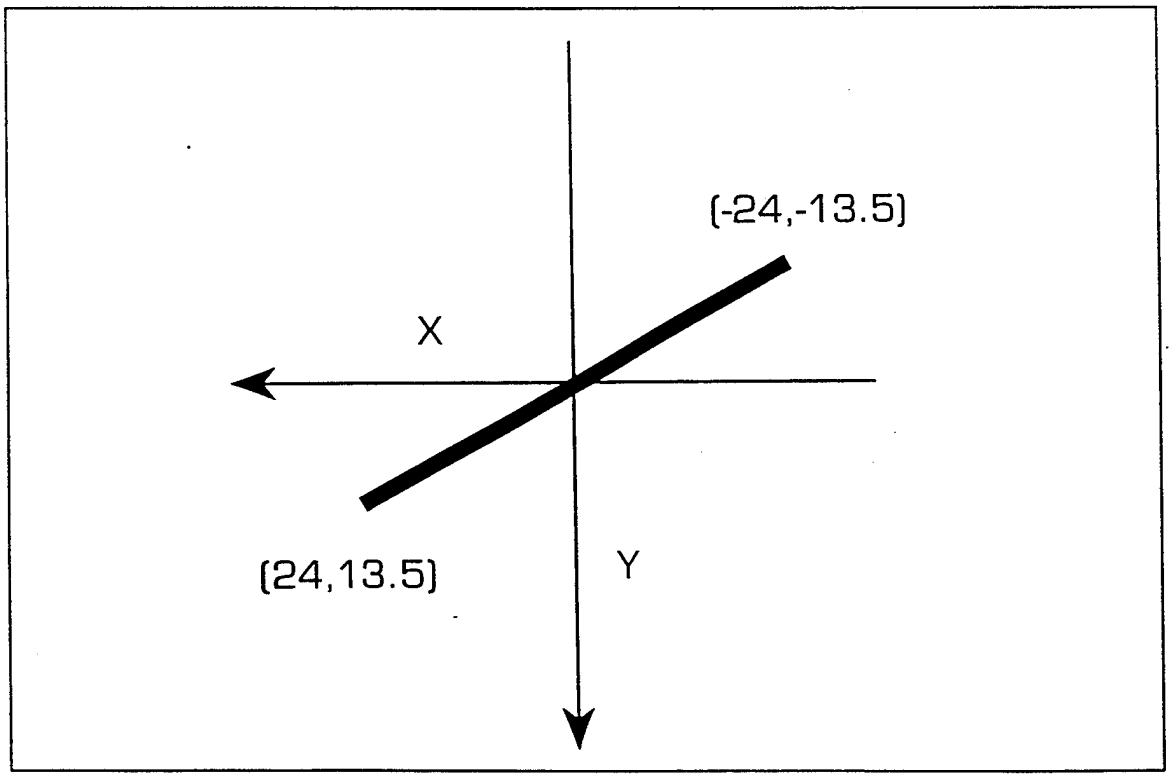

Figure 6. Plate no. 3 with Coordinate System at Center of gravity.

APPENDIX D. NORMAL BENDING STRESS CALCULATIONS

The normal bending stress is determined with the equation

$$\sigma = \frac{M_{total} * c}{I_{xx\ total}} \left(12 \frac{in}{ft}\right) \qquad (1)$$

where M_{total} = the total bending moment $\{ft*lb_f\}$

c = the distance form the neutral axis to point of interest

= 54.6 in (at station 10)

$I_{xx\ total}$ = the second moment of inertia of the cross section.

= 201,312 in^4.

The total bending moment is the sum of the calm water bending moment and the design extreme dynamic bending moment which is 2.15 times the significant dynamic bending moment

$$M_{total} = M_{CWBM} + 2.15 M_{DYN} \qquad (2)$$

where M_{CWBM} = the calm water bending moment

= 1,439,300 $ft*lb_f$ (at station 10)

M_{DYN} = the significant dynamic bending moment.

The significant dynamic bending moments and the normal bending stresses for station 10:

Dynamic Bending Moment for Station 10, Moments are in 10^6 ft*lbf.

10 Knots Heading	SS 2	SS 3	SS 4	SS 5	SS 6
0	0.0557	0.0971	0.1690	0.3000	0.4270
15.0000	0.0181	0.0653	0.1570	0.2980	0.4270
30.0000	0.0374	0.0900	0.1890	0.3290	0.4530
45.0000	0.0155	0.0759	0.2320	0.3840	0.5010
60.0000	0.0786	0.2740	0.4650	0.6110	0.7030
75.0000	0.0093	0.1530	0.3930	0.5480	0.6360
90.0000	0.0083	0.0719	0.3010	0.4290	0.4890
105.0000	0.0091	0.0543	0.2390	0.4380	0.5480
120.0000	0.0115	0.0612	0.4480	0.9220	1.2000
135.0000	0.0128	0.0716	1.3900	2.8700	3.6200
150.0000	0.0184	0.0702	0.8760	1.9400	2.6900
165.0000	0.0136	0.0915	0.4780	1.3800	2.3100
180.0000	0.0317	0.1110	0.4460	1.3800	2.3900

15 Knots Heading	SS 2	SS 3	SS 4	SS 5	SS 6
0	0.0252	0.1090	0.1850	0.2610	0.3610
15.0000	0.0538	0.1670	0.2230	0.2910	0.3860
30.0000	0.0750	0.1650	0.2080	0.2900	0.3990
45.0000	0.0273	0.0851	0.1610	0.2970	0.4300
60.0000	0.0297	0.0901	0.2630	0.4340	0.5630
75.0000	0.0491	0.3530	0.5000	0.6090	0.6940
90.0000	0.0092	0.0655	0.2090	0.2820	0.3240
105.0000	0.0080	0.0548	0.2390	0.4380	0.5620
120.0000	0.0136	0.0651	0.7570	1.5600	1.9900
135.0000	0.0161	0.0884	0.3960	0.8970	1.3500
150.0000	0.0234	0.0881	0.3180	0.8600	1.4500
165.0000	0.0162	0.0807	0.3060	0.9270	1.6200
180.0000	0.0393	0.0971	0.3150	0.9580	1.6800

20 Knots Heading	SS 2	SS 3	SS 4	SS 5	SS 6
0	0.0474	0.5120	0.6950	0.7790	0.8440
15.0000	0.0230	0.2110	0.3800	0.4970	0.5870
30.0000	0.0136	0.0892	0.2200	0.3260	0.4310
45.0000	0.0249	0.1020	0.1790	0.2800	0.3930
60.0000	0.0267	0.0651	0.1580	0.2870	0.4010
75.0000	0.0440	0.1230	0.1990	0.2880	0.3640
90.0000	0.0105	0.0704	0.1890	0.2430	0.2650
105.0000	0.0122	0.0708	0.2740	0.4920	0.6160
120.0000	0.0140	0.0723	0.7460	1.5200	1.9100
135.0000	0.0193	0.0734	0.2910	0.7050	1.1300
150.0000	0.0290	0.0897	0.3360	0.8660	1.4700
165.0000	0.0203	0.1190	0.4390	1.0700	1.8200
180.0000	0.0483	0.1480	0.4900	1.1600	1.9700

Dynamic Bending Moment for Station 10, Moments are in 10^6 ft*lbf.

25 Knots

Heading	SS 2	SS 3	SS 4	SS 5	SS 6
0	0.0306	0.1320	0.3280	0.4660	0.5470
15.0000	0.0184	0.4190	0.6940	0.8430	0.9220
30.0000	0.0183	0.1360	0.3000	0.4190	0.4870
45.0000	0.0163	0.0947	0.2320	0.3120	0.3660
60.0000	0.0281	0.0809	0.1270	0.1930	0.2580
75.0000	0.0350	0.0650	0.1350	0.2050	0.2580
90.0000	0.0111	0.0753	0.1870	0.2360	0.2540
105.0000	0.0122	0.0862	0.3070	0.5520	0.6860
120.0000	0.0165	0.0965	0.3520	0.6950	0.9580
135.0000	0.0232	0.0910	0.3330	0.7620	1.2300
150.0000	0.0329	0.1320	0.4110	1.0300	1.7700
165.0000	0.0237	0.1240	0.3640	1.3000	2.3700
180.0000	0.0573	0.1450	0.3660	1.5300	2.8400

30 Knots

Heading	SS 2	SS 3	SS 4	SS 5	SS 6
0	0.0380	0.3280	0.7320	0.9390	1.1100
15.0000	0.0163	0.2760	0.6130	0.7880	0.9120
30.0000	0.0227	0.1620	0.3780	0.5260	0.6160
45.0000	0.0126	0.1070	0.2780	0.3970	0.4620
60.0000	0.0846	0.2540	0.3200	0.3560	0.3840
75.0000	0.0627	0.1160	0.1630	0.2100	0.2470
90.0000	0.0122	0.0830	0.1930	0.2390	0.2580
105.0000	0.0142	0.0886	0.3280	0.6030	0.7490
120.0000	0.0199	0.0705	0.2950	0.6250	0.9160
135.0000	0.0249	0.1240	0.4040	0.8930	1.4500
150.0000	0.0381	0.1190	0.3570	1.4400	2.6500
165.0000	0.0250	0.1390	0.7800	6.4200	12.3000
180.0000	0.0626	0.1740	0.4880	2.2000	4.1000

Total Bending Moment for Station 10, Moments are in 10^6 ft*lbf.

10 Knots

Heading	SS 2	SS 3	SS 4	SS 5	SS 6
0	1.5591	1.6481	1.8027	2.0843	2.3573
15.0000	1.4782	1.5797	1.7769	2.0800	2.3573
30.0000	1.5197	1.6328	1.8457	2.1467	2.4133
45.0000	1.4726	1.6025	1.9381	2.2649	2.5164
60.0000	1.6083	2.0284	2.4390	2.7529	2.9508
75.0000	1.4593	1.7683	2.2843	2.6175	2.8067
90.0000	1.4572	1.5939	2.0865	2.3617	2.4907
105.0000	1.4588	1.5560	1.9531	2.3810	2.6175
120.0000	1.4640	1.5709	2.4025	3.4216	4.0193
135.0000	1.4668	1.5932	4.4278	7.6098	9.2223
150.0000	1.4789	1.5902	3.3227	5.6103	7.2228
165.0000	1.4685	1.6360	2.4670	4.4063	6.4058
180.0000	1.5075	1.6780	2.3982	4.4063	6.5778

Total Bending Moment for Station 10, Moments are in 10^6 ft*lbf.

15 Knots

Heading	SS 2	SS 3	SS 4	SS 5	SS 6
0	1.4935	1.6737	1.8371	2.0004	2.2155
15.0000	1.5550	1.7983	1.9187	2.0650	2.2692
30.0000	1.6005	1.7940	1.8865	2.0628	2.2971
45.0000	1.4980	1.6223	1.7854	2.0779	2.3638
60.0000	1.5032	1.6330	2.0048	2.3724	2.6498
75.0000	1.5449	2.1982	2.5143	2.7487	2.9314
90.0000	1.4590	1.5801	1.8886	2.0456	2.1359
105.0000	1.4565	1.5571	1.9531	2.3810	2.6476
120.0000	1.4685	1.5793	3.0669	4.7933	5.7178
135.0000	1.4739	1.6294	2.2907	3.3678	4.3418
150.0000	1.4896	1.6287	2.1230	3.2883	4.5568
165.0000	1.4741	1.6128	2.0972	3.4324	4.9223
180.0000	1.5238	1.6481	2.1166	3.4990	5.0513

20 Knots

Heading	SS 2	SS 3	SS 4	SS 5	SS 6
0	1.5412	2.5401	2.9335	3.1141	3.2539
15.0000	1.4888	1.8929	2.2563	2.5078	2.7014
30.0000	1.4685	1.6311	1.9123	2.1402	2.3660
45.0000	1.4928	1.6586	1.8241	2.0413	2.2843
60.0000	1.4967	1.5793	1.7790	2.0564	2.3014
75.0000	1.5339	1.7038	1.8672	2.0585	2.2219
90.0000	1.4619	1.5907	1.8457	1.9618	2.0090
105.0000	1.4655	1.5915	2.0284	2.4971	2.7637
120.0000	1.4694	1.5947	3.0432	4.7073	5.5458
135.0000	1.4808	1.5971	2.0650	2.9550	3.8688
150.0000	1.5016	1.6322	2.1617	3.3012	4.5998
165.0000	1.4829	1.6951	2.3832	3.7398	5.3523
180.0000	1.5431	1.7575	2.4928	3.9333	5.6748

25 Knots

Heading	SS 2	SS 3	SS 4	SS 5	SS 6
0	1.5051	1.7231	2.1445	2.4412	2.6153
15.0000	1.4789	2.3401	2.9314	3.2517	3.4216
30.0000	1.4786	1.7317	2.0843	2.3401	2.4863
45.0000	1.4743	1.6429	1.9381	2.1101	2.2262
60.0000	1.4997	1.6132	1.7124	1.8542	1.9940
75.0000	1.5146	1.5791	1.7295	1.8800	1.9940
90.0000	1.4632	1.6012	1.8414	1.9467	1.9854
105.0000	1.4655	1.6246	2.0993	2.6261	2.9142
120.0000	1.4748	1.6468	2.1961	2.9335	3.4990
135.0000	1.4892	1.6349	2.1553	3.0776	4.0838
150.0000	1.5100	1.7231	2.3230	3.6538	5.2448
165.0000	1.4903	1.7059	2.2219	4.2343	6.5348
180.0000	1.5625	1.7510	2.2262	4.7288	7.5453

Total Bending Moment for Station 10, Moments are in 10^6 ft*lbf.

30 Knots Heading	SS 2	SS 3	SS 4	SS 5	SS 6
0	1.5210	2.1445	3.0131	3.4581	3.8258
15.0000	1.4743	2.0327	2.7572	3.1335	3.4001
30.0000	1.4881	1.7876	2.2520	2.5702	2.7637
45.0000	1.4664	1.6693	2.0370	2.2929	2.4326
60.0000	1.6212	1.9854	2.1273	2.2047	2.2649
75.0000	1.5741	1.6887	1.7897	1.8908	1.9704
90.0000	1.4655	1.6178	1.8542	1.9531	1.9940
105.0000	1.4698	1.6298	2.1445	2.7357	3.0497
120.0000	1.4821	1.5909	2.0736	2.7830	3.4087
135.0000	1.4928	1.7059	2.3079	3.3592	4.5568
150.0000	1.5212	1.6951	2.2069	4.5353	7.1368
165.0000	1.4930	1.7382	3.1163	15.2423	27.8843
180.0000	1.5739	1.8134	2.4885	6.1693	10.2543

Normal Bending Stress at Station 10, Stresses are in Kpsi.

10 Knots Heading	SS 2	SS 3	SS 4	SS 5	SS 6
0	5.0742	5.3639	5.8670	6.7837	7.6723
15.0000	4.8111	5.1414	5.7830	6.7697	7.6723
30.0000	4.9461	5.3142	6.0069	6.9866	7.8543
45.0000	4.7929	5.2155	6.3078	7.3715	8.1902
60.0000	5.2344	6.6017	7.9383	8.9599	9.6037
75.0000	4.7496	5.7550	7.4344	8.5190	9.1348
90.0000	4.7426	5.1875	6.7907	7.6863	8.1062
105.0000	4.7479	5.0644	6.3568	7.7493	8.5190
120.0000	4.7649	5.1127	7.8193	11.1361	13.0814
135.0000	4.7740	5.1854	14.4109	24.7672	30.0154
150.0000	4.8132	5.1756	10.8142	18.2596	23.5077
165.0000	4.7796	5.3247	8.0292	14.3410	20.8486
180.0000	4.9062	5.4611	7.8053	14.3410	21.4084

15 Knots Heading	SS 2	SS 3	SS 4	SS 5	SS 6
0	4.8608	5.4471	5.9790	6.5108	7.2105
15.0000	5.0609	5.8530	6.2449	6.7207	7.3855
30.0000	5.2092	5.8390	6.1399	6.7137	7.4764
45.0000	4.8754	5.2799	5.8110	6.7627	7.6933
60.0000	4.8922	5.3149	6.5248	7.7213	8.6240
75.0000	5.0280	7.1545	8.1832	8.9459	9.5407
90.0000	4.7486	5.1428	6.1469	6.6577	6.9516
105.0000	4.7405	5.0679	6.3568	7.7493	8.6170
120.0000	4.7796	5.1400	9.9815	15.6005	18.6094
135.0000	4.7971	5.3030	7.4554	10.9612	14.1310
150.0000	4.8482	5.3009	6.9096	10.7023	14.8308
165.0000	4.7978	5.2491	6.8257	11.1711	16.0204
180.0000	4.9594	5.3639	6.8886	11.3880	16.4402

Normal Bending Stress at Station 10, Stresses are in Kpsi.

20 Knots Heading	SS 2	SS 3	SS 4	SS 5	SS 6
0	5.0161	8.2671	9.5477	10.1355	10.5903
15.0000	4.8454	6.1609	7.3435	8.1622	8.7919
30.0000	4.7796	5.3086	6.2239	6.9656	7.7003
45.0000	4.8587	5.3982	5.9370	6.6437	7.4344
60.0000	4.8713	5.1400	5.7900	6.6927	7.4904
75.0000	4.9923	5.5451	6.0769	6.6997	7.2315
90.0000	4.7579	5.1770	6.0069	6.3848	6.5388
105.0000	4.7698	5.1798	6.6017	8.1272	8.9949
120.0000	4.7824	5.1903	9.9045	15.3206	18.0496
135.0000	4.8195	5.1980	6.7207	9.6177	12.5916
150.0000	4.8873	5.3121	7.0356	10.7442	14.9707
165.0000	4.8265	5.5171	7.7563	12.1717	17.4199
180.0000	5.0224	5.7200	8.1132	12.8015	18.4695

25 Knots Heading	SS 2	SS 3	SS 4	SS 5	SS 6
0	4.8985	5.6081	6.9796	7.9453	8.5120
15.0000	4.8132	7.6164	9.5407	10.5833	11.1361
30.0000	4.8125	5.6361	6.7837	7.6164	8.0922
45.0000	4.7985	5.3471	6.3078	6.8676	7.2455
60.0000	4.8810	5.2505	5.5731	6.0349	6.4898
75.0000	4.9293	5.1393	5.6291	6.1189	6.4898
90.0000	4.7621	5.2113	5.9929	6.3358	6.4618
105.0000	4.7698	5.2876	6.8326	8.5470	9.4847
120.0000	4.7999	5.3597	7.1475	9.5477	11.3880
135.0000	4.8468	5.3212	7.0146	10.0165	13.2913
150.0000	4.9146	5.6081	7.5604	11.8918	17.0700
165.0000	4.8503	5.5521	7.2315	13.7812	21.2685
180.0000	5.0854	5.6991	7.2455	15.3906	24.5573

30 Knots Heading	SS 2	SS 3	SS 4	SS 5	SS 6
0	4.9503	6.9796	9.8066	11.2551	12.4516
15.0000	4.7985	6.6157	8.9739	10.1984	11.0661
30.0000	4.8433	5.8180	7.3295	8.3651	8.9949
45.0000	4.7726	5.4331	6.6297	7.4624	7.9173
60.0000	5.2764	6.4618	6.9236	7.1755	7.3715
75.0000	5.1232	5.4961	5.8250	6.1539	6.4128
90.0000	4.7698	5.2652	6.0349	6.3568	6.4898
105.0000	4.7838	5.3044	6.9796	8.9039	9.9255
120.0000	4.8237	5.1777	6.7487	9.0579	11.0941
135.0000	4.8587	5.5521	7.5114	10.9332	14.8308
150.0000	4.9510	5.5171	7.1825	14.7608	23.2278
165.0000	4.8594	5.6571	10.1425	49.6083	90.7536
180.0000	5.1225	5.9020	8.0992	20.0789	33.3742

LIST OF REFERENCES

American Society for Metals (ASM), "Metals Hand Book, 9th ed., Vol 2," pp.103 - 104, 1979.

Beck, R. F., and Troesch, A. W., "Documentation and User's Manual for the Computer Program SHIPMO.BM,"Report No. 89-2, 1989.

Gupta,S. K., and Schmidt, T. W., "Developments in Swath Technology," Naval Engineers Journal, May 1986.

Lesh, D. B., "Seakeeping Characteristics of the SLICE Hulls: A Motion Study in Six Degrees Of Freedom," M.S. Thesis, Naval Postgraduate School, Monterey, CA, 1995.

Lewis, E. V., "Principles of Naval Architecture," The Society of Naval Architectures and Marine Engineers, vol III, 1989.

Lockheed Missile and Space Company, Inc. (LMSC), "SLICE Lines and Profile," Drawing No. P1-100-01, Sheet 1 and 2, Dec. 1994.

Muckle, W., "Muckle's Naval Architecture," Butterworth and Company Ltd., 1987.

Papoulias, F. A., "Dynamics of Marine Vehicles," Informal Lecture Notes for ME4823, Naval Postgraduate School, Monterey, CA, Summer 1993.

Roberts, D. J., "Structural Responses of the SLICE Advanced Technology Demonstrator,"M.S. Thesis, Naval Postgraduate School, Monterey, CA, 1995.

Rodriguez, M., "Structural Response of SLICE Hulls," M.S. Thesis, Naval Postgraduate School, Monterey, CA, 1995.

Salvesen, N., Tuck, E. O., and Faltinsen, O., "Ship Motions and Sea Loads," Transactions of the Society of Naval Architects and Marine Engineers, vol. 78, pp 250-287, 1970.

INITIAL DISTRIBUTION LIST

		No. Copies
1.	Defense Technical Information Center 8725 John J. Kingman Rd., STE 0944 Ft. Belvoir, VA 22060-6218	2
2.	Dudlley Knox Library, Naval Postgraduate School 411 Dyer Rd. Monterey, CA 93943-5101	2
3.	Chairman, Code ME Department of Mechanical Engineering Naval Postgraduate School Monterey, CA 93943-5000	1
4.	Professor Fotis A. Papoulias, Code ME/PA Department of Mechanical Engineering Naval Postgraduate School Monterey, CA 93943-5000	6
5.	Professor Charles N. Calvano, Code ME/PA Department of Mechanical Engineering Naval Postgraduate School Monterey, CA 93943-5000	2
6.	Naval Engineering Curricular Office, Code 34 Naval Postgraduate School Monterey, CA 93943-5000	1
7.	LT Dennis W. McFadden 2432 So. St. Louis Tulsa, OK 74114	2